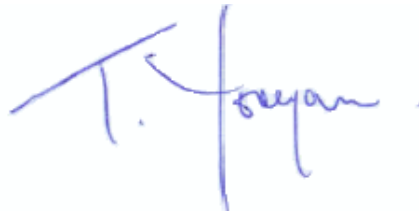


Thesis presented to the Faculty of the Department of Graduate Studies of the Aeronautics Institute of Technology, in partial fulfillment of the requirements for the Degree of Doctor in Science in the Program of Electronic Engineering and Computer Science, Field of Systems and Control

**Davi Antônio dos Santos**

**FAULT-TOLERANT STATE ESTIMATION OF  
LINEAR GAUSSIAN SYSTEMS SUBJECT TO  
ADDITIVE FAULTS**

Thesis approved in its final version by signatories below:



Prof. Takashi Yoneyama

Advisor

Prof. Celso Missaki Hirata

Head of the Faculty of the Department of Graduate Studies

Campo Montenegro  
São José dos Campos, SP - Brazil  
2011

**Cataloging-in Publication Data**  
**Documentation and Information Division/DCTA**

Santos, Davi Antônio dos  
Fault-tolerant state estimation of linear Gaussian Systems Subject to Additive Faults / Davi Antônio dos Santos.  
São José dos Campos, 2011.  
130f.

Thesis of Doctor in Science – Course of Electronic Engineering and Computer Science. Area of Systems and Control – Aeronautical Institute of Technology, 2011. Advisor: Prof. Takashi Yoneyama.

1. Fault-Tolerant State Estimation. 2. Filtering Theory. 3. Statistical Signal Processing. 4. Bayesian Detection. 5. Model Predictive Control. 6. Satellite Attitude Control. I. Aeronautics Institute of Technology. II. Title.

**BIBLIOGRAPHIC REFERENCE**

SANTOS, Davi Antônio dos. **Fault-tolerant state estimation of linear Gaussian Systems Subject to Additive Faults**. 2011. 130f. Thesis of Doctor in Science in Systems and Control – Technological Institute of Aeronautics, São José dos Campos.

**CESSION OF RIGHTS**

AUTHOR NAME: Davi Antônio dos Santos

PUBLICATION TITLE: Fault-tolerant state estimation of linear Gaussian Systems Subject to Additive Faults.

TYPE OF PUBLICATION/YEAR: Thesis / 2011

It is granted to Aeronautics Institute of Technology permission to reproduce copies of this thesis and to only loan or to sell copies for academic and scientific purposes. The author reserves other publication rights and no part of this thesis can be reproduced without the authorization of the author.

---

Davi Antônio dos Santos  
Praça Marechal Eduardo Gomes, 50 – Vila das Acácias  
CEP 12.228-900 – São José dos Campos–SP

# FAULT-TOLERANT STATE ESTIMATION OF LINEAR GAUSSIAN SYSTEMS SUBJECT TO ADDITIVE FAULTS

Davi Antônio dos Santos

Thesis Committee Composition:

Prof. Dr.	Elder Moreira Hemerly	Chairperson	-	ITA
Prof.	Takashi Yoneyama	Advisor	-	ITA
Prof. Dr.	Oswaldo Luiz do Valle Costa		-	USP
Dr.	Hélio Koiti Kuga		-	INPE
Prof. Dr.	David Fernandes		-	ITA

This thesis is dedicated to my  
parents Antônio and Filomena  
Santos for their love, encour-  
agement and moral support.

# Acknowledgments

I would like to thank all the people who either directly or indirectly contributed to the development of this thesis. Specially, I am grateful to Professor Takashi Yoneyama, whose guidance and encouragement enabled me to learn how to conduct a scientific research. I owe my deepest gratitude to my parents Antônio and Filomena Santos for their love and moral support. This research was realized with the financial support given by the Fundação de Amparo à Pesquisa do Estado de São Paulo (FAPESP) under grant 07/58501-4.

*"The only way of finding the limits of the possible  
is by going beyond them into the impossible."*

— SIR ARTHUR C. CLARKE

# Resumo

Devido à demanda por atributos tais como segurança, manutenibilidade e confiabilidade em dispositivos atuais de engenharia, verifica-se uma crescente investigação sobre o uso de métodos de tolerância a falhas em projetos de sistemas de controle. Em particular, caso os estados do sistema não possam ser diretamente medidos pelos sensores existentes, a adoção de um método tolerante a falhas para estimação de estados é fundamental. Neste contexto, a presente tese formula um problema de estimação de estados que consiste na estimação conjunta da falha e dos estados do sistema de forma recursiva. Considera-se que a dinâmica do sistema possa ser descrita por um modelo em espaço de estados, discreto no tempo, com ruídos Gaussianos e sujeito a falhas aditivas que afetem tanto a equação de estados quanto a de medidas. Considera-se que a sequência de vetores de falha seja parametrizável por três parâmetros: a magnitude da falha, o instante de início da falha, e o índice do modo da falha. Adicionalmente, considera-se que esses parâmetros sejam realizações de variáveis aleatórias (VA) definidas de forma a representar conhecimento *a priori* sobre possíveis falhas. Para tratar o problema acima, propõe-se uma abordagem de filtragem de dois estágios (FTTS), da qual três diferentes filtros FTTS são derivados levando-se em conta três caracterizações alternativas da VA subjacente à magnitude da falha. Com base em simulação computacional, um dos filtros é ilustrado num esquema de controle preditivo tolerante a falhas para controle de atitude de um satélite rígido.

# Abstract

Owing to the need for the satisfaction of attributes such as safety, maintainability, and reliability in modern critical engineering devices, the design of automatic feedback control systems has increasingly demanding fault-tolerant methods. In particular, if the system states cannot directly be measured by the available suite of sensors, a fault-tolerant state estimation method turns out to be of paramount importance for achieving fault tolerance. In this context, the present thesis formulates a fault-tolerant state estimation (FTSE) problem consisting of a joint state and fault estimation of linear systems subject to additive faults. The system is described by a discrete-time linear Gaussian state-space model, where the fault appears as unknown inputs affecting both the state and measurement equations. The sequence of fault inputs is assumed to be parameterizable by three fault parameters: the fault magnitude, the fault instant, and the fault mode index. Moreover, these parameters are treated as unknown realizations of random variables (RV) that are defined so as to account for prior knowledge about possible faults. For tackling the above FTSE problem, the present work introduces a fault-tolerant two-stage (FTTS) filtering approach, from which three different FTTS filters are derived by considering three plausible alternative characterizations of the fault magnitude RV. On the basis of computational simulations, one of the FTTS filters is illustrated on a fault-tolerant model predictive control (MPC) scheme for satellite attitude control.



# Contents

LIST OF FIGURES . . . . .	xii
LIST OF TABLES . . . . .	xiv
LIST OF ABBREVIATIONS . . . . .	xv
LIST OF SYMBOLS . . . . .	xvii
<b>1 INTRODUCTION . . . . .</b>	<b>20</b>
<b>1.1 Motivation . . . . .</b>	<b>20</b>
<b>1.2 Historical background . . . . .</b>	<b>22</b>
1.2.1 Recursive linear minimum variance unbiased approach . . . . .	24
1.2.2 Decision-theoretic approach . . . . .	25
1.2.3 Bayesian filtering approach . . . . .	26
<b>1.3 Text organization . . . . .</b>	<b>27</b>
<b>1.4 Contributions of the thesis . . . . .</b>	<b>28</b>
<b>2 PROBLEM STATEMENT . . . . .</b>	<b>30</b>
<b>2.1 Fault-tolerant state estimation problem . . . . .</b>	<b>30</b>
<b>2.2 Some comments upon the proposed fault-prone system model . . . . .</b>	<b>34</b>
2.2.1 Examples of fault modes . . . . .	34
2.2.2 The prior information on the fault parameters . . . . .	35

---

<b>2.3</b>	<b>Summary</b> . . . . .	39
<b>3</b>	<b>THEORETICAL BACKGROUND</b> . . . . .	40
<b>3.1</b>	<b>Parameter estimation</b> . . . . .	40
<b>3.2</b>	<b>State estimation</b> . . . . .	41
<b>3.3</b>	<b>Detection of signals corrupted by noise</b> . . . . .	47
<b>4</b>	<b>FAULT-TOLERANT TWO-STAGE FILTERS</b> . . . . .	52
<b>4.1</b>	<b>The structure of the filters</b> . . . . .	52
<b>4.2</b>	<b>Stage 1: Fault estimation</b> . . . . .	53
4.2.1	Case 1: Fault magnitude with Gaussian distribution . . . . .	57
4.2.2	Case 2: Fault magnitude with <i>gamma</i> distribution . . . . .	61
4.2.3	Case 3: Fault magnitude with discrete distribution . . . . .	66
<b>4.3</b>	<b>Stage 2: state estimation</b> . . . . .	69
<b>4.4</b>	<b>Illustrative Examples</b> . . . . .	71
4.4.1	System modeling . . . . .	71
4.4.2	Simulation-based evaluation of the FTTS filters . . . . .	73
<b>4.5</b>	<b>Comments on performance analysis</b> . . . . .	77
4.5.1	Fault estimation . . . . .	78
4.5.2	State estimation . . . . .	79
<b>4.6</b>	<b>Summary</b> . . . . .	80
<b>5</b>	<b>A FAULT-TOLERANT MODEL PREDICTIVE SATELLITE ATTITUDE CONTROLLER</b> . . . . .	81
<b>5.1</b>	<b>Fault-prone system model</b> . . . . .	81
<b>5.2</b>	<b>The fault-tolerant control method</b> . . . . .	83
5.2.1	The scheme for fault-tolerant control . . . . .	84

---

5.2.2	Fault-tolerant attitude determination . . . . .	84
5.2.3	Reconfigurable MPC . . . . .	86
<b>5.3</b>	<b>Simulation Results</b> . . . . .	<b>95</b>
5.3.1	Simulation of the satellite motion . . . . .	95
5.3.2	Configuration of the FTMP SAC . . . . .	96
5.3.3	Monte Carlo simulation results . . . . .	97
<b>5.4</b>	<b>Summary</b> . . . . .	<b>101</b>
<b>6</b>	<b>CONCLUSION</b> . . . . .	<b>103</b>
	<b>BIBLIOGRAPHY</b> . . . . .	<b>107</b>
	<b>APPENDIX A – SATELLITE ATTITUDE DYNAMICS</b> . . . . .	<b>117</b>
<b>A.1</b>	<b>Preliminary definitions</b> . . . . .	<b>117</b>
<b>A.2</b>	<b>System Modeling</b> . . . . .	<b>120</b>
A.2.1	Satellite attitude dynamics . . . . .	121
A.2.2	Measurement models . . . . .	124
<b>A.3</b>	<b>Linearized state-space model</b> . . . . .	<b>125</b>
<b>A.4</b>	<b>Discretized state-space model</b> . . . . .	<b>128</b>

# List of Figures

FIGURE 1.1 – Block diagram of a typical active FTC system. . . . .	21
FIGURE 2.1 – Effects of the <i>actuator faults</i> ( $s = 1, 2, 3, 4$ ) on the system output measurements. . . . .	36
FIGURE 2.2 – Effects of the <i>sensor faults</i> ( $s = 5, 6, 7, 8$ ) on the system output measurements. . . . .	37
FIGURE 2.3 – Some <i>gamma</i> PDFs with shape parameter $\alpha = 2$ . . . . .	38
FIGURE 2.4 – A truncated exponential PMF for characterizing the prior knowledge about the fault instant. . . . .	39
FIGURE 4.1 – Physical model of the servomechanism. . . . .	72
FIGURE 4.2 – The state estimation index – Case 1. . . . .	75
FIGURE 4.3 – Realizations of the innovation sequence of the fault-free KF for different fault modes. . . . .	76
FIGURE 4.4 – The state estimation index – Case 2. . . . .	77
FIGURE 4.5 – The state estimation index – Case 3. . . . .	79
FIGURE 5.1 – The overall fault-tolerant control scheme. . . . .	84
FIGURE 5.2 – The fault-tolerant attitude determination method. . . . .	86
FIGURE 5.3 – Simulation results for scenario A and $M_1 = 10$ . . . . .	99
FIGURE 5.4 – Simulation results for scenario B and $M_1 = 10$ . . . . .	100
FIGURE 5.5 – Simulation results for scenario C and $M_1 = 10$ . . . . .	101

---

FIGURE 5.6 – State estimation errors obtained with the MPC-KF scheme under scenarios A, B, and C. . . . .	101
FIGURE A.1 – Cartesian coordinate systems. . . . .	118
FIGURE A.2 – A cubic rigid-body satellite and its sensors and actuators. . . . .	120

# List of Tables

TABLE 2.1 – Examples of fault mode realizations. . . . .	35
TABLE 4.1 – Physical parameters of the servomechanism. . . . .	71
TABLE 4.2 – The fault modes for the illustrative example. . . . .	73
TABLE 4.3 – The prior statistics of the fault magnitudes in SI units. . . . .	74
TABLE 4.4 – The fault parameter estimation errors – Case 1. . . . .	76
TABLE 4.5 – The fault parameter estimation errors – Case 2. . . . .	78
TABLE 4.6 – The fault parameter estimation errors – Case 3. . . . .	78
TABLE 5.1 – The illustrative fault modes. . . . .	83
TABLE 5.2 – The dimensions of the RMPC matrices. . . . .	92
TABLE 5.3 – Orbital parameters. . . . .	95
TABLE 5.4 – Covariance matrices of the measurement noises. . . . .	96
TABLE 5.5 – Parameters of the FTAD module in SI units. . . . .	97
TABLE 5.6 – Parameters of the RMPC in SI units. . . . .	97
TABLE 5.7 – The fault parameter estimation errors. . . . .	102

# List of Abbreviations

ACS	Attitude Control System
AD	Attitude Determination
ADS	Attitude Determination System
CCS	Cartesian Coordinate System
CM	Center of Mass
DC	Direct Current
FTAD	Fault-Tolerant Attitude Determination
FTC	Fault-Tolerant Control
FTMPC	Fault-Tolerant Model Predictive Control/Controller
FTMPSAC	Fault-Tolerant Model Predictive Satellite Attitude Control/Controller
FTSE	Fault-Tolerant State Estimation
FTTF	Fault-Tolerant Two-Stage Filter
GLR	Generalized Likelihood Ratio
GMT	Greenwich Mean Time
IMM	Interacting Multiple Model
KF	Kalman Filter
LMVU	Linear Minimum Variance Unbiased
LR	Likelihood Ratio
LS	Least-Squares

---

MAP	Maximum <i>a Posteriori</i>
MC	Monte Carlo
ML	Maximum Likelihood
MMSE	Minimum Mean Squared Error
MPC	Model Predictive Control/Controller
MPE	Minimum Probability of Error
MRP	Modified Rodrigues Parameters
MVU	Minimum Variance Unbiased
NP	Neyman-Pearson
PDF	Probability Density Function
PF	Particle Filter
PMF	Probability Mass Function
QP	Quadratic Programming
RMPC	Reconfigurable Model Predictive Controller
RV	Random Variable/Vector
SI	International System of Units
SIS	Sequential Importance Sampling
WMM2005	World Magnetic Model - epoch 2005



# List of Symbols

$a$	Scalar
$\mathbf{a}$	Vector
$a_1$	The first component of $\mathbf{a}$
$a_{1,k}$	The first component of $\mathbf{a}_k$
$\mathbf{A}$	Matrix
$\mathbf{A}'$	Transposed matrix
$\hat{a}$	Estimate of $a$
$\mathbf{I}_n$	Identity matrix of order $n$
$\mathbf{0}_{n \times m}$	Zero matrix of dimension $n \times m$
$\det(\cdot)$	Determinant of a matrix
$\text{diag}(\cdot)$	Diagonal or block-diagonal matrix
$\ln(\cdot)$	Natural logarithm function
$k$	Discrete time index
$\mathbf{a}_k/\mathbf{A}_k$	Vector/matrix at instant $k$
$b_f$	Fault magnitude
$k_f$	Fault instant
$\mathfrak{B}_f$	Domain of $b_f$
$\mathfrak{K}_f$	Domain of $k_f$

$s$	Fault mode index
$\mathbf{e}_j \in \mathbb{R}^n$	Unit vector of dimension $n$ and with the $j$ -th component equal to 1
$\delta_{k-k_f}$	Kronecker delta at instant $k_f$
$\mathbf{1}_{k-k_f}$	Unit step sequence with step time $k_f$
$\{\mathbf{x}_k\}$	Infinite sequence $\mathbf{x}_1, \mathbf{x}_2, \mathbf{x}_3, \dots$
$\mathbf{x}_{k_1:k_2}$	Finite sequence $\mathbf{x}_{k_1}, \mathbf{x}_{k_1+1}, \dots, \mathbf{x}_{k_2}$
$h$	Number of fault modes
$\mathcal{J}$	$\{1, 2, \dots, h\}$
$\vartheta^{(s)}(\cdot)$	Fault profile function corresponding to the $s$ -th mode
$k_a$	Alarm instant
$k_\delta$	Alarm delay, $k_\delta \triangleq k_a - k_f$
$\sim$	Distributed as
$m(\cdot)$	Probability mass function
$p(\cdot)$	Probability density function
$P(\cdot)$	Probability of an event
$P(\cdot \cdot)$	Conditional probability of an event
$\mathcal{N}_b(\mu, \sigma^2)$	$\frac{1}{\sqrt{2\pi\sigma}} \exp\left\{-\frac{(b-\mu)^2}{2\sigma^2}\right\}$ , $b \in \mathbb{R}$ (PDF of a Gaussian distributed RV $b$ with mean $\mu$ and variance $\sigma^2$ )
$\mathcal{G}_b(\alpha, \beta)$	$\frac{b^{\alpha-1}}{\Gamma(\alpha)\beta^\alpha} \exp\left\{-\frac{b}{\beta}\right\}$ , $b \in \mathbb{R}_+$ (PDF of a <i>gamma</i> distributed RV $b$ with shape parameter $\alpha$ and scale parameter $\beta$ )
$\Gamma(\alpha)$	$\int_0^\infty x^{\alpha-1} \exp(-x) dx$ ( <i>Gamma</i> function)
$\mathcal{U}_k([k_1, k_2])$	$\sum_{\bar{k}=k_1}^{k_2} \frac{1}{k_2-k_1+1} \delta_{k-\bar{k}}$ (PMF of a discrete RV $k$ with uniform distribution in the interval $[k_1, k_2]$ )
$\mathcal{K}_s(P(1), \dots, P(h))$	$\sum_{\bar{s}=1}^h P(\bar{s}) \delta_{s-\bar{s}}$ , $s \in \{1, 2, \dots, h\}$ (PMF of a discrete RV $s$ with a

---

	general distribution in $\{1, 2, \dots, h\}$ )
$\mathbf{r}_k$	Innovation vector at instant $k$
$\mathbf{V}_k$	Covariance of $\mathbf{r}_k$
$M_1$	Length of the data set for fault estimation
$\mathcal{D}_{k_a}$	$\mathbf{r}_{k_a:k_a+M_1-1}$ (Data set for fault estimation)
$H_j$	Statistical hypothesis
$T_i \stackrel{H_i}{>} T_j$	Decision rule that decides for $H_i$ if and only if $T_i > T_j, \forall j \neq i$
$T$	Sample period
$SO(3)$	Special Orthogonal Group
$ \cdot $	Magnitude of a scalar
$\ \cdot\ $	Norm of a vector
$k_c$	$k_a + M_1 - 1$ (Instant of correction)
$N_c$	Number of correct identification of the fault mode
$P_c$	Probability of correct identification of the fault mode
$\hat{\mathbf{x}}_{k k}$	Estimate of $\mathbf{x}_k$ based upon the measurements $\mathbf{y}_1, \mathbf{y}_2, \dots, \mathbf{y}_k$
$\check{\mathbf{x}}_{k k}$	Estimate provided by the fault-free KF
$S_b$	Body CCS
$S_i$	Inertial CCS
$S_r$	Reference CCS

# 1 Introduction

This thesis is concerned with the fault-tolerant state estimation of discrete-time linear Gaussian systems subject to additive faults. The present chapter is organized in the following manner. Section 1.1 gives some motivations for investigating the fault-tolerant state estimation problem. Section 1.2 presents a historical background on state estimation of linear systems subject general to unknown inputs. Section 1.3 outlines the following chapters. Finally, Section 1.4 pinpoints the main contributions of the thesis.

## 1.1 Motivation

The Feedback Control Theory for linear systems with sensors, actuators, and internal components that do not undergo any fault is well-established in the literature ([FRANKLIN \*et al.\*, 2010](#); [SHINNERS, 1992](#); [OGATA, 1970](#)). However, in practical systems, faults may arise due to various causes such as component ageing, wear, wrong design, and lack of maintenance ([ISERMANN, 2006](#)). The faults could degrade the system performance or even interrupt its operation. Primarily motivated by a growing demand on dependability requirements of critical engineering systems, the Fault-Tolerant Control (FTC) area has experienced intensive development since the early 1980s. Among the literature in the field, one can find the review papers: ([PATTON, 1997](#); [ZHANG; JIANG, 2003](#); [BLANKE \*et al.\*, 1997](#)); and the books: ([BLANKE \*et al.\*, 2003](#); [MAHMOUD \*et al.\*, 2003](#)).

A FTC system is defined as a setting that can maintain an acceptable degree of performance in the presence of faults ([MAHMOUD \*et al.\*, 2003](#)). In general, the FTC methods fall into two categories ([PATTON, 1997](#)): *passive* and *active*. The passive methods

rely on robust control techniques to design a fixed control law that makes the system almost insensitive to a limited class of anticipated faults. On the other hand, in the active methods, the control law is updated *online*. In order to accomplish adaptation, a *Fault Diagnosis* module is used to provide *online* information about the current fault, while a *Reconfiguration Mechanism* is used for properly modifying the control law. The active approach is particularly suitable for tackling unanticipated faults, which in fact are quite common in practice (ZHANG; JIANG, 2003).

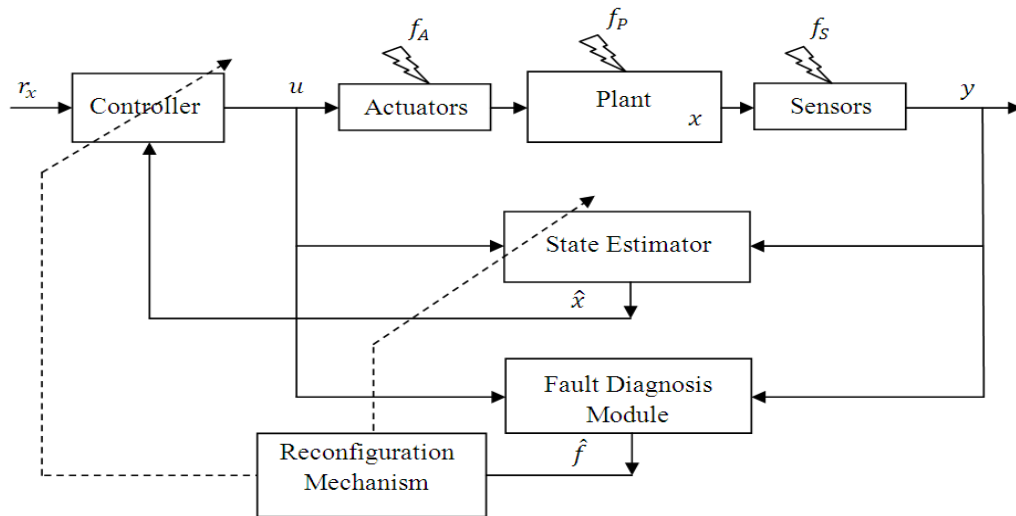


FIGURE 1.1 – Block diagram of a typical active FTC system.

Figure 1.1 shows a block diagram of a typical active FTC system that may undergo actuator faults,  $f_A$ , sensor faults,  $f_S$ , and plant component faults,  $f_P$ . Suppose that the illustrative system aims at making the states of the plant,  $x$ , to track the specified reference trajectory,  $r_x$ . To attain this goal, the following subsystems may be employed:

- a *state estimator*, which provides the estimate,  $\hat{x}$ , of the hidden state,  $x$ ;
- a *controller*, which implements a feedback control law from which the control input,  $u$ , is computed;
- a *fault diagnosis module*, which provides an estimate,  $\hat{f}$ , of a fault; and
- a *reconfiguration mechanism*, which, in the presence of a fault, will properly reconfigure both the state estimator and the controller in order to accommodate the fault

effects.

As illustrated in Figure 1.1, the fault diagnosis and the state estimation procedures are both carried out on the basis of data obtained from the control inputs,  $u$ , and from the output sensors,  $y$ . Henceforth, the main guideline of the present thesis is to unify the state estimation and the fault diagnosis procedures into a single task, which is herein called *Fault-Tolerant State Estimation*. One could realize that in spite of the need for reliable state estimators to design fault-tolerant control systems, rather little attention has been paid on the joint state and fault estimation problem.

Regarding the applicability of FTSE techniques, a satellite Attitude Determination System (ADS) is a notable example of a mission-critical engineering device. The ADS is essentially composed of sensors (e.g., solar sensors, star sensors, magnetometers, etc.) and an attitude estimation method implemented in the onboard computer of the satellite. Consider an hypothetical satellite equipped with a camera, which is required to be pointed towards the Earth throughout the mission lifetime. In this case, to satisfy the mission requirements, the ADS needs to provide the control system with sufficiently accurate attitude estimates, even in the presence of sensor faults.

## 1.2 Historical background

The Estimation Theory has its origin in the Least-Squares (LS) method, which was invented by the mathematician Johann Carl Friedrich Gauss around 1795 to estimate the orbit of Ceres (KAILATH, 1974). The LS method turns out to be suitable for estimating the constant parameters of a signal model from a set of observations by minimizing the residuals between the observations and their theoretically expected values. It is a deterministic method in the sense that it does not rely on any probabilistic model of either the data or the prior knowledge about the unknown parameters. Nevertheless, in his work, Gauss had already made conjectures on most of the essential characteristics of the modern stochastic approaches to signal estimation (SORENSEN, 1970).

About one and a half century after the Gauss' work on the LS method, the stochastic approach to the signal estimation problem began to be investigated mainly by [WIENER \(1949\)](#) and [KOLMOGOROV \(1941\)](#). In their theory, the signal and the observation noise are both assumed to be stationary stochastic processes with known spectral densities. The optimal Minimum Mean Squared Error (MMSE) solution to this problem is given by the *Wiener filter*, which is a linear time-invariant filter ([KAILATH \*et al.\*, 2000](#)). During the 1950s, some researchers attempted to extend the Wiener filter so as to make it appropriate for estimating nonstationary and multivariable signals. However, the resulting methods often required cumbersome calculations ([GELB, 1974](#)).

One decade later, the well-known Kalman filter (KF) ([KALMAN, 1960](#)) was proposed as a new approach to the signal estimation problem. The KF turned out to be a natural form of dealing with nonstationary and multivariable signals. The Kalman's work changed the conventional formulation of the signal estimation problem by describing the signal dynamics and observations with a linear state-space model driven by white Gaussian noises. Nowadays, the KF (as well as its suboptimal extensions) is widely used in numerous fields such as navigation, control, signal processing, finance, communication, etc. ([BARSHALOM; LI, 1993](#); [GELB, 1974](#); [JAZWINSKI, 1970](#); [KAILATH \*et al.\*, 2000](#); [SORENSEN, 1985](#); [ANDERSON; MOORE, 1979](#)).

In order to perform optimally in the MMSE sense, the KF requires the availability of an accurate linear Gaussian model for describing the dynamics of the system of interest. However, in practice, the system might be subject to environmental changes or even to faults in its sensors, actuators, or internal components. Such events may cause a significant mismatch between the real system behavior and its model. In many applications, this system-model mismatch can be represented by changing parameters. In such cases, the simpler form of tackling the estimation problem consists of augmenting the state-space model so as to include the changing parameters as extra state components. Hence, the faulty parameters and the original states can jointly be estimated with an augmented KF. This method is effective only when the number of changing parameters is small and, additionally, their changes can be well-represented by constant biases [see, e.g., ([BAR-](#)

SHALOM; LI, 1993), pp. 484–488]. The following subsections review the literature on the three most common approaches to tackle the state estimation problem for linear systems subject to unknown inputs such as additive faults.

### 1.2.1 Recursive linear minimum variance unbiased approach

Consider a linear system subject to additive faults that can be represented by unknown constant inputs into both the state and measurement equations. As argued before, the augmented KF can appropriately be used to estimate the states of such a system. In order to improve computational efficiency, FRIEDLAND (1969) proposed a two-stage filter that decomposes the augmented KF into a bias estimator and a bias-free state estimator. Since the Friedland’s estimator is equivalent to the augmented KF, it indeed corresponds to the optimal MMSE estimator. Considerable attention was paid to this method, which was rederived and extended in various aspects (IGNAGNI, 1981; IGNAGNI, 1990; HSIEH; CHEN, 1999; IGNAGNI, 2000; MENDEL, 1976; CAGLAYAN; LANCRAFT, 1983; KIM *et al.*, 2009).

In particular, the work by IGNAGNI (1981) eliminated the requirement of statistical uncorrelation between the state and the bias at the filter initialization, which had contrarily been taken into account by Friedland. Later, some investigators dealt with slowly varying inputs by describing them as discrete-time random-walk processes (IGNAGNI, 1990; HSIEH; CHEN, 1999; IGNAGNI, 2000). It is worth mentioning that the Friedland’s idea has also been extended to nonlinear systems, though in a suboptimal manner (MENDEL, 1976; CAGLAYAN; LANCRAFT, 1983; ZHOU *et al.*, 1993; KIM *et al.*, 2009).

In order to treat varying parameters without relying on a random-walk model, a Linear Minimum-Variance Unbiased (LMVU) estimator was proposed by KITANIDIS (1987). Although this work did not address the global optimality, the resulting estimator has shown a satisfactory performance in a practical environmental application. In this method, only the state equation was assumed to be affected by the unknown inputs. Later, DAROUACH *et al.* (2003) proposed an extension that included the case in which the output measurements are also subject to unknown inputs. None of the above methods deals with the



explicit estimation of the unknown inputs.

The above LMVU estimators have recently been extended to carry out the joint state and input estimation (GILLIJNS; MOOR, 2007a; GILLIJNS; MOOR, 2007b; HSIEH, 2009). Firstly, GILLIJNS; MOOR (2007a) considered the problem in which the unknown input affects only the state equation. Secondly, in a separate paper, the same authors treated the more general problem in which the input is also assumed to affect the measurement equation (GILLIJNS; MOOR, 2007b). In these works, a linear recursive two-stage estimator structure was established. In such structure, the input estimate is computed in stage 1 based on the observation of a single innovation vector. Then, the state estimate is computed in state 2 by an input-corrected form of the KF. Later, the above method was improved by eliminating a full-rank condition on the direct feedthrough matrix (HSIEH, 2009).

More recently, HMIDA *et al.* (2010) proposed an estimator specifically suitable for the joint state and fault estimation. In this method, the system is assumed to be subject to additive faults on both the state and measurement equations. Additionally, the system is allowed to undergo state disturbances. The estimator consists of a recursive filter that provides LMVU estimates of the states and faults, while decoupling the effects of the state disturbances from the filter output.

### 1.2.2 Decision-theoretic approach

A decision-theoretic approach to the problem of state estimation of systems subject to unknown additive inputs has also been considered by some investigators, specially during the 1970s and 1980s (MCAULAY; DENLINGER, 1973; WILLSKY; JONES, 1976; SANYAL; SHEN, 1974; BUENO *et al.*, 1976; CHANG; DUNN, 1979; CHAN *et al.*, 1979; WAHNON *et al.*, 1991; WILLSKY, 1986; NARASIMHAN; MAH, 1988). The essential element of the decision-theoretic methods consists of a KF implemented with a model that neglects the presence of the unknown inputs. In general, these methods involve two interconnected stages. The first stage carries out input detection and estimation by statistically processing the inno-

vation sequence of the KF. On the other hand, the second stage performs state estimation by correcting the KF outputs by using the input estimates provided by the first stage.

The method proposed by [WILLSKY; JONES \(1976\)](#) is one of the most popular of this category. It considers the class of linear Gaussian systems that are subject to an impulsive input whose magnitude and instant of occurrence are both unknown. To detect and estimate the input, this method processes the innovation sequence of the KF by using the Generalized Likelihood Ratio (GLR) test. Later, this method was extended in order to include more general input forms, such as stepwise, sinusoidal, etc. ([NARASIMHAN; MAH, 1988](#)). This method has been applied to the fault diagnosis of process control systems ([PRAKASH \*et al.\*, 2002](#); [PRAKASH \*et al.\*, 2005](#)). Particularly, [PRAKASH \*et al.\* \(2005\)](#) proposed a fault-tolerant model predictive controller (FTMPC) that integrates the GLR method with a conventional state-space formulation of the MPC.

To implement a decision-theoretic method, the input form (impulsive, stepwise, sinusoidal, etc.) needs to be previously hypothesized. Therefore, such methods indeed rely on prior knowledge concerning the dynamics of the unknown inputs. However, it is worth noting that none of the mentioned methods has considered the availability of any prior knowledge concerning the values of the input parameters (magnitude and instant of occurrence), which are supposed to be unknown deterministic constants.

### 1.2.3 Bayesian filtering approach

The Bayesian filtering approach to solve the problem of joint fault and state estimation has recently attracted attention of some investigators ([FREITAS, 2002](#); [VERMA, 2004](#); [ORCHARD, 2007](#); [RAPOPORT; OSHMAN, 2004b](#); [RAPOPORT; OSHMAN, 2004a](#); [ZHANG; LI, 1998](#); [SIGALOV; OSHMAN, 2010](#)). These works described the fault modes as discrete states and devised appropriate schemes for computing the posterior PDF of the hybrid continuous-discrete states in a recursive filtering manner. The explicit implementation of such filters turns out to be quite difficult, requiring some kind of approximation.

In the work by [FREITAS \(2002\)](#), a Rao-backwellized particle filter (PF) is employed to

tackle the joint state estimation and fault diagnosis of systems subject to multiplicative (rather than additive) faults. The discrete states are assumed to evolve as a finite-state Markov process. In this scheme, the PDF of the discrete states is approximated by using the Sequential Importance Sampling (SIS) method (DOUCET *et al.*, 2001), while the PDF of the continuous states are approximated by a Gaussian mixture via a bank of KFs. As verified by the author himself, this method does not perform well when the fault is considered to be a very rare event. Moreover, this method is not able to deal with faults of unknown magnitudes. Some other PFs that outperform the aforementioned Rao-backwellized PF when dealing with rare events have appeared in the literature (VERMA, 2004; RAPOPORT; OSHMAN, 2004b; ORCHARD, 2007). However, the fault modes need to be exactly hypothesized in all of these methods, since they cannot treat faults with unknown magnitudes.

Besides the PF technique, the Interacting Multiple Model (IMM) estimator has also been adopted by some author with the purpose of approximating the Bayesian filter for joint fault and state estimation (ZHANG; LI, 1998; RAPOPORT; OSHMAN, 2004a; SIGALOV; OSHMAN, 2010). In these methods, the dynamical behavior of the fault modes is also described by a Markov process. Again, none of these works addressed faults with unknown magnitudes.

### 1.3 Text organization

The remainder of the thesis is organized in the following form:

- Chapter 2 formally defines the *Fault-Tolerant State Estimation* (FTSE) problem as being the joint state and fault estimation of discrete-time linear Gaussian systems subject to additive faults. Particularly, the faults are considered to be realizations of a structured random sequence parameterized by three fault parameters: the fault magnitude, the fault instant, and the fault mode index. This is the main problem with which the thesis is concerned.

- Chapter 3 reviews the theoretical background necessary to understand the technical terms, notations, and some existing results on the Statistical Processing Theory that will be used throughout the thesis. It focuses on three topics: *(i)* parameter estimation, *(ii)* state estimation of linear Gaussian systems, and *(iii)* detection of signals corrupted by Gaussian noise.
- Chapter 4 proposes a two-stage recursive filtering approach to solve the FTSE problem defined in Chapter 2. By considering different ways of modeling the fault parameters, three estimators are derived. The first stage of the estimators carries out fault estimation by processing the innovation sequence of a Kalman filter(KF) implemented with the model of the system operating under fault-free conditions. The second stage provides estimates of the state by correcting the KF's output using the fault estimate computed in the first stage. The proposed estimators are called Fault-Tolerant Two-Stage (FTTS) filters. They can be classified as decision-theoretic methods.
- Chapter 5 illustrates one of the FTTS filters by applying it to a simulation-based Attitude Control System (ACS) of a rigid satellite. The control strategy adopted therein consists of a state-space formulation of the Model Predictive Control (MPC) that is properly modified in order to compensate for the fault effects. The resulting overall scheme is a Fault-Tolerant Model Predictive Control (FTMPC) method that can be used in other control applications.
- Chapter 6 presents the conclusions of the thesis and suggests some topics for future works.

## 1.4 Contributions of the thesis

The present thesis contributes to the field of state estimation of linear systems subject to additive faults. The main contributions are the following:

- A mathematical model for describing fault-prone dynamic systems. It is a discrete-time linear Gaussian state-space model subject to additive faults. These faults are assumed to be realizations of a structured random sequence parameterized by: a fault magnitude, a fault instant (the onset of the fault), and a fault mode index. Moreover, a Fault-Tolerant State Estimation (FTSE) problem is defined as the joint state and fault estimation of systems described by the proposed fault-prone system model. For details, see Section 2.1.
- A two-stage filtering approach to solve the FTSE problem, leading to three Fault-Tolerant Two-Stage (FTTS) filters. The FTTS filters account for the three alternative forms established to represent prior knowledge about the fault parameters. The FTTS filters belong to the class of Decision-Theoretic approaches to the joint state and input estimation [Subsection 1.2.2]. For details, see Chapter 4.
- A scheme for fault-tolerant satellite attitude control based on a Model Predictive Control (MPC) strategy. This scheme integrates an FTTS filter with a state-space formulation of the MPC that is properly modified in order to compensate for the fault effects. For details, see Chapter 5.

Some partial results of the thesis were hitherto published in the following papers: (SANTOS; YONEYAMA, 2009), (SANTOS; YONEYAMA, 2010), and (SANTOS; YONEYAMA, 2011).

## 2 Problem Statement

This chapter is concerned with a formal definition of the main problem treated in the present thesis. This is a state estimation problem for linear Gaussian systems subject to additive faults. Most of the literature on state estimation of this class of systems do not take into account any prior knowledge about the faults ([WILLSKY, 1986](#); [HMIDA \*et al.\*, 2010](#); [GILLIJNS; MOOR, 2007b](#)). On the contrary, this chapter considers that the additive fault is a structured random sequence parameterized by: a *fault magnitude*, a *fault instant*, and a *fault mode index*. These parameters are assumed to be realizations of random variables (RV) with known distributions. The chapter is organized in the following manner. Section 2.1 formally defines a Fault-Tolerant State Estimation (FTSE) problem as being the joint state and input estimation for a fault-prone system whose model is stated at the beginning of the section. Section 2.2 presents some comments and insights into the proposed fault-prone system model. Finally, Section 2.3 summarizes the present chapter.

### 2.1 Fault-tolerant state estimation problem

Let the dynamics of a fault-prone system be described by the following discrete-time linear Gaussian state-space model:

$$\mathbf{x}_{k+1} = \mathbf{A}_k \mathbf{x}_k + \mathbf{B}_k \mathbf{u}_k + \mathbf{\Gamma}_k \mathbf{w}_k + \mathbf{\Xi}_k \mathbf{f}_k \quad (2.1)$$

$$\mathbf{y}_k = \mathbf{C}_k \mathbf{x}_k + \mathbf{v}_k + \mathbf{\Theta}_k \mathbf{f}_k \quad (2.2)$$

where  $\mathbf{x}_k \in \mathbb{R}^{n_x}$  is the state vector;  $\mathbf{y}_k \in \mathbb{R}^{n_y}$  is the vector of observed outputs;  $\mathbf{u}_k \in \mathbb{R}^{n_u}$  is the vector of control inputs;  $\mathbf{f}_k \in \mathbb{R}^{n_f}$  is the fault vector. The fault sequence,  $\{\mathbf{f}_k\}$ , is assumed to be a realization of a particular structured random sequence, which will be defined below;  $\mathbf{A}_k, \mathbf{B}_k, \mathbf{\Gamma}_k, \mathbf{C}_k, \mathbf{\Xi}_k$ , and  $\mathbf{\Theta}_k$  are known deterministic matrices with appropriate dimensions;  $\{\mathbf{w}_k\}$  and  $\{\mathbf{v}_k\}$  are mutually independent, zero-mean, white, Gaussian sequences with known covariances,  $\mathbf{Q}_k$  and  $\mathbf{R}_k$ , respectively. These sequences are also assumed to be statistically independent of the initial state  $\mathbf{x}_0$ , which is modeled as a Gaussian RV with a known mean,  $\bar{\mathbf{x}}_0$ , and a known covariance,  $\mathbf{P}_0$ .

**Definition 2.1** Let  $\{\mathbf{f}_k\}$  be a structured sequence with the  $k$ -th term given by

$$\mathbf{f}_k = b_f \mathbf{e}_{j(s)} \vartheta^{(s)}(k - k_f), \quad (2.3)$$

where  $b_f \in \mathbb{R}$  is the *fault magnitude*,  $k_f \in \mathbb{Z}_+$  is the *fault instant*, and  $s \in \mathcal{J} \triangleq \{1, 2, \dots, h\}$  is the *fault mode index*, with  $h$  being the *number of fault modes*. The quantities  $b_f, k_f$ , and  $s$  are generally referred to as the fault parameters. The unit vector  $\mathbf{e}_{j(s)} \in \mathbb{R}^{n_f}$  represents the *fault location*. The map  $\vartheta^{(s)} : \mathbb{Z} \mapsto \mathbb{R}$  is a discrete-time function specifying the *fault form*. It satisfies the condition  $\vartheta^{(s)}(l) = 0, \forall l < 0$ .

The fault parameters appearing in the above definition have the following meanings. The fault magnitude,  $b_f$ , quantifies the severity of the fault in the sense that the larger it is, the graver will be its effects on the system behavior. The fault instant,  $k_f$ , corresponds to the onset time of the fault, i.e.,  $\mathbf{f}_k = \mathbf{0}, \forall k < k_f$ . Finally, the fault mode index,  $s$ , has the role of identifying both the fault location and the form of the fault sequence along the time (e.g., stepwise, ramp-type, sinusoidal, etc.). Subsection 2.2.1 will present some examples of fault modes as well as their effects on the output measurements of a particular system.

In order to account for prior knowledge about the fault parameters,  $s, k_f, b_f$ , they

are assumed to be realizations of RVs with known distributions. Before specifying such probability distributions, it is necessary to make some considerations. Suppose that the overall system contains a *fault detection* module that triggers an alarm signal at the occurrence of some fault. Hereafter, the time instant of such alarm occurrence will be called *alarm instant* and will be denoted by  $k_a$ . Now, the following assumption establishes a relationship between the true fault instant,  $k_f$ , and the alarm instant,  $k_a$ .

**Assumption 2.2** Define the alarm delay  $k_\delta \triangleq k_a - k_f$ . Assume that the alarm signal provided by the fault detection module is always correct, and that the corresponding alarm delay satisfies the condition  $k_\delta < M_2$ , where  $M_2 \in \mathbb{Z}_+$ ,  $M_2 < k_a$ .

**Assumption 2.3** Assume that the fault parameters ( $b_f$ ,  $k_f$ , and  $s$ ) are realizations of the mutually independent RVs characterized by the following PDFs/PMFs<sup>1</sup>:

- **Fault magnitude:** Three cases are considered in this work,

1. *Gaussian case:*

$$p(b_f|s) = \mathcal{N}_{b_f}(\mu_s, \sigma_s^2), \quad b_f \in \mathbb{R}, \quad (2.4)$$

where  $\mu_s$  and  $\sigma_s^2$  are, respectively, the mean and the variance of the  $s$ -mode conditioned PDF  $p(b_f|s)$ .

2. *Gamma case:*

$$p(b_f|s) = \mathcal{G}_{b_f}(\alpha_s, \beta_s), \quad b_f \in \mathbb{R}_+, \quad (2.5)$$

where  $\alpha_s$  and  $\beta_s$  are, respectively, the shape and the scale parameters of the  $s$ -mode conditioned PDF  $p(b_f|s)$ .

3. *Discrete case:*

$$m(b_f|s) = \mathcal{K}_{b_f}(P(b_L|s), P(b_M|s), P(b_H|s)), \quad b_f \in \{b_L, b_M, b_H\}, \quad (2.6)$$

---

<sup>1</sup>The List of Symbols given at the beginning of the thesis presents the explicit forms of the PDFs/PMFs mentioned here.



where the three possible values  $b_L$ ,  $b_M$ , and  $b_H$  represent, respectively, low, medium and high fault magnitude levels. The parameters  $P(b_L|s)$ ,  $P(b_M|s)$ , and  $P(b_H|s)$  are the  $s$ -mode conditioned probabilities of the fault magnitude being low, medium, and high, respectively.

- **Fault instant:**

$$m(k_f|s, k_a) = \mathcal{U}_{k_f}([k_a - M_2 + 1, k_a]), \quad (2.7)$$

where  $k_a$  is the alarm instant and the parameter  $M_2$  is defined in Assumption 2.2.

- **Fault mode index:**

$$m(s) = \mathcal{K}_s(P(1), P(2), \dots, P(h)), \quad s \in \mathcal{I}, \quad (2.8)$$

where  $h$  is the number of fault modes and  $P(i)$ ,  $i \in \mathcal{I}$ , is the prior probability of the  $i$ -th mode being in effect.

The parameters of the models (2.4)-(2.8) are all assumed to be known *a priori*.

Now that the model of the fault-prone system has been defined as a whole, the central thesis problem can be stated.

**Problem 2.4** Consider a fault-prone system described by (2.1)-(2.2), with the fault sequence established by Definition 2.1 and Assumption 2.3. The *Fault-Tolerant State Estimation* (FTSE) problem is to estimate, in a recursive filtering manner, both the system state sequence,  $\{\mathbf{x}_k\}$ , and the fault sequence,  $\{\mathbf{f}_k\}$ . For this end, the system model, the control input sequence,  $\{\mathbf{u}_k\}$ , and the output measurement sequence,  $\{\mathbf{y}_k\}$ , are assumed to be available.

It is worth pointing out that the afore-defined problem is similar to the joint state and input estimation problem for linear systems (FRIEDLAND, 1969; DAROUACH *et al.*, 2003; GILLIJNS; MOOR, 2007b; HSIEH, 2010). Nevertheless, none of the cited works attempted to propose a particular form of modeling the unknown inputs in order to make the resulting

method specially suitable to represent faults. On the contrary, the present work takes into consideration the existence of prior knowledge about both the fault dynamics (Definition 2.1) and the values of the fault parameters (Assumption 2.3).

## 2.2 Some comments upon the proposed fault-prone system model

This section is intended to provide the reader with some more insights into the proposed fault-prone system model. Subsection 2.2.1 presents some fault mode examples. Subsection 2.2.2 makes some comments on the prior statistical models defined in Assumption 2.3.

### 2.2.1 Examples of fault modes

It is worth noting that the structured fault sequence given in Definition 2.1 is a quite general description for additive faults in the sense that it can represent a variety of fault modes, with different time forms and acting on different locations. Table 2.1 presents eight examples of fault mode realizations. For illustration purposes, a simple simulation-based example is given in order to provide some insights into the effects caused by these faults on the output measurements of a particular system.

Consider the system described by (2.1)-(2.2), with  $\mathbf{A}_k = 0.7$ ,  $\mathbf{B}_k = 1$ ,  $\mathbf{C}_k = 1$ ,  $\mathbf{\Gamma}_k = 1$ ,  $\mathbf{\Xi}_k = [1 \ 0]$ ,  $\mathbf{\Theta}_k = [0 \ 1]$ ,  $\mathbf{Q}_k = 0.01$ , and  $\mathbf{R}_k = 0.01$ . Let the system be excited by the open-loop control law  $\mathbf{u}_k = \sin(0.04\pi k)$ . By inspection of either  $\mathbf{\Xi}_k$  or  $\mathbf{\Theta}_k$ , it can be concluded that the fault vector,  $\mathbf{f}_k$ , is two-dimensional. Moreover, its first component,  $f_{1,k}$ , represents actuator faults, whereas its second component,  $f_{2,k}$ , represents sensor faults.

Computational simulations were carried out by using the afore-defined model and by considering the fault mode realizations of Table 2.1. The resulting output measurements are depicted in Figures 2.1 and 2.2, each of which has four graphics. In its turn, each

TABLE 2.1 – Examples of fault mode realizations.

Description	$s$	$k_f$	$b_f$	$\mathbf{e}_{j(s)}$	$\vartheta^{(s)}(k - k_f)$
Impulsive actuator fault	1	50	3.0	$\mathbf{e}_1$	$\delta_{k-k_f}$
Stepwise actuator fault	2	50	1.0	$\mathbf{e}_1$	$1_{k-k_f}$
Ramp-type actuator fault	3	50	0.05	$\mathbf{e}_1$	$(k - k_f)1_{k-k_f}$
Sinusoidal actuator fault	4	50	1.0	$\mathbf{e}_1$	$\sin[0.2\pi(k - k_f)]1_{k-k_f}$
Impulsive sensor fault	5	50	3.0	$\mathbf{e}_2$	$\delta_{k-k_f}$
Stepwise sensor fault	6	50	1.0	$\mathbf{e}_2$	$1_{k-k_f}$
Ramp-type sensor fault	7	50	0.05	$\mathbf{e}_2$	$(k - k_f)1_{k-k_f}$
Sinusoidal sensor fault	8	50	1.0	$\mathbf{e}_2$	$\sin[0.2\pi(k - k_f)]1_{k-k_f}$

graphic contains three curves representing: 1) the fault sequence, 2) the output measurements of the faulty system, and 3) the output measurements of the fault-free system.

Figure 2.1 shows the effects of the actuator faults ( $s = 1, 2, 3, 4$ ) on the system output measurements, whereas Figure 2.2 presents the effects of the sensor faults ( $s = 5, 6, 7, 8$ ). As expected, in all the cases, at the outset of the faults, the output measurements start diverging from the values that they would assume in fault-free conditions. Such divergence depends on the severity of the fault. Owing to the dynamics of the system, the effects of the actuator faults are memorized in all the output samples after the occurrence. On the other hand, the sensor fault effects just appear as instantaneous shifts on the output. In the latter case, one could reason that the effects of the faults on the output measurements can be suppressed (or reduced) by simply subtracting an estimate of them from the samples.

Note that, as established by Problem 2.4, it is necessary to process faulty output measurements such as those shown in Figures 2.1 and 2.2 in order to carry out both input and state estimation.

## 2.2.2 The prior information on the fault parameters

Assumption 2.3 has defined that the fault parameters  $b_f$ ,  $k_f$ , and  $s$  are realizations of specific RVs with known probability distributions. The PDFs/PMFs given by equa-

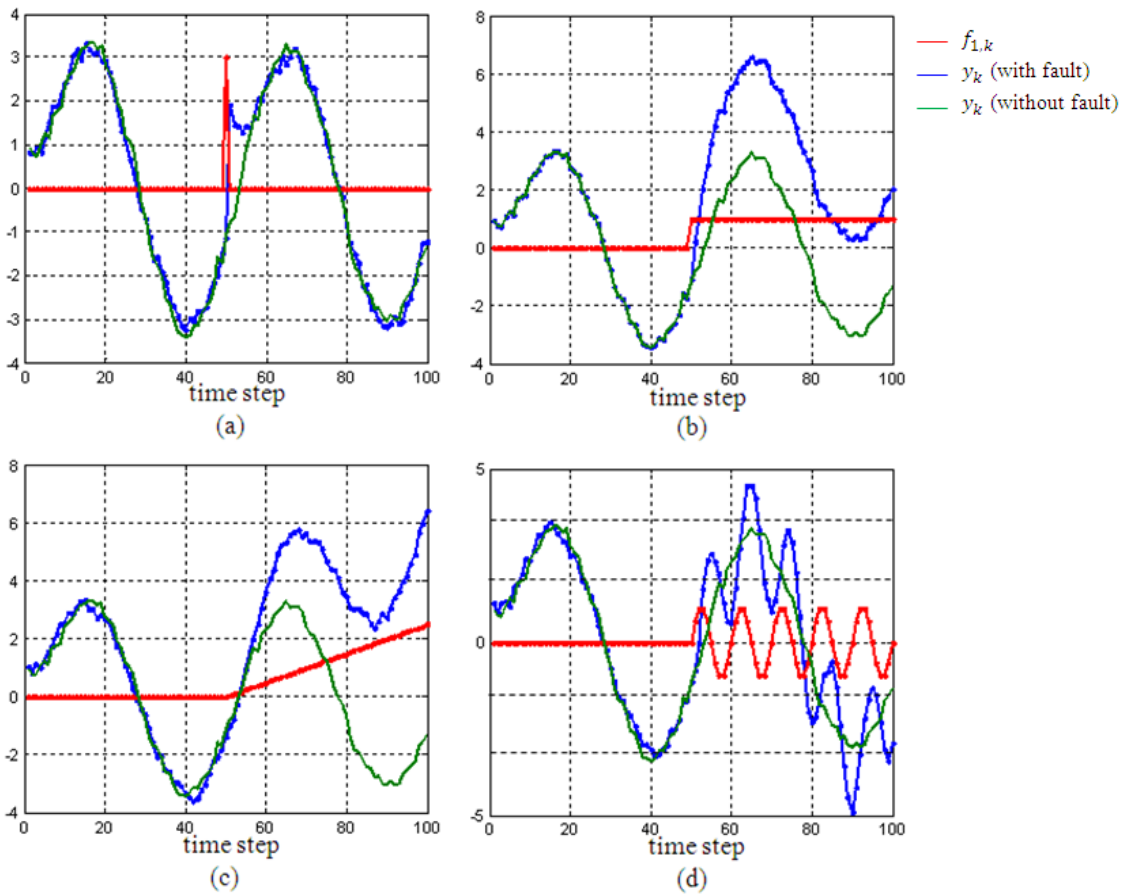


FIGURE 2.1 – Effects of the *actuator faults* ( $s = 1, 2, 3, 4$ ) on the system output measurements.

tions (2.4)-(2.8) could be viewed as compact representations of the prior knowledge about the fault parameters. In practice, such statistical models might be obtained by properly processing a large amount of historical experimental data. This is an identification problem (GOODWIN; PAYNE, 1977), with which the present thesis is not concerned. It is rather provided some comments on the meaning of the probabilistic models established in Assumption 2.3.

- *Fault magnitude:*

Three alternative probability distributions have been considered for describing the RV that underlies the fault magnitude parameter. The first one is the Gaussian distribution, which has been taken into account since it is a widely used model of random phenomena in physical systems. Moreover, as will be verified in Chapter 4, such distribution yields, in general, simpler mathematical derivations.

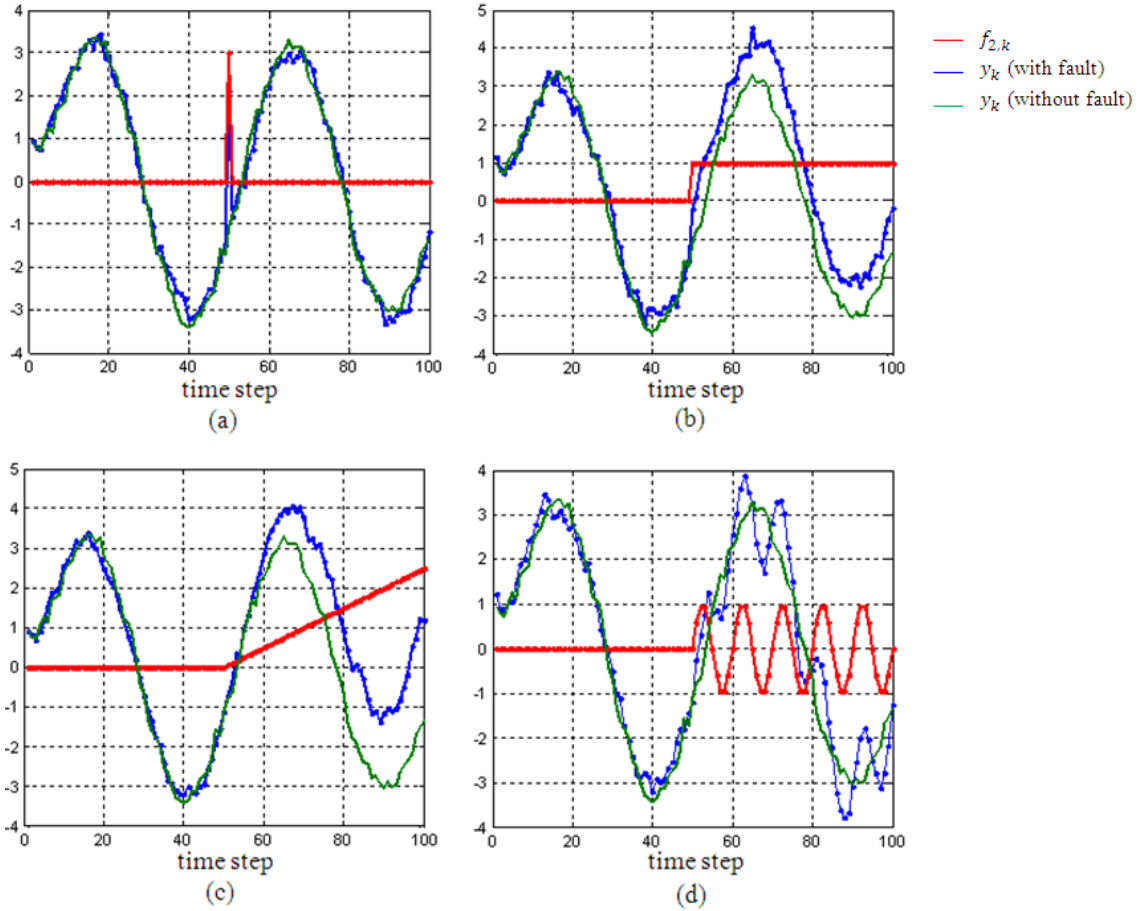


FIGURE 2.2 – Effects of the *sensor faults* ( $s = 5, 6, 7, 8$ ) on the system output measurements.

The second type of distribution is the *gamma*. It is argued that this is an interesting model owing to two factors. Figure 2.3 shows three *gamma* PDFs with shape parameter  $\alpha = 2$ . First, since this is a positive RV, one can use it to account for prior knowledge about the signal of the fault magnitude. Second, by using the *gamma* distribution, one means that faults with both very small and very large magnitudes rarely occur (see Figure 2.3). The very small faults can rather be dealt with the noise models,  $\{\mathbf{w}_k\}$  and  $\{\mathbf{v}_k\}$ . On the other hand, very large faults probably might cause a complete system breakdown, and in this case one is no more interested in state and fault estimation.

The third type of fault magnitude RV is a discrete one that may assume three alternative values: low, medium, and high. This model has been considered since, in most practical situations, only an approximation of the severity of the fault would be required. For such situations, it is argued that the proposed discrete model is

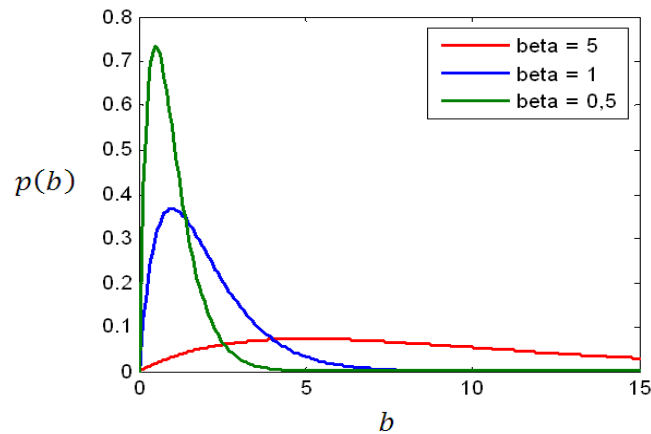


FIGURE 2.3 – Some *gamma* PDFs with shape parameter  $\alpha = 2$ .

a plausible one. For example, in the aeronautical industry, it is quite common to have green-yellow-red indications on the pilot's instrumentation. Moreover, as will be verified in Chapter 4, this is a very simple model, with which it is easier to derive optimal decision rules and fault parameter estimators.

- *Fault instant:*

Only one model has been adopted for the RV underlying the fault instant: a discrete uniform distribution. Its discrete-time characteristic is forthwith justified by the focus of the thesis on discrete-time systems. On the other hand, its uniformity corresponds to the assumption that there exists no additional information about this parameter besides that given by Assumption 2.2. Nevertheless, it is conjectured that more sophisticated discrete distributions (other than the uniform one) could have been adopted. An example could be a sampled and truncated exponential function that increases along the time interval  $[k_a - M_2 + 1, k_a]$ . See Figure 2.4. Note that by this model one means that the onset of the fault has a larger probability of being near the alarm event.

- *Fault mode index:*

The most general form of discrete distributions has been adopted for the RV underlying the fault mode index. Once again, it is argued that experiments might be conducted in order to obtain the number of fault modes,  $h$ , as well as the fault

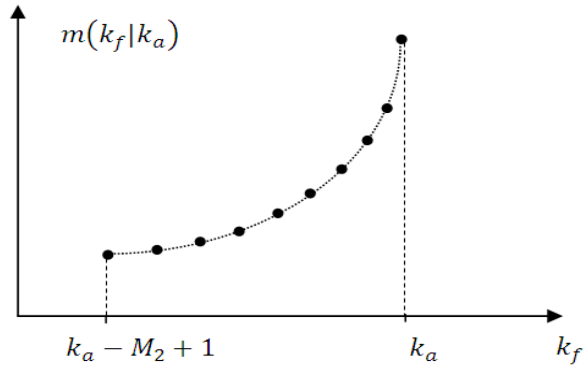


FIGURE 2.4 – A truncated exponential PMF for characterizing the prior knowledge about the fault instant.

mode probabilities,  $P(1), P(2), \dots, P(h)$ . However, without loss of generality, in most of the examples given throughout the thesis, such distribution are particularized to a uniform one, i.e.,  $P(1) = P(2) = \dots = P(h) = 1/h$ .

## 2.3 Summary

This chapter defined the central problem of the present thesis. It is a joint state and fault estimation problem for systems subject to additive faults. Its originality resides on the manner by which the fault was described, namely, as a realization of a structured random sequence parameterized by three RVs representing the prior knowledge about the fault magnitude, the fault instant, and the fault mode index.

# 3 Theoretical Background

This chapter is devoted to the review of some mathematical tools concerning the statistical signal processing theory, on the basis of which the main problem of the thesis will be approached. The material presented herein has mostly been collected from (KAY, 1998a), (KAY, 1998b), (SCHARF, 1991), and (ANDERSON; MOORE, 1979). The text is organized as follows. Section 3.1 reviews the Maximum a Posteriori (MAP) criterion for estimating an unknown random parameter from a noisy data set. Section 3.2 reviews the Kalman filter (KF) as well as some of its properties that will be invoked in the remaining chapters. Finally, Section 3.3 reviews the detection problem formulated as a multiple composite hypothesis testing.

## 3.1 Parameter estimation

The present section is concerned with the problem of estimating the parameters of a measurable signal,  $\mathbf{y}_k \in \mathbb{R}^{n_y}$ ,  $k = 1, 2, \dots, N$ , which can be described by the following algebraic model:

$$\mathbf{y}_k = \boldsymbol{\psi}_k(\boldsymbol{\lambda}) + \mathbf{n}_k, \quad k = 1, 2, \dots, N, \quad (3.1)$$

where  $\boldsymbol{\psi}_k : \mathbb{R}^{n_\lambda} \mapsto \mathbb{R}^{n_y}$  is a known map, and  $\mathbf{n}_k \in \mathbb{R}^{n_y}$  is a zero-mean Gaussian random vector (RV) with known covariance  $\mathbf{R}_k$ . Moreover, the sequence  $\{\mathbf{n}_k\}$  is assumed to be white. The vector  $\boldsymbol{\lambda} \in \mathbb{R}^{n_\lambda}$  consists of the parameter vector, which is an unknown realization of the RV characterized by the prior PDF  $p(\boldsymbol{\lambda})$ .

The problem at hand is to estimate the parameter vector  $\boldsymbol{\lambda}$  by using the prior informa-



tion  $p(\boldsymbol{\lambda})$  and the measurement information contained in the data set  $\mathcal{D} \triangleq \{\mathbf{y}_1, \mathbf{y}_2, \dots, \mathbf{y}_N\}$ . The framework so established is known as the Bayesian approach to parameter estimation (KAY, 1998b). In general, any point estimation technique based on the Bayesian approach stems from the posterior PDF of  $\boldsymbol{\lambda}$ , given the data set  $\mathcal{D}$ ,  $p(\boldsymbol{\lambda}|\mathcal{D})$ . By using the Bayes rule, such PDF can be written as

$$p(\boldsymbol{\lambda}|\mathcal{D}) = \frac{p(\mathcal{D}|\boldsymbol{\lambda})p(\boldsymbol{\lambda})}{p(\mathcal{D})}, \quad (3.2)$$

where  $p(\mathcal{D})$  is the marginal PDF of the data set, and  $p(\mathcal{D}|\boldsymbol{\lambda})$  is the likelihood function, which can be obtained immediately from model (3.1).

In order to determine a point estimate of  $\boldsymbol{\lambda}$  from the posterior PDF  $p(\boldsymbol{\lambda}|\mathcal{D})$ , a criterion needs to be chosen. The most usual criteria are the mean, the mode, and the median of  $p(\boldsymbol{\lambda}|\mathcal{D})$  (KAY, 1998b; SCHARF, 1991). In this work, the mode criterion is adopted. The resulting estimate is known as the *Maximum a Posteriori* (MAP) estimate and, in general, is given by

$$\hat{\boldsymbol{\lambda}}_{MAP} = \arg \left\{ \max_{\boldsymbol{\lambda}} p(\boldsymbol{\lambda}|\mathcal{D}) \right\}. \quad (3.3)$$

In spite of its conceptual simplicity, the above MAP estimator can rarely be characterized in closed form and, therefore, some numerical approximation is usually required. Additionally, difficulties can often be found when trying to derive analytical expressions for the mean and the covariance of such an estimator. In this case, in order to evaluate its performance, a common practice is to rely on Monte Carlo simulations (KAY, 1998b).

## 3.2 State estimation

Consider the system described by the following linear Gaussian model:

$$\mathbf{x}_{k+1} = \mathbf{A}_k \mathbf{x}_k + \mathbf{B}_k \mathbf{u}_k + \mathbf{\Gamma}_k \mathbf{w}_k + \mathbf{\Xi}_k \mathbf{f}_k, \quad (3.4)$$

$$\mathbf{y}_k = \mathbf{C}_k \mathbf{x}_k + \mathbf{v}_k + \mathbf{\Theta}_k \mathbf{f}_k, \quad (3.5)$$

where  $\mathbf{x}_k \in \mathbb{R}^{n_x}$  is the state vector,  $\mathbf{y}_k \in \mathbb{R}^{n_y}$  is the vector of observed outputs,  $\mathbf{u}_k \in \mathbb{R}^{n_u}$  is the vector of control inputs,  $\mathbf{f}_k \in \mathbb{R}^{n_f}$  is the fault vector, which is, by the time being, assumed to be exactly known. The quantities  $\mathbf{A}_k, \mathbf{B}_k, \mathbf{\Gamma}_k, \mathbf{C}_k, \mathbf{\Xi}_k$ , and  $\mathbf{\Theta}_k$  are known deterministic matrices with appropriate dimensions. The signals  $\{\mathbf{w}_k\}$  and  $\{\mathbf{v}_k\}$  are mutually independent, zero-mean, white, Gaussian sequences with known covariances  $\mathbf{Q}_k$  and  $\mathbf{R}_k$ , respectively. These sequences are also assumed to be statistically independent of the initial state  $\mathbf{x}_0$ , which is assumed to be a Gaussian RV with known mean,  $\bar{\mathbf{x}}_0$ , and covariance,  $\mathbf{P}_0$ .

Considering the Minimum Mean Squared Error (MMSE) criterion, it is well-known that the optimal estimate of  $\mathbf{x}_{k+1}$  based on the measurement sequence  $\mathbf{y}_{1:k+1}$  is recursively given by the Kalman Filter (KF) (KALMAN, 1960). The proof of this fundamental result can be found in several books, e.g., (ANDERSON; MOORE, 1979), (KAY, 1998b), (JAZWINSKI, 1970), (BAR-SHALOM; LI, 1993), and (GELB, 1974). The following algorithm summarizes the KF equations.

**Algorithm 3.1** Let  $\hat{\mathbf{x}}_{k+1|k+1}$  denote the optimal MMSE estimate of  $\mathbf{x}_{k+1}$  based on  $\mathbf{y}_{1:k+1}$ . The  $k$ -th iteration of the Kalman filter is given by

1. Prediction phase:

$$\hat{\mathbf{x}}_{k+1|k} = \mathbf{A}_k \hat{\mathbf{x}}_{k|k} + \mathbf{B}_k \mathbf{u}_k + \mathbf{\Xi}_k \mathbf{f}_k \quad (3.6)$$

$$\mathbf{P}_{k+1|k} = \mathbf{A}_k \mathbf{P}_{k|k} \mathbf{A}'_k + \mathbf{\Gamma}_k \mathbf{Q}_k \mathbf{\Gamma}'_k \quad (3.7)$$

2. Updating phase:

$$\mathbf{K}_{k+1} = \mathbf{P}_{k+1|k} \mathbf{C}'_{k+1} (\mathbf{C}_{k+1} \mathbf{P}_{k+1|k} \mathbf{C}'_{k+1} + \mathbf{R}_{k+1})^{-1} \quad (3.8)$$

$$\hat{\mathbf{x}}_{k+1|k+1} = \hat{\mathbf{x}}_{k+1|k} + \mathbf{K}_{k+1} (\mathbf{y}_{k+1} - \mathbf{C}_{k+1}\hat{\mathbf{x}}_{k+1|k} - \mathbf{\Theta}_{k+1}\mathbf{f}_{k+1}) \quad (3.9)$$

$$\mathbf{P}_{k+1|k+1} = (\mathbf{I}_{n_x} - \mathbf{K}_{k+1}\mathbf{C}_{k+1}) \mathbf{P}_{k+1|k} \quad (3.10)$$

with initial conditions given by  $\hat{\mathbf{x}}_{0|0} = \bar{\mathbf{x}}_0$  and  $\mathbf{P}_{0|0} = \mathbf{P}_0$ .

In the above recursive algorithm, the *updated state estimate*, which is denoted by  $\hat{\mathbf{x}}_{k+1|k+1}$ , is computed in two phases. In the prediction phase, the estimate obtained in the previous iteration,  $\hat{\mathbf{x}}_{k|k}$ , is predicted one time-step ahead by propagating it using the state equation (3.4), giving rise to the *predicted state estimate*, which is denoted by  $\hat{\mathbf{x}}_{k+1|k}$ . The matrix  $\mathbf{P}_{k+1|k}$  is the covariance of the state estimation error corresponding to  $\hat{\mathbf{x}}_{k+1|k}$ . In the updating phase,  $\hat{\mathbf{x}}_{k+1|k}$  is updated on the basis of the measurement information,  $\mathbf{y}_{k+1}$ , thus yielding the estimate  $\hat{\mathbf{x}}_{k+1|k+1}$  and the covariance of the corresponding estimation error,  $\mathbf{P}_{k+1|k+1}$ . The matrix  $\mathbf{K}_{k+1}$  is the Kalman gain.

In the next two chapters, the KF implemented with the model of the system operating under fault-free conditions will often be invoked. Hereafter, this KF will be called *fault-free KF*. A formal definition is presented in the sequel.

**Definition 3.2** The *fault-free KF* is given by Algorithm 3.1, but assuming that  $\mathbf{f}_k = \mathbf{0}, \forall k \in \mathbb{Z}_+$ . Its predicted and updated estimates are denoted by  $\check{\mathbf{x}}_{k+1|k}$  and  $\check{\mathbf{x}}_{k+1|k+1}$ , respectively.

In the presence of a fault, by simply inspecting equations (3.6) and (3.9), one can see that the state estimate,  $\hat{\mathbf{x}}_{k+1|k+1}$ , provided by Algorithm 3.1 differs from that provided by the fault-free KF,  $\check{\mathbf{x}}_{k+1|k+1}$ . As given by the following lemma, such difference is a known linear function of the fault sequence,  $\{\mathbf{f}_k\}$ . In Chapter 4, this property will be considered in the proposal of a fault compensation mechanism.

**Lemma 3.3** Let the system dynamics be described by equations (3.4)-(3.5) and suppose that the fault sequence  $\{\mathbf{f}_k\}$  is known. In this context, the estimate  $\hat{\mathbf{x}}_{k+1|k+1}$  provided by

Algorithm 3.1 and the estimate  $\check{\mathbf{x}}_{k+1|k+1}$  provided by the fault-free KF are related to each other by

$$\hat{\mathbf{x}}_{k+1|k+1} = \check{\mathbf{x}}_{k+1|k+1} + \mathbf{h}_{k+1}, \quad (3.11)$$

with  $\mathbf{h}_{k+1}$  given recursively by

$$\mathbf{h}_{k+1} = (\mathbf{I}_{n_x} - \mathbf{K}_{k+1}\mathbf{C}_{k+1})\mathbf{A}_k\mathbf{h}_k + \boldsymbol{\rho}_{k+1}, \quad (3.12)$$

where  $\boldsymbol{\rho}_{k+1} \triangleq (\mathbf{I}_{n_x} - \mathbf{K}_{k+1}\mathbf{C}_{k+1})\boldsymbol{\Xi}_k\mathbf{f}_k - \mathbf{K}_{k+1}\boldsymbol{\Theta}_{k+1}\mathbf{f}_{k+1}$ , and the initial condition is  $\mathbf{h}_0 = \mathbf{0}$ .

**Proof.** By substituting equation (3.6) into (3.9), the following recursive equation on the updated state estimates can be obtained as

$$\hat{\mathbf{x}}_{k+1|k+1} = \bar{\mathbf{K}}_{k+1}\mathbf{A}_k\hat{\mathbf{x}}_{k|k} + \bar{\mathbf{K}}_{k+1}\mathbf{B}_k\mathbf{u}_k + \mathbf{K}_{k+1}\mathbf{y}_{k+1} + \boldsymbol{\rho}_{k+1}, \quad (3.13)$$

where  $\bar{\mathbf{K}}_k \triangleq (\mathbf{I}_{n_x} - \mathbf{K}_k\mathbf{C}_k)$  and  $\boldsymbol{\rho}_{k+1} \triangleq \bar{\mathbf{K}}_{k+1}\boldsymbol{\Xi}_k\mathbf{f}_k - \mathbf{K}_{k+1}\boldsymbol{\Theta}_{k+1}\mathbf{f}_{k+1}$ . By considering  $\mathbf{f}_k = \mathbf{0}, \forall k \in \mathbb{Z}_+$ , the corresponding fault-free KF equation is immediately obtained:

$$\check{\mathbf{x}}_{k+1|k+1} = \bar{\mathbf{K}}_{k+1}\mathbf{A}_k\check{\mathbf{x}}_{k|k} + \bar{\mathbf{K}}_{k+1}\mathbf{B}_k\mathbf{u}_k + \mathbf{K}_{k+1}\mathbf{y}_{k+1}. \quad (3.14)$$

Note that both filters are initialized at instant  $k = 0$  with  $\bar{\mathbf{x}}_0$  and, therefore,  $\hat{\mathbf{x}}_{0|0} = \check{\mathbf{x}}_{0|0}$ . By using equations (3.13)-(3.14),  $\hat{\mathbf{x}}_{1|1}$  can immediately be written in terms of  $\check{\mathbf{x}}_{1|1}$  as

$$\hat{\mathbf{x}}_{1|1} = \check{\mathbf{x}}_{1|1} + \boldsymbol{\rho}_1. \quad (3.15)$$

Similarly, the estimate  $\hat{\mathbf{x}}_{2|2}$  can be written in terms of  $\check{\mathbf{x}}_{2|2}$  by using equations (3.13)-(3.15), resulting

$$\hat{\mathbf{x}}_{2|2} = \check{\mathbf{x}}_{2|2} + \boldsymbol{\rho}_2 + \bar{\mathbf{K}}_2\mathbf{A}_1\boldsymbol{\rho}_1 \quad (3.16)$$

Thus, by repeating the above procedure up to some arbitrary instant  $k > 1$ , the result of Lemma 3.3 is obtained.  $\square$

The sequence  $\{\mathbf{r}_k\}$ , with general term

$$\mathbf{r}_k \triangleq \mathbf{y}_k - \mathbf{C}_k \tilde{\mathbf{x}}_{k|k-1}, \quad (3.17)$$

consists of the *innovation sequence* of the fault-free KF. When the system is in fact operating under fault-free conditions, such innovation sequence is a zero-mean, white, Gaussian sequence. Moreover, the covariance of  $\mathbf{r}_k$ , which can be computed within the KF iterations, is given by

$$\mathbf{V}_k = \mathbf{C}_k \mathbf{P}_{k|k-1} \mathbf{C}_k' + \mathbf{R}_k. \quad (3.18)$$

The proofs of the aforementioned properties can be found in (ANDERSON; MOORE, 1979). In the presence of a fault, the innovation sequence of the fault-free KF remains white and its covariance is unchanged. However, its mean is not zero any more. This mean is referred to as the *signature* of the fault on the innovation of the fault-free KF. The following lemma provides an expression for computing such a fault signature assuming that the fault is known. In Chapter 4, this property will be of paramount importance to recast the problem of identifying the fault mode index into the convenient form of a statistical hypothesis testing.

**Lemma 3.4** Let the system dynamics be described by equations (3.4)-(3.5) and suppose that the fault sequence  $\{\mathbf{f}_k\}$  is known. In this context, the innovation sequence of the fault-free KF,  $\{\mathbf{r}_k\}$ , is such that,  $\forall k \in \mathbb{Z}_+$ ,

$$\mathbf{r}_k = \boldsymbol{\nu}_k + \mathbf{g}_k, \quad (3.19)$$

where  $\{\boldsymbol{\nu}_k\}$  is a zero-mean, white, Gaussian sequence. The covariance of  $\boldsymbol{\nu}_k$ , denoted by  $\mathbf{V}_k$ , is given by equation (3.18). The vector  $\mathbf{g}_k \in \mathbb{R}^{n_y}$  is the *signature*, at instant  $k$ , of the fault sequence  $\{\mathbf{f}_k\}$  on the innovation sequence  $\{\mathbf{r}_k\}$ . This vector is given by

$$\mathbf{g}_k = \mathbf{C}_k \tilde{\mathbf{g}}_k + \boldsymbol{\Theta}_k \mathbf{f}_k, \quad (3.20)$$

where  $\tilde{\mathbf{g}}_k$  can recursively be computed by

$$\tilde{\mathbf{g}}_k = \bar{\mathbf{A}}_{k-1} \tilde{\mathbf{g}}_{k-1} + \bar{\mathbf{B}}_{k-1} \mathbf{f}_{k-1}, \quad (3.21)$$

with initial condition  $\tilde{\mathbf{g}}_0 = \mathbf{0}$ ;  $\bar{\mathbf{A}}_k \triangleq \mathbf{A}_k \bar{\mathbf{K}}_k$ , and  $\bar{\mathbf{B}}_{k-1} \triangleq (\bar{\boldsymbol{\Xi}}_{k-1} - \mathbf{A}_{k-1} \mathbf{K}_{k-1} \boldsymbol{\Theta}_{k-1})$ .

**Proof.** By substituting the measurement equation (3.5) into equation (3.17), it follows that

$$\mathbf{r}_k = \mathbf{C}_k \check{\mathbf{e}}_{k|k-1} + \mathbf{v}_k + \boldsymbol{\Theta}_k \mathbf{f}_k, \quad (3.22)$$

where  $\check{\mathbf{e}}_{k|k-1} \triangleq \mathbf{x}_k - \check{\mathbf{x}}_{k|k-1}$  is the estimation error regarding the predicted estimate provided by the fault-free KF.

On the other hand, by substituting equation (3.9) into (3.6), a recursive expression is obtained for  $\check{\mathbf{x}}_{k|k-1}$ . By letting  $\mathbf{f}_k = \mathbf{0}, \forall k \in \mathbb{Z}_+$ , one gets the corresponding fault-free expression:

$$\check{\mathbf{x}}_{k+1|k} = \mathbf{A}_k \check{\mathbf{x}}_{k|k-1} + \mathbf{B}_k \mathbf{u}_k + \mathbf{A}_k \mathbf{K}_k \mathbf{r}_k. \quad (3.23)$$

Now, by using equations (3.4) and (3.23), the estimation error  $\check{\mathbf{e}}_{k+1|k}$  can be rewritten as

$$\check{\mathbf{e}}_{k+1|k} = \mathbf{A}_k \check{\mathbf{e}}_{k|k-1} + \boldsymbol{\Gamma}_k \mathbf{w}_k + \bar{\boldsymbol{\Xi}}_k \mathbf{f}_k - \mathbf{A}_k \mathbf{K}_k \mathbf{r}_k, \quad (3.24)$$

which can finally be rewritten by taking into account equation (3.22), yielding

$$\check{\mathbf{e}}_{k+1|k} = \bar{\mathbf{A}}_k \check{\mathbf{e}}_{k|k-1} + \bar{\mathbf{B}}_k \mathbf{f}_k + \boldsymbol{\eta}_k, \quad (3.25)$$

where  $\bar{\mathbf{A}}_k \triangleq \mathbf{A}_k (\mathbf{I}_{n_x} - \mathbf{K}_k \mathbf{C}_k)$ ,  $\bar{\mathbf{B}}_{k-1} \triangleq (\bar{\boldsymbol{\Xi}}_{k-1} - \mathbf{A}_{k-1} \mathbf{K}_{k-1} \boldsymbol{\Theta}_{k-1})$ , and  $\boldsymbol{\eta}_k \triangleq \boldsymbol{\Gamma}_k \mathbf{w}_k - \mathbf{A}_k \mathbf{K}_k \mathbf{v}_k$ . Now, introduce the notation  $\tilde{\mathbf{g}}_k \triangleq E \{ \check{\mathbf{e}}_{k|k-1} \}$ . Then, by taking the expectation of (3.25), one can obtain equation (3.21). Finally, define  $\mathbf{g}_k \triangleq E \{ \mathbf{r}_k \}$ . Thus, by taking the expectation of equation (3.22), the desired signature vector given by equation (3.20) can be obtained.  $\square$

### 3.3 Detection of signals corrupted by noise

This section reviews the central problem of Detection Theory: deciding from which of the  $h$  hypothesized sources a given noisy data set has been observed. To start, let a measurable signal,  $\mathbf{y}_k$ ,  $k = 1, 2, \dots, N$ , be described by one of the following  $h$  hypothetical algebraic models:

$$\mathbf{y}_k = \boldsymbol{\psi}_k^{(j)}(\boldsymbol{\lambda}) + \mathbf{n}_k, \quad k = 1, 2, \dots, N; \quad j = 1, 2, \dots, h, \quad (3.26)$$

where  $\boldsymbol{\psi}_k^{(j)} : \mathbb{R}^{n_\lambda} \mapsto \mathbb{R}^{n_y}$  is a known map, and  $\mathbf{n}_k \in \mathbb{R}^{n_y}$  is a zero-mean Gaussian RV with known covariance  $\mathbf{R}_k$ . Moreover, the sequence  $\{\mathbf{n}_k\}$  is assumed to be white. The vector  $\boldsymbol{\lambda} \in \mathbb{R}^{n_\lambda}$  denotes the parameter vector. Under the  $j$ -th signal model,  $\boldsymbol{\lambda}$  is assumed to be an unknown realization of the RV characterized by the prior PDF  $p(\boldsymbol{\lambda}|H_j)$ . In this context, the aforementioned problem can be stated as a multiple composite hypothesis testing that, on the basis of a given optimality criterion, picks out the best among the following hypotheses:

$$\begin{aligned} H_1 : \mathbf{y}_k &= \boldsymbol{\psi}_k^{(1)}(\boldsymbol{\lambda}) + \mathbf{n}_k, & k = 1, 2, \dots, N \\ H_2 : \mathbf{y}_k &= \boldsymbol{\psi}_k^{(2)}(\boldsymbol{\lambda}) + \mathbf{n}_k, & k = 1, 2, \dots, N \\ & \vdots \\ H_h : \mathbf{y}_k &= \boldsymbol{\psi}_k^{(h)}(\boldsymbol{\lambda}) + \mathbf{n}_k, & k = 1, 2, \dots, N \end{aligned} \quad (3.27)$$

When  $h = 2$ , the above problem reduces to a binary hypothesis testing. In this case, the most common criterion is that established by the Neyman-Pearson (NP) Lemma, which provides the decision rule with the maximum probability of detection for any specified probability of false alarm (SCHARF, 1991). Although the NP Lemma can be reformulated for the general case in which  $h > 2$ , this is rarely carried out in practice (KAY, 1998a). The present work adopts the Bayesian criterion, which is detailed in the sequel.

Let each hypothesis  $H_j$  be a random event with a known prior probability  $P(j)$ . Let  $C_{ij}$  denote the cost of deciding  $H_i$  when  $H_j$  is true. The Bayesian risk is defined to be the

expected cost given by

$$\mathcal{R} = \sum_{i=1}^h \sum_{j=1}^h C_{ij} P(H_i, H_j), \quad (3.28)$$

where  $P(H_i, H_j)$  denotes the joint probability of deciding  $H_i$  and  $H_j$  being the true hypothesis. By the definition of conditional probabilities [see (PAPOULIS; PILLAI, 2002), p. 28], it follows that  $P(H_i, H_j) = P(H_i|H_j)P(H_j)$ , with  $P(H_i|H_j)$  being the conditional probability of deciding  $H_i$ , given that  $H_j$  is true.

Let the data set be denoted by  $\mathcal{D} \triangleq \{\mathbf{y}_1, \mathbf{y}_2, \dots, \mathbf{y}_N\}$ . As shown in KAY (1998a), the decision rule that minimizes the Bayes risk decides for the hypothesis  $H_i$  that minimizes

$$C_i(\mathcal{D}) \triangleq \sum_{j=1}^h C_{ij} P(H_j|\mathcal{D}), \quad (3.29)$$

where  $P(H_j|\mathcal{D})$  is the posterior probability of  $H_j$  being the true hypothesis, given the measurement sequence  $\mathcal{D}$ .

A particular form of the minimum Bayes risk criterion will be adopted in this work. Namely, the minimum probability of error criterion, which is obtained from the general Bayesian criterion by choosing  $C_{ii} = 0$  and  $C_{ij} = 1$  (for  $i \neq j$ ). It is worth noting that, in this case, the Bayes risk is just the probability of error, i.e.,  $\mathcal{R} = P_e$ . The resulting decision rule is summarized in the following lemma.

**Lemma 3.5** The optimal rule (in the minimum probability of error sense) that solves the multiple hypothesis testing of equation (3.27) is given by

$$P(H_i|\mathcal{D}) \stackrel{H_i}{>} P(H_j|\mathcal{D}), \quad j = 1, \dots, h, j \neq i. \quad (3.30)$$

**Proof.** By replacing  $C_{ii} = 0$  and  $C_{ij} = 1$  in (3.29), it follows that

$$C_i(\mathcal{D}) = \sum_{j=1, j \neq i}^h P(H_j|\mathcal{D}),$$



which can be rewritten as

$$C_i(\mathcal{D}) = -P(H_i|\mathcal{D}) + 1. \quad (3.31)$$

Since the last term of equation (3.31) does not depend on  $i$ , in order to minimize  $C_i(\mathcal{D})$ , it suffices to maximize  $P(H_i|\mathcal{D})$ .  $\square$

For implementing the Maximum a Posteriori (MAP) decision rule given in Lemma 3.5, one needs to obtain an explicit expression for the posterior probabilities  $P(H_j|\mathcal{D})$ , for  $j = 1, \dots, h$ . By using the Bayes rule [see (PAPOULIS; PILLAI, 2002), p. 102], such probabilities can be expressed as

$$P(H_j|\mathcal{D}) = \frac{p(\mathcal{D}|H_j)P(H_j)}{p(\mathcal{D})}, \quad (3.32)$$

where  $P(H_j)$  is the prior probability of hypothesis  $H_j$  being the true one. The PDF  $p(\mathcal{D})$  is only a normalizing factor, which does not depend on  $H_j$ . The PDF  $p(\mathcal{D}|H_j)$  is the likelihood of  $\mathcal{D}$ , given that  $H_j$  is true. This likelihood can be obtained by the integration of the joint PDF  $p(\mathcal{D}, \boldsymbol{\lambda}|H_j)$  over the domain of the random parameter  $\boldsymbol{\lambda}$ :

$$p(\mathcal{D}|H_j) = \int p(\mathcal{D}, \boldsymbol{\lambda}|H_j)d\boldsymbol{\lambda}, \quad (3.33)$$

which, by using the chain rule, can be rewritten as

$$p(\mathcal{D}|H_j) = \int p(\mathcal{D}|\boldsymbol{\lambda}, H_j)p(\boldsymbol{\lambda}|H_j)d\boldsymbol{\lambda}, \quad (3.34)$$

where  $p(\boldsymbol{\lambda}|H_j)$  is the prior PDF of the unknown parameter. From the signal model of equation (3.26) corresponding to hypothesis  $H_j$ , it follows that

$$p(\mathcal{D}|\boldsymbol{\lambda}, H_j) = \prod_{k=1}^N p(\mathbf{y}_k|\boldsymbol{\lambda}, H_j), \quad (3.35)$$

with

$$p(\mathbf{y}_k|\boldsymbol{\lambda}, H_j) = \mathcal{N}_{\mathbf{y}_k} \left( \boldsymbol{\psi}_k^{(j)}(\boldsymbol{\lambda}), \mathbf{R}_k \right). \quad (3.36)$$

As pointed out in the literature on Detection Theory, there are two major difficulties associated with the use of the Bayesian approach to hypothesis testing (KAY, 1998a; SCHARF, 1991). The first one consists of the selection of a meaningful prior PDF,  $p(\boldsymbol{\lambda}|H_j)$ , for the unknown parameter vector corresponding to each hypothesis. This is a modeling problem that, in order to be solved, requires physical arguments as well as a large set of historical realizations of the parameter vector. The second difficulty is that the multidimensional integration given by equation (3.34) is usually not possible to be carried out in closed form. In this case, numerical approximations are required.

Although, in this work, the Bayesian method has been elected for tackling the fault estimation problem, it is worth briefly presenting a very popular approach used for circumventing the aforementioned difficulties: the Generalized Likelihood Ratio (GLR) approach. In order to derive an explicit formula for the likelihood  $p(\mathcal{D}|H_j)$ , rather than taking the expectation of  $p(\mathcal{D}|\boldsymbol{\lambda}, H_j)$  with respect to  $\boldsymbol{\lambda}$ , the GLR approach considers the maximum of  $p(\mathcal{D}|\boldsymbol{\lambda}, H_j)$  over the domain of  $\boldsymbol{\lambda}$ . Therefore, from equations (3.30) and (3.33), the GLR rule is given by

$$\frac{[\max_{\boldsymbol{\lambda}} p(\mathcal{D}|\boldsymbol{\lambda}, H_i)] P(H_i)}{p(\mathcal{D})} \underset{H_i}{>} \frac{[\max_{\boldsymbol{\lambda}} p(\mathcal{D}|\boldsymbol{\lambda}, H_j)] P(H_j)}{p(\mathcal{D})}, \quad (3.37)$$

which can be rewritten, by using the Bayes rule, as

$$\max_{\boldsymbol{\lambda}} p(H_i|\mathcal{D}, \boldsymbol{\lambda}) \underset{H_i}{>} \max_{\boldsymbol{\lambda}} p(H_j|\mathcal{D}, \boldsymbol{\lambda}). \quad (3.38)$$

Moreover, by considering  $P(H_1) = P(H_2) = \dots = P(H_h) = 1/h$ , and denoting the value of  $\boldsymbol{\lambda}$  that maximizes  $p(\mathcal{D}|\boldsymbol{\lambda}, H_j)$  by  $\hat{\boldsymbol{\lambda}}_j$ , equation (3.38) can be rewritten as

$$p(\mathcal{D}|\hat{\boldsymbol{\lambda}}_i, H_i) \underset{H_i}{>} p(\mathcal{D}|\hat{\boldsymbol{\lambda}}_j, H_j). \quad (3.39)$$

It is well-known that  $\hat{\boldsymbol{\lambda}}_j$  is just the Maximum Likelihood (ML) estimate of  $\boldsymbol{\lambda}$ , assuming that  $H_j$  is the true hypothesis (KAY, 1998a). In other words, in order to yield an explicit decision rule, the GLR method considers an estimate of the parameter vector in place of

its unknown true value.

After deriving an explicit form of a decision rule, it is desirable to obtain an analytical expression for the corresponding probability of error  $P_e$ . Such expression would be useful for analyzing the performance of the rule. However, in most applications, this is a very hard problem. It is worth mentioning a simple application in which  $P_e$  can be explicitly determined. It consists of the communication of multiple orthogonal symbols [see (KAY, 1998a), p. 119]. In this case, the hypothesized signals  $\boldsymbol{\psi}_k^{(j)}, j = 1, \dots, h$  are exactly known (i.e., they do not depend on unknown parameters) and, moreover, they are mutually orthogonal, i.e.,

$$\left(\boldsymbol{\psi}_k^{(i)}\right)' \boldsymbol{\psi}_k^{(j)} = 0, \quad j = 1, \dots, h; \quad j \neq i. \quad (3.40)$$

As will be discussed in the next chapter, such simplifying conditions cannot be extended to the fault estimation problem with which the present thesis is concerned. Therefore, Monte Carlo simulations will be adopted for evaluating the performance of the proposed decision rules.

# 4 Fault-Tolerant Two-Stage Filters

The present chapter proposes a two-stage filtering structure to tackle the Fault-Tolerant State Estimation (FTSE) problem defined in Chapter 2. This method is called Fault-Tolerant Two-Stage (FTTS) filtering. The three alternative statistical models established in Assumption 2.3 for representing the prior knowledge about the fault magnitude are considered separately. Therefore, three variants of Fault-Tolerant Two-Stage (FTTS) filters are derived. The function of Stage 1 is to estimate the fault by statistically processing the innovation sequence of a fault-free Kalman filter (KF). This stage relies on the Bayesian approach for the detection of signals in noise (see Section 3.3). The role of Stage 2 is to estimate the system states by correcting the fault-free KF on the basis of the fault estimate provided by Stage 1. The present chapter is organized in the following manner. Section 4.1 defines the structure of the FTTS filters. Section 4.2 details the first stage of the filters, while Section 4.3 elaborates on their second stage. Section 4.4 illustrates the methods by applying them to a simulated rotational DC servomechanism. Section 4.5 concerns the performance analysis of the filters. Finally, Section 4.6 summarizes the essential points of the chapter.

## 4.1 The structure of the filters

For the purpose of providing easily realizable solutions to Problem 2.4, consider the two-stage filtering structure defined below.

**Definition 4.1** The FTTS filters are considered to have a recursive structure composed

of the following two stages:

- *STAGE 1: Fault estimation.* Its function is to estimate the fault parameters ( $s$ ,  $b_f$ , and  $k_f$ ) by using a Bayesian statistical processing of the fault-free KF innovation sequence.
- *STAGE 2: State estimation.* Its function is to estimate the system states by correcting the fault-free KF by using the fault estimate provided by Stage 1.

It is worth noting that the fault estimation problem addressed in Stage 1 is similar to the one treated in [WILLSKY; JONES 1976](#) (see Section 1.2.2). However, here, prior probabilistic information on the fault parameters are considered, whereas in that work, the fault parameters are assumed to be unknown deterministic constants.

The following two sections detail both stages.

## 4.2 Stage 1: Fault estimation

To estimate a fault sequence such as those established in Definition 2.1, it suffices to estimate the fault parameters:  $s$  (fault mode index),  $k_f$  (fault instant), and  $b_f$  (fault magnitude). Here, the fault estimation is carried out on the basis of a finite set of innovation vectors provided by the fault-free KF, which has been defined in Section 3.2.

**Definition 4.2** The data set used for estimating the fault parameters is given by  $\mathcal{D}_{k_a} \triangleq \mathbf{r}_{k_a:k_a+M_1-1}$ , where  $M_1 \in \mathbb{Z}_+ - \{0\}$  is the design parameter specifying the length of the data set,  $k_a$  is the alarm instant, and  $\mathbf{r}_k$  is the innovation vector of the fault-free KF at instant  $k$ .

The fault estimation subproblem is divided into two parts. The first part aims at estimating the fault mode index,  $s$ , by a multiple composite hypothesis test. The second part is responsible for the estimation of the fault instant,  $k_f$ , and the fault magnitude,  $b_f$ , by solving a parameter estimation problem. This is formalized below.

**Problem 4.3** Consider the system described by equations (2.1)-(2.2), with the additive fault,  $\mathbf{f}_k = b_f \mathbf{e}_{j(s)} \vartheta^{(s)}(k - k_f)$ , given in Definition 2.1. Moreover, let the fault parameters  $s$ ,  $k_f$ , and  $b_f$  be realizations of the RVs defined in Assumption 2.3. In this context, given the data set  $\mathcal{D}_{k_a}$ ,

- a . the estimate of the fault mode index,  $\hat{s}$ , is obtained by solving the following multiple composite hypothesis testing:

$$H_i : \mathcal{D}_{k_a} = \boldsymbol{\nu}_{k_a:k_a+M_1-1} + b_f \mathbf{g}_{k_a:k_a+M_1-1}^{(i)}(k_f), i = 1, 2, \dots, h. \quad (4.1)$$

where  $\boldsymbol{\nu}_{k_a:k_a+M_1-1}$  is an uncorrelated sequence of Gaussian distributed RVs belonging to  $\mathbb{R}^{n_y}$ , with zero means and covariances,  $\mathbf{V}_{k_a:k_a+M_1-1}$ , computed by the fault-free KF, equation (3.18). The sequence  $b_f \mathbf{g}_{k_a:k_a+M_1-1}^{(i)}(k_f)$  is the signature of the  $i$ -th fault mode on the innovation sequence of the fault-free KF along the discrete time interval  $[k_a, k_a + M_1 - 1]$ .

- b . and both the estimate of the fault instant,  $\hat{k}_f$ , and the estimate of the fault magnitude,  $\hat{b}_f$ , are obtained by assuming that the true fault mode is  $\hat{s}$  and by using the Maximum a Posteriori (MAP) criterion.

To start dealing with Problem 4.3, the following lemma provides a general-form solution to the hypothesis test expressed in equation (4.1). This solution is based on the Minimum Probability of Error (MPE) criterion, which was reviewed in Section 3.3.

**Lemma 4.4** Let  $\hat{s}$  and  $j \neq \hat{s}$  belong to the set of fault mode indices  $\mathfrak{J} = \{1, 2, \dots, h\}$ . The optimal MPE solution,  $\hat{s}$ , to the multiple composite hypothesis test (4.1) is given by the following MAP decision rule:

$$P(\hat{s} | \mathcal{D}_{k_a}) \stackrel{H_{\hat{s}}}{>} P(j | \mathcal{D}_{k_a}), \forall j \neq \hat{s} \quad (4.2)$$

where,  $\forall i \in \mathfrak{J}$ ,  $P(i | \mathcal{D}_{k_a})$  is the posterior probability of  $i$  being the true fault mode index.

**Proof.** This is just the result given by Lemma 3.5, but using the notation of Problem 4.3.

□

By means of the Bayes' rule, the decision rule given by equation (4.2) can immediately be rewritten as

$$p(\mathcal{D}_{k_a}|\hat{s})P(\hat{s}) \stackrel{H_{\hat{s}}}{>} p(\mathcal{D}_{k_a}|j)P(j), \forall j \neq \hat{s}, \quad (4.3)$$

where,  $\forall i \in \mathfrak{I}$ ,  $P(i)$  is the prior probability of  $i$  being the true fault mode index and  $p(\mathcal{D}_{k_a}|i)$  is the likelihood of  $\mathcal{D}_{k_a}$  assuming that  $i$  is the true fault mode index. To obtain an equivalent but explicit form of the decision rule given by equation (4.3), it is necessary to specify the likelihood function  $p(\mathcal{D}_{k_a}|i)$ ,  $\forall i \in \mathfrak{I}$ .

The following two lemmas are useful to simplify the forthcoming presentations.

**Lemma 4.5** Let  $s$ ,  $k_f$ , and  $b_f$  be the true fault parameters. In this case, the data set  $\mathcal{D}_{k_a}$  is a sample of the PDF

$$p(\mathcal{D}_{k_a}|s, k_f, b_f) = a_1 \exp \left\{ -\frac{1}{2} b_f^2 \xi^{(s)}(k_f) + b_f \zeta^{(s)}(k_f) \right\}, \quad (4.4)$$

where

$$a_1 \triangleq \frac{1}{(2\pi)^{\frac{M_1 n_y}{2}}} \left( \prod_{k=k_a}^{k_a+M_1-1} \det(\mathbf{V}_k)^{-\frac{1}{2}} \right) \exp \left\{ -\frac{1}{2} \sum_{n=k_a}^{k_a+M_1-1} \mathbf{r}'_n \mathbf{V}_n^{-1} \mathbf{r}_n \right\},$$

$$\xi^{(s)}(k_f) \triangleq \sum_{k=k_a}^{k_a+M_1-1} \left( \mathbf{g}_k^{(s)}(k_f) \right)' \mathbf{V}_k^{-1} \mathbf{g}_k^{(s)}(k_f),$$

$$\zeta^{(s)}(k_f) \triangleq \sum_{k=k_a}^{k_a+M_1-1} \left( \mathbf{g}_k^{(s)}(k_f) \right)' \mathbf{V}_k^{-1} \mathbf{r}_k.$$

**Proof.** From Section 3.2, it is known that  $\mathbf{r}_k \sim \mathcal{N}_{r_k} \left( b_f \mathbf{g}_k^{(s)}(k_f), \mathbf{V}_k \right)$ , or equivalently,

$$p(\mathbf{r}_k|s, b_f, k_f) = \frac{1}{\sqrt{(2\pi)^{n_y} \det(\mathbf{V}_k)}} \exp \left\{ -\frac{1}{2} \left( \mathbf{r}_k - b_f \mathbf{g}_k^{(s)}(k_f) \right)' \mathbf{V}_k^{-1} \left( \mathbf{r}_k - b_f \mathbf{g}_k^{(s)}(k_f) \right) \right\}. \quad (4.5)$$

Furthermore, owing to the uncorrelatedness of the innovation sequence,  $\{\mathbf{r}_k\}$ , the joint

PDF of the RVs belonging to  $\mathcal{D}_{k_a}$  is given by the following product:

$$p(\mathcal{D}_{k_a}|s, k_f, b_f) = \prod_{k=k_a}^{k_a+M_1-1} p(\mathbf{r}_k|s, k_f, b_f). \quad (4.6)$$

Therefore, equation (4.4) can be obtained by substituting equation (4.5) into (4.6) and manipulating the resulting expression accordingly.  $\square$

**Lemma 4.6** Let  $\mathfrak{B}_f$  and  $\mathfrak{K}_f$  denote the supports of  $b_f$  and  $k_f$ , respectively. The likelihood of the data set,  $\mathcal{D}_{k_a}$ , assuming that  $i$  is the true fault mode index, is given by the following two alternative expressions:

- If the fault magnitude RV is continuous (Gaussian or *gamma*),

$$p(\mathcal{D}_{k_a}|i) = \int_{\mathfrak{B}_f} \sum_{k_f \in \mathfrak{K}_f} p(\mathcal{D}_{k_a}|i, k_f, b_f) p(b_f|i) m(k_f|i, k_a) db_f \quad (4.7)$$

- If the fault magnitude RV is discrete,

$$p(\mathcal{D}_{k_a}|i) = \sum_{b_f \in \mathfrak{B}_f} \sum_{k_f \in \mathfrak{K}_f} p(\mathcal{D}_{k_a}|i, k_f, b_f) m(b_f|i) m(k_f|i, k_a) \quad (4.8)$$

where  $p(\mathcal{D}_{k_a}|i, k_f, b_f)$  is given by the previous lemma, and  $p(b_f|i)$ ,  $m(b_f|i)$ , and  $m(k_f|i, k_a)$  are the prior PDF/PMFs of the fault magnitude and fault instant (see Assumption 2.3).

**Proof.** Firstly, consider the continuous fault magnitude case. The likelihood of the data set is obtained by marginalizing  $p(\mathcal{D}_{k_a}, b_f, k_f|i)$  over  $b_f$  and  $k_f$ , i.e.,

$$p(\mathcal{D}_{k_a}|i) = \int_{\mathfrak{B}_f} \sum_{k_f \in \mathfrak{K}_f} p(\mathcal{D}_{k_a}, b_f, k_f|i) db_f. \quad (4.9)$$

By means of the chain rule, the summand in equation (4.9) can be rewritten as

$$p(\mathcal{D}_{k_a}, b_f, k_f|i) = p(\mathcal{D}_{k_a}|i, k_f, b_f) p(b_f, k_f|i).$$

By using the assumption of statistical independence between the RVs underlying the fault



magnitude and the fault instant (see Assumption 2.3), the above equation becomes

$$p(\mathcal{D}_{k_a}, b_f, k_f|i) = p(\mathcal{D}_{k_a}|i, b_f, k_f) p(b_f|i) m(k_f|i, k_a) \quad (4.10)$$

Therefore, by combining equations (4.10) and (4.9), equation (4.7) can be obtained.

Now, for the case of discrete fault magnitudes, corresponding to equation (4.8), replace  $p(b_f|i)$  by  $m(b_f|i)$  in equation (4.10) and, instead of the integration carried out in equation (4.9), take the summation over  $\mathfrak{B}_f$ .  $\square$

Note that the first part of Problem 4.3 can be solved independently of the second one. This is made possible by the marginalization of the joint PDF  $p(\mathcal{D}_{k_a}, b_f, k_f|i)$  over  $b_f$  and  $k_f$ , which was carried out in Lemma 4.6. This characteristic is not found in the GLR method, in which the fault instant and the fault magnitude need to be estimated for each fault mode hypothesis (WILLSKY; JONES, 1976) and, therefore, the two parts have to be solved in an intertwined form. In the following three subsections, the prior statistics of the fault parameters are explicitly taken into account. Each subsection looks upon one of the three alternative fault magnitude models defined in Assumption 2.3.

### 4.2.1 Case 1: Fault magnitude with Gaussian distribution

Let the fault parameters,  $s$ ,  $k_f$ , and  $b_f$  be drawn from the corresponding RVs defined in Assumption 2.3. Regarding to the fault magnitude,  $b_f$ , for which three alternative cases have been considered, let it be drawn from the *Gaussian* RV with the PDF given by equation (2.4). In this context, the present subsection provides an explicit solution to Problem 4.3. Particularly, Theorem 4.7 is concerned with the first part of the problem, while Theorem 4.8 refers to its second part.

**Theorem 4.7** Let  $i \in \mathfrak{I}$  denote an arbitrary fault mode index. If  $b_f$  is a sample of the PDF  $p(b_f|i) = \mathcal{N}_{b_f}(\mu_i, \sigma_i^2)$ , with support  $\mathfrak{B}_f = \mathbb{R}$ , and  $k_f$  is a sample of the PMF  $m(k_f|i, k_a) = \mathcal{U}_{k_f}([k_a, k_a - M_2 + 1])$ , with support  $\mathfrak{R}_f = [k_a, k_a - M_2 + 1]$ , then, by using

the MPE criterion, the solution to part *a* of Problem 4.3 is given by

$$T_{\hat{s}}(\mathcal{D}_{k_a}) \stackrel{H_{\hat{s}}}{>} T_j(\mathcal{D}_{k_a}), \forall j \neq \hat{s}, \quad (4.11)$$

where, for  $\forall i$ ,

$$T_i(\mathcal{D}_{k_a}) \triangleq \frac{P(i) \exp\{-\mu_i^2/2\sigma_i^2\}}{\sigma_i} \sum_{l \in \mathfrak{R}_f} \frac{1}{\sqrt{\sigma_i^{-2} + \xi^{(i)}(l)}} \exp\left\{\frac{(\mu_i \sigma_i^{-2} + \zeta^{(i)}(l))^2}{2(\sigma_i^{-2} + \xi^{(i)}(l))}\right\}, \quad (4.12)$$

with  $\zeta^{(i)}(l)$  and  $\xi^{(i)}(l)$  as defined in Lemma 4.5.

**Proof.** Note that, in the present case, the appropriate likelihood function is given by equation (4.7). For clarity, denote its summand by  $q(b_f, k_f)$ , which can be rewritten as  $q(b_f, k_f) = q_1 q_2(b_f, k_f)$ , with  $q_1 \triangleq a_1 \exp\left\{-\frac{\mu_i^2}{2\sigma_i^2}\right\} / (\sigma_i M_2 \sqrt{2\pi})$  and

$$q_2(b_f, k_f) \triangleq \sum_{l \in \mathfrak{R}_f} \delta_{k_f-l} \exp\left\{-\frac{1}{2} b_f^2 (\xi^{(i)}(k_f) + \sigma_i^{-2}) + b_f (\zeta^{(i)}(k_f) + \mu_i \sigma_i^{-2})\right\}.$$

Once  $q_1$  does not depend on  $b_f$  and  $k_f$ , equation (4.7) can be rearranged, yielding

$$p(\mathcal{D}_{k_a}|i) = q_1 \sum_{l \in \mathfrak{R}_f} \int_{\mathfrak{B}_f} \sum_{k_f \in \mathfrak{R}_f} \delta_{k_f-l} \exp\left\{-\frac{1}{2} b_f^2 \left(\xi^{(i)}(k_f) + \frac{1}{\sigma_i^2}\right) + b_f \left(\zeta^{(i)}(k_f) + \frac{\mu_i}{\sigma_i^2}\right)\right\} db_f.$$

By taking the sum over  $k_f$  and completing the square of the resulting exponent, one gets

$$p(\mathcal{D}_{k_a}|i) = q_1 \sum_{l \in \mathfrak{R}_f} \int_{\mathfrak{B}_f} \exp\left\{-\frac{1}{2} (\xi^{(i)}(l) + \sigma_i^{-2}) \left(b_f - \frac{\zeta^{(i)}(l) + \mu_i \sigma_i^{-2}}{\xi^{(i)}(l) + \sigma_i^{-2}}\right)^2\right\} db_f \dots$$

$$\times \exp\left\{\frac{(\zeta^{(i)}(l) + \mu_i \sigma_i^{-2})^2}{2(\xi^{(i)}(l) + \sigma_i^{-2})}\right\}.$$

Note that the integrand of the above expression is proportional to a Gaussian PDF. Since the integral of any PDF over its entire support is unitary, one can immediately compute

the integral over  $b_f$ , obtaining

$$p(\mathcal{D}_{k_a}|i) = q_1 \sum_{l \in \mathfrak{R}_f} \sqrt{\frac{2\pi}{\xi^{(i)}(l) + \sigma_i^{-2}}} \exp \left\{ \frac{(\zeta^{(i)}(l) + \mu_i \sigma_i^{-2})^2}{2(\xi^{(i)}(l) + \sigma_i^{-2})} \right\}. \quad (4.13)$$

Therefore, by substituting equation (4.13) into (4.3) and making some algebraic manipulations, the decision rule of equation (4.11) can be obtained.  $\square$

**Theorem 4.8** Let  $\hat{s}$  be the estimate of the fault mode index provided by Theorem 4.7. If  $b_f$  is a sample of the PDF  $p(b_f|\hat{s}) = \mathcal{N}_{b_f}(\mu_{\hat{s}}, \sigma_{\hat{s}}^2)$ , with support  $\mathfrak{B}_f = \mathbb{R}$ , and  $k_f$  is a sample of the PMF  $m(k_f|\hat{s}, k_a) = \mathcal{U}_{k_f}([k_a, k_a - M_2 + 1])$ , with support  $\mathfrak{R}_f = [k_a, k_a - M_2 + 1]$ , then the solution to part *b* of Problem 4.3 is given by

$$\hat{k}_f = \arg \left\{ \min_{k_f \in \mathfrak{R}_f} z(k_f) \right\}, \quad (4.14)$$

$$\hat{b}_f = \bar{b}(\hat{k}_f), \quad (4.15)$$

where

$$z(k_f) \triangleq -\frac{(\zeta^{(\hat{s})}(k_f) + \mu_{\hat{s}} \sigma_{\hat{s}}^{-2})^2}{\xi^{(\hat{s})}(k_f) + \sigma_{\hat{s}}^{-2}}, \quad (4.16)$$

$$\bar{b}(k_f) \triangleq \frac{\zeta^{(\hat{s})}(k_f) + \mu_{\hat{s}} \sigma_{\hat{s}}^{-2}}{\xi^{(\hat{s})}(k_f) + \sigma_{\hat{s}}^{-2}}, \quad (4.17)$$

with  $\zeta^{(\hat{s})}(k_f)$  and  $\xi^{(\hat{s})}(k_f)$  as defined in Lemma 4.5.

**Proof.** In general, by the MAP criterion, the optimal estimates of  $k_f$  and  $b_f$  are given by

$$\left\{ \hat{k}_f, \hat{b}_f \right\} \triangleq \arg \left\{ \max_{k_f \in \mathfrak{R}_f, b_f \in \mathfrak{B}_f} J(b_f, k_f) \right\}, \quad (4.18)$$

where  $J(b_f, k_f)$  is the joint posterior PDF of the RVs underlying  $k_f$  and  $b_f$ . It can be rewritten, by means of the Bayes' rule, as

$$J(b_f, k_f) = \frac{p(\mathcal{D}_{k_a} | \hat{s}, k_f, b_f) p(b_f | \hat{s}) m(k_f | \hat{s}, k_a)}{p(\mathcal{D}_{k_a} | \hat{s})}.$$

Note that the denominator of the right-hand side of the above expression does not depend on  $b_f$  and  $k_f$ , and, moreover,  $m(k_f | \hat{s}, k_a)$  is a non-informative PMF. Therefore, one can use the reduced cost function  $\bar{J}(b_f, k_f) = p(\mathcal{D}_{k_a} | \hat{s}, k_f, b_f) p(b_f | \hat{s})$ . From both Lemma 4.5 and the explicit form of  $p(b_f | \hat{s}) = \mathcal{N}_{b_f}(\mu_{\hat{s}}, \sigma_{\hat{s}}^2)$ ,  $\bar{J}$  can be rewritten as

$$\bar{J}(b_f, k_f) = \left[ \frac{a_1}{\sqrt{2\pi}} \exp \left\{ -\frac{\mu_{\hat{s}}^2}{2\sigma_{\hat{s}}^2} \right\} \right] \exp \left\{ -\frac{1}{2} b_f^2 (\xi^{(\hat{s})}(k_f) + \sigma_{\hat{s}}^{-2}) + b_f (\zeta^{(\hat{s})}(k_f) + \mu_{\hat{s}} \sigma_{\hat{s}}^{-2}) \right\}.$$

By eliminating the factor in brackets, which does not depend on  $b_f$  and  $k_f$ , and by applying the natural logarithmic function, the optimization given by (4.18) can be seen to be equivalent to

$$\left\{ \hat{k}_f, \hat{b}_f \right\} = \arg \left\{ \min_{k_f \in \mathfrak{K}_f, b_f \in \mathfrak{B}_f} \check{J}(b_f, k_f) \right\},$$

where  $\check{J}(b_f, k_f) = b_f^2 (\xi^{(\hat{s})}(k_f) + \sigma_{\hat{s}}^{-2}) - 2b_f (\zeta^{(\hat{s})}(k_f) + \mu_{\hat{s}} \sigma_{\hat{s}}^{-2})$ .

Finally, note that for each  $k_f \in \mathfrak{K}_f$ ,  $\check{J}$  is quadratic in  $b_f$  and  $\partial^2 \check{J} / \partial b_f^2 = 2 (\xi^{(\hat{s})}(k_f) + \sigma_{\hat{s}}^{-2}) > 0, \forall b_f \in \mathfrak{B}_f$ . Then, for each value of  $k_f$ , the minimum of  $\check{J}$  is attained at  $b_f = \bar{b}(k_f)$ , which is given by  $\partial \check{J} / \partial b_f(b_f, k_f)|_{b_f = \bar{b}(k_f)} = 0$ . Hence,  $\bar{b}(k_f)$  is given by equation (4.17). Now, by defining  $z(k_f) \triangleq \check{J}(\bar{b}(k_f), k_f)$ , one can see that the desired estimate of the fault instant,  $\hat{k}_f$ , is the value of  $k_f$  that minimizes  $z(k_f)$ . On the other hand, the estimate of  $b_f$  is obtained by substituting  $k_f$  by  $\hat{k}_f$  in  $\bar{b}(k_f)$ .  $\square$

On the basis of the above two theorems, the following algorithm summarizes Stage 1 of the FTTS filter that is suitable for Gaussian fault magnitudes.

**Algorithm 4.9** Stage 1 of the FTTS filter for Gaussian fault magnitudes:

1. Estimation of  $s$ :

- for  $\forall i \in \mathcal{I}$ , compute  $T_i(\mathcal{D}_{k_a})$  using equation (4.12);

- $\hat{s} = \arg \{ \max_{i \in \mathfrak{J}} T_i(\mathcal{D}_{k_a}) \}$ ;

2. Estimation of  $k_f$  and  $b_f$ :

- $\hat{k}_f = \arg \{ \min_{k_f \in \mathfrak{R}_f} z(k_f) \}$ , where  $z(\cdot)$  is given by equation (4.16);
- $\hat{b}_f = \bar{b}(\hat{k}_f)$ , where  $\bar{b}(\cdot)$  is given by equation (4.17).

## 4.2.2 Case 2: Fault magnitude with *gamma* distribution

Similar to the previous subsection, let the fault parameters  $s$ ,  $k_f$ , and  $b_f$  be drawn from the corresponding RVs defined in Assumption 2.3. But now, assume that the fault magnitude is drawn from the *gamma* RV with PDF given by equation (2.5). Particularly, assume that the shape parameter of this PDF is fixed at  $\alpha_s = 2$ . Therefore, the scale parameter  $\beta_s$  is the only degree of freedom available to model the prior knowledge about the fault magnitude<sup>1</sup>. In this context, the following two theorems provide a quasi-explicit solution to Problem 4.3.

**Theorem 4.10** Let  $i \in \mathfrak{J}$  denote an arbitrary fault mode index. If  $b_f$  is a sample of the PDF  $p(b_f|i) = \mathcal{G}_{b_f}(2, \beta_i)$ , with support  $\mathfrak{B}_f = \mathbb{R}_+$ , and  $k_f$  is a sample of the PMF  $m(k_f|s, k_a) = \mathcal{U}_{k_f}([k_a, k_a - M_2 + 1])$ , with support  $\mathfrak{R}_f = [k_a, k_a - M_2 + 1]$ , then, by using the MPE criterion, the solution to part *a* of Problem 4.3 is given by

$$T_{\hat{s}}(\mathcal{D}_{k_a}) \stackrel{H_{\hat{s}}}{>} T_j(\mathcal{D}_{k_a}), \forall j \neq \hat{s}, \quad (4.19)$$

where,  $\forall i$ ,

$$T_i(\mathcal{D}_{k_a}) \triangleq \frac{P(i)}{\beta_i^2} \sum_{l \in \mathfrak{R}_f} \exp \left\{ \frac{\left( \zeta^{(i)}(l) - \frac{1}{\beta_i} \right)^2}{2\xi^{(i)}(l)} \right\} (c_1 + c_2 + c_3), \quad (4.20)$$

<sup>1</sup>Note that the *gamma* PDF with  $\alpha = 2$  and an arbitrary  $\beta$  is equivalent to the Erlang-2 PDF with rate parameter  $\lambda = 1/2\beta$  [see (PAPOULIS; PILLAI, 2002), p.87].

with  $c_1 \triangleq I_i(l) \frac{\zeta^{(i)}(l) - \frac{1}{\beta_i}}{\xi^{(i)}(l)}$ ,  $c_2 \triangleq \frac{1}{\xi^{(i)}(l)} \exp \left\{ \frac{\left( \zeta^{(i)}(l) - \frac{1}{\beta_i} \right)^2}{2\xi^{(i)}(l)} \right\}$ ,  $c_3 \triangleq \frac{\zeta^{(i)}(l) - \frac{1}{\beta_i}}{2\xi^{(i)}(l)} \sqrt{\frac{2\pi}{\xi^{(i)}(l)}}$ ,

$$I_i(l) \triangleq \int_{-\frac{\zeta^{(i)}(l) - \frac{1}{\beta_i}}{\xi^{(i)}(l)}}^0 \exp \left\{ -\frac{1}{2} \zeta^{(i)}(l) b^2 \right\} db, \quad (4.21)$$

and both  $\zeta^{(i)}(l)$  and  $\xi^{(i)}(l)$  are as defined in Lemma 4.5.

**Proof.** Note that, in the present case, the appropriate likelihood function is again given by equation (4.7). For clarity, denote its summand by  $q(b_f, k_f)$ , which can be rewritten as  $q(b_f, k_f) = q_1 q_2(b_f, k_f)$ , with  $q_1 \triangleq a_1 / (\beta_i^2 M_2 \Gamma(2))$ , and

$$q_2(b_f, k_f) \triangleq b_f \sum_{l \in \mathfrak{R}_f} \delta_{k_f - l} \exp \left\{ -\frac{1}{2} b_f^2 \xi^{(i)}(k_f) + b_f \left( \zeta^{(i)}(k_f) - \frac{1}{\beta_i} \right) \right\}.$$

Once  $q_1$  does not depend on  $b_f$  and  $k_f$ , equation (4.7) can be rearranged, yielding

$$p(\mathcal{D}_{k_a} | i) = q_1 \sum_{l \in \mathfrak{R}_f} \int_{\mathfrak{B}_f} b_f \sum_{k_f \in \mathfrak{R}_f} \delta_{k_f - l} \exp \left\{ -\frac{1}{2} b_f^2 \xi^{(i)}(k_f) + b_f \left( \zeta^{(i)}(k_f) - \frac{1}{\beta_i} \right) \right\} db_f.$$

By taking the sum over  $k_f$  and completing the square of the resulting exponent, one gets

$$p(\mathcal{D}_{k_a} | i) = q_1 \sum_{l \in \mathfrak{R}_f} \int_0^\infty b_f \exp \left\{ -\frac{\xi^{(i)}(l)}{2} \left( b_f - \frac{\zeta^{(i)}(l) - \frac{1}{\beta_i}}{\xi^{(i)}(l)} \right)^2 \right\} db_f \exp \left\{ \frac{\left( \zeta^{(i)}(l) - \frac{1}{\beta_i} \right)^2}{2\xi^{(i)}(l)} \right\}.$$

By considering the change of variable given by  $\tilde{b} \triangleq b_f - (\zeta^{(i)}(l) - \beta_i^{-1}) / \xi^{(i)}(l)$ , and carrying out the integration over  $\mathfrak{B}_f$ , the above expression becomes

$$p(\mathcal{D}_{k_a} | i) = q_1 \sum_{l \in \mathfrak{R}_f} \exp \left\{ \frac{\left( \zeta^{(i)}(l) - \frac{1}{\beta_i} \right)^2}{2\xi^{(i)}(l)} \right\} (c_1 + c_2 + c_3), \quad (4.22)$$

where  $c_1$ ,  $c_2$ , and  $c_3$  are defined after equation (4.20). Finally, by substituting equation (4.22) into (4.3) and making some algebraic manipulations, the decision rule of equation (4.19) can be obtained.  $\square$

Since the integral  $I_i(l)$  defined in (4.21) does not have an exact analytical solution,

the decision rule given by the above theorem is rather a quasi-closed solution to part *a* of Problem 4.3. In this case, for the purpose of obtaining a corresponding closed solution, a numerical approximation is needed to compute  $I_i(l)$ . The following lemma suggests such an approximation.

**Lemma 4.11** The approximation of  $I_i(l)$  that is obtained by means of expanding its integrand into a Maclaurin series of degree  $n$  is given by the following finite alternating series:

$$I_i^n(l) = \sum_{q=0}^n \frac{(-1)^q \xi^{(i)}(l)^{-q-1} (\zeta^{(i)}(l) - \beta_i^{-1})^{2q+1}}{2^q (q!) (2q+1)}. \quad (4.23)$$

**Proof.** The Maclaurin series expansion of the integrand of  $I_i(l)$  in equation (4.21) corresponds to the converging series  $\exp\{\nu\} = \sum_{q=0}^{\infty} \nu^q / q!$ , where  $\nu \triangleq -\frac{1}{2} \xi^{(i)}(l) b^2$  (ATKINSON, 1989). Therefore, by neglecting the terms with the order greater than  $n$  and analytically integrating the resulting expression, one gets  $I_i^n(l)$ .  $\square$

Thus, by using  $I_i^n(l)$  in place of  $I_i(l)$  to compute the test statistics expressed by equation (4.20), the ensuing rule (4.19) turns out to be explicit.

**Theorem 4.12** Let  $\hat{s}$  be the estimate of the fault mode index provided by Theorem 4.10. If  $b_f$  is a sample of the PDF  $p(b_f | \hat{s}) = \mathcal{G}_{b_f}(2, \beta_{\hat{s}})$ , with support  $\mathfrak{B}_f = \mathbb{R}_+$ , and  $k_f$  is a sample of the PMF  $m(k_f | \hat{s}, k_a) = \mathcal{U}_{k_f}([k_a, k_a - M_2 + 1])$ , with support  $\mathfrak{K}_f = [k_a, k_a - M_2 + 1]$ , then the solution to part *b* of Problem 4.3 is given by

$$\hat{k}_f = \arg \left\{ \max_{k_f \in \mathfrak{K}_f} z(k_f) \right\}, \quad (4.24)$$

$$\hat{b}_f = \bar{b}(\hat{k}_f), \quad (4.25)$$

where

$$z(k_f) \triangleq \ln \bar{b}(k_f) - \frac{1}{2} \xi^{(\hat{s})}(k_f) \bar{b}^2(k_f) + \left( \zeta^{(\hat{s})}(k_f) - \frac{1}{\beta_{\hat{s}}} \right) \bar{b}(k_f), \quad (4.26)$$

$$\bar{b}(k_f) \triangleq \frac{\left(\zeta^{(\hat{s})}(k_f) - \frac{1}{\beta_{\hat{s}}}\right) + \sqrt{\left(\zeta^{(\hat{s})}(k_f) - \frac{1}{\beta_{\hat{s}}}\right)^2 + 4\xi^{(\hat{s})}(k_f)}}{2\xi^{(\hat{s})}(k_f)}, \quad (4.27)$$

with  $\zeta^{(\hat{s})}(k_f)$  and  $\xi^{(\hat{s})}(k_f)$  as defined in Lemma 4.5.

**Proof.** In general, by the MAP criterion, the optimal estimates of  $k_f$  and  $b_f$  are given by

$$\{\hat{k}_f, \hat{b}_f\} \triangleq \arg \left\{ \max_{k_f \in \mathfrak{K}_f, b_f \in \mathfrak{B}_f} J(b_f, k_f) \right\}, \quad (4.28)$$

where  $J(b_f, k_f)$  is the joint posterior PDF of the RVs underlying  $k_f$  and  $b_f$ . It can be rewritten, by means of the Bayes' rule, as

$$J(b_f, k_f) = \frac{p(\mathcal{D}_{k_a} | \hat{s}, k_f, b_f) p(b_f | \hat{s}) m(k_f | \hat{s}, k_a)}{p(\mathcal{D}_{k_a} | \hat{s})}.$$

Note that the denominator of the right-hand side of the above expression does not depend on  $b_f$  and  $k_f$ , and, moreover,  $m(k_f | \hat{s}, k_a)$  is a non-informative PMF. Therefore, one can use the reduced cost function  $\bar{J}(b_f, k_f) = p(\mathcal{D}_{k_a} | \hat{s}, k_f, b_f) p(b_f | \hat{s})$ . From both Lemma 4.5 and the explicit form of  $p(b_f | \hat{s}) = \mathcal{G}_{b_f}(2, \beta_{\hat{s}})$ ,  $\bar{J}$  can be written as

$$\bar{J}(b_f, k_f) = \left[ \frac{a_1}{\Gamma(2)\beta_{\hat{s}}^2} \right] b_f \exp \left\{ -\frac{1}{2} b_f^2 \xi^{(\hat{s})}(k_f) + b_f \left( \zeta^{(\hat{s})}(k_f) - \frac{1}{\beta_{\hat{s}}} \right) \right\}.$$

By eliminating the factor in brackets, which does not depend on  $b_f$  and  $k_f$ , and by applying the natural logarithmic function, the optimization in (4.28) can be seen to be equivalent to

$$\{\hat{k}_f, \hat{b}_f\} = \arg \left\{ \max_{k_f \in \mathfrak{K}_f, b_f \in \mathfrak{B}_f} \check{J}(b_f, k_f) \right\},$$

where  $\check{J}(b_f, k_f) = \ln b_f - \frac{1}{2} \xi^{(\hat{s})}(k_f) b_f^2 + \left( \zeta^{(\hat{s})}(k_f) - \frac{1}{\beta_{\hat{s}}} \right) b_f$ .

Note that for each  $k_f \in \mathfrak{K}_f$ ,  $\check{J}$  is differentiable with respect to  $b_f$  in  $\mathfrak{B}_f - \{0\}$ . Additionally, when  $b_f \rightarrow 0^+$ ,  $\check{J} \rightarrow -\infty$ . Then, for each  $k_f$ , the maximum of  $\check{J}$  occurs at some of the critical points given by  $\partial \check{J} / \partial b_f(b_f, k_f)|_{b_f=b^*(k_f)} = 0$ . Explicitly, these critical points are



the following two:

$$b_{1,2}^*(k_f) = \frac{\left(\zeta^{(\hat{s})}(k_f) - \frac{1}{\beta_{\hat{s}}}\right) \pm \sqrt{\left(\zeta^{(\hat{s})}(k_f) - \frac{1}{\beta_{\hat{s}}}\right)^2 + 4\xi^{(\hat{s})}(k_f)}}{2\xi^{(\hat{s})}(k_f)}.$$

Since  $\xi^{(\hat{s})}(k_f) > 0, \forall k_f$ , the value of the square root in the above expression is always greater than  $|\zeta^{(\hat{s})}(k_f) - \beta_{\hat{s}}^{-1}|$ . Thus, there exists only one critical point in  $\mathfrak{B}_f$ , i.e.,

$$\bar{b}(k_f) = \frac{\left(\zeta^{(\hat{s})}(k_f) - \frac{1}{\beta_{\hat{s}}}\right) + \sqrt{\left(\zeta^{(\hat{s})}(k_f) - \frac{1}{\beta_{\hat{s}}}\right)^2 + 4\xi^{(\hat{s})}(k_f)}}{2\xi^{(\hat{s})}(k_f)}.$$

Finally, note that  $\partial^2 \check{J} / \partial b_f^2 = -(b_f^{-2} + \xi^{(\hat{s})}(k_f)) < 0, \forall b_f \in \mathfrak{B}_f$ . Then, in fact, for each value of  $k_f$ , the maximum of  $\check{J}$  occurs at  $b_f = \bar{b}(k_f)$ . Therefore, by defining  $z(k_f) \triangleq \check{J}(\bar{b}(k_f), k_f)$ , one can see that the estimate of the fault instant,  $\hat{k}_f$ , is the value of  $k_f$  that maximizes  $z(k_f)$ . On the other hand, the estimate of  $b_f$  is obtained by substituting  $k_f$  by  $\hat{k}_f$  into  $\bar{b}(k_f)$ .  $\square$

On the basis of Theorem 4.10, Lemma 4.11, and Theorem 4.12, the following algorithm summarizes Stage 1 of the FTTS filter that are suitable for *gamma* fault magnitudes.

**Algorithm 4.13** Stage 1 of the FTTS filter for *gamma* fault magnitudes:

1. Estimation of  $s$ :

- for  $\forall i \in \mathfrak{I}$ , compute  $T_i(\mathcal{D}_{k_a})$  using equation (4.20) by approximating  $I_i(l)$  with  $I_i^n(l)$ , which is given by equation (4.23);
- $\hat{s} = \arg \{\max_{i \in \mathfrak{I}} T_i(\mathcal{D}_{k_a})\}$ ;

2. Estimation of  $k_f$  and  $b_f$ :

- $\hat{k}_f = \arg \{\max_{k_f \in \mathfrak{R}_f} z(k_f)\}$ , where  $z(\cdot)$  is given by equation (4.26);
- $\hat{b}_f = \bar{b}(\hat{k}_f)$ , where  $\bar{b}(\cdot)$  is given by equation (4.27).

### 4.2.3 Case 3: Fault magnitude with discrete distribution

Similar to the previous subsections, let the fault parameters  $s$ ,  $k_f$ , and  $b_f$  be drawn from the corresponding RVs defined in Assumption 2.3. But now, assume that the fault magnitude is drawn from the discrete RV whose PMF is given by equation (2.6). In this context, the following two theorems provide the explicit solution, respectively, to part  $a$  and part  $b$  of Problem 4.3.

**Theorem 4.14** Let  $i \in \mathfrak{J}$  denote an arbitrary fault mode index. If  $b_f$  is a sample of the PMF  $m(b_f|i) = \mathcal{K}_{b_f}(P(b_L|i), P(b_M|i), P(b_H|i))$ , with support  $\mathfrak{B}_f = \{b_L, b_M, b_H\}$ , and  $k_f$  is a sample of the PMF  $m(k_f|i, k_a) = \mathcal{U}_{k_f}([k_a, k_a - M_2 + 1])$ , with support  $\mathfrak{K}_f = [k_a, k_a - M_2 + 1]$ , then, by using the MPE criterion, the solution to part  $a$  of Problem 4.3 is given by

$$T_{\hat{s}}(\mathcal{D}_{k_a}) \stackrel{H_{\hat{s}}}{>} T_j(\mathcal{D}_{k_a}), \forall j \neq \hat{s}, \quad (4.29)$$

where, for  $\forall i$ ,

$$T_i(\mathcal{D}_{k_a}) \triangleq P(i) \sum_{l \in \mathfrak{K}_f} \sum_{b \in \mathfrak{B}_f} P(b|i) \exp \left\{ -\frac{1}{2} b^2 \xi^{(i)}(l) + b \zeta^{(i)}(l) \right\}, \quad (4.30)$$

with  $\zeta^{(i)}(l)$  and  $\xi^{(i)}(l)$  as defined in Lemma 4.5.

**Proof.** Note that, in the present case, the likelihood of the data set is appropriately given by equation (4.8). Denote the summand of such expression by  $q(b_f, k_f)$ , which can be rewritten as  $q(b_f, k_f) = q_1 q_2(b_f, k_f)$ , with  $q_1 \triangleq a_1/M_2$ , and

$$q_2(b_f, k_f) \triangleq \sum_{l \in \mathfrak{K}_f} \sum_{b \in \mathfrak{B}_f} P(b|i) \delta_{b_f-b} \delta_{k_f-l} \exp \left\{ -\frac{1}{2} b_f^2 \xi^{(i)}(k_f) + b_f \zeta^{(i)}(k_f) \right\}.$$

Since  $q_1$  does not depend on  $b_f$  and  $k_f$ , equation (4.8) can be written as

$$p(\mathcal{D}_{k_a}|i) = q_1 \sum_{b_f \in \mathfrak{B}_f} \sum_{k_f \in \mathfrak{K}_f} \sum_{b \in \mathfrak{B}_f} \sum_{l \in \mathfrak{K}_f} P(b|i) \delta_{b_f-b} \delta_{k_f-l} \exp \left\{ -\frac{1}{2} b_f^2 \xi^{(i)}(k_f) + b_f \zeta^{(i)}(k_f) \right\}.$$

By taking the sum over  $k_f$ , the above expression becomes

$$p(\mathcal{D}_{k_a}|i) = q_1 \sum_{b_f \in \mathfrak{B}_f} \sum_{b \in \mathfrak{B}_f} \sum_{l \in \mathfrak{K}_f} P(b|i) \delta_{b_f-b} \exp \left\{ -\frac{1}{2} b_f^2 \xi^{(i)}(l) + b_f \zeta^{(i)}(l) \right\},$$

or equivalently,

$$p(\mathcal{D}_{k_a}|i) = q_1 \sum_{l=k_a-M_2+1}^{k_a} \sum_{b \in \mathfrak{B}_f} P(b|i) \sum_{b_f \in \mathfrak{B}_f} \delta_{b_f-b} \exp \left\{ -\frac{1}{2} b_f^2 \xi^{(i)}(l) + b_f \zeta^{(i)}(l) \right\}.$$

Now, by taking the sum over  $b_f$ , one gets

$$p(\mathcal{D}_{k_a}|i) = q_1 \sum_{l \in \mathfrak{K}_f} \sum_{b \in \mathfrak{B}_f} P(b|i) \exp \left\{ -\frac{1}{2} b^2 \xi^{(i)}(l) + b \zeta^{(i)}(l) \right\}. \quad (4.31)$$

Therefore, by substituting equation (4.31) into (4.3) and making some algebraic manipulations, the decision rule given by equation (4.29) can be obtained.  $\square$

**Theorem 4.15** Let  $\hat{s}$  be the estimate of the fault mode index provided by Theorem 4.14. If  $b_f$  is a sample of the PMF  $m(b_f|\hat{s}) = \mathcal{K}_{b_f}(P(b_L|\hat{s}), P(b_M|\hat{s}), P(b_H|\hat{s}))$ , with support  $\mathfrak{B}_f = \{b_L, b_M, b_H\}$ , and  $k_f$  is a sample of the PMF  $m(k_f|\hat{s}, k_a) = \mathcal{U}_{k_f}([k_a, k_a - M_2 + 1])$ , with support  $\mathfrak{K}_f = [k_a, k_a - M_2 + 1]$ , then the solution to part b of Problem 4.3 is given by

$$\{\hat{b}_f, \hat{k}_f\} = \arg \left\{ \min_{k_f \in \mathfrak{K}_f, b_f \in \mathfrak{B}_f} \check{J}(b_f, k_f) \right\}, \quad (4.32)$$

where

$$\check{J}(b_f, k_f) \triangleq b_f^2 \xi^{(\hat{s})}(k_f) - 2b_f \zeta^{(\hat{s})}(k_f) - 2 \ln \left( \sum_{b \in \mathfrak{B}_f} P(b|\hat{s}) \delta_{b_f-b} \right), \quad (4.33)$$

with  $\zeta^{(\hat{s})}(k_f)$  and  $\xi^{(\hat{s})}(k_f)$  as defined in Lemma 4.5.

**Proof.** In general, by the MAP criterion, the optimal estimates of  $k_f$  and  $b_f$  are given by

$$\{\hat{k}_f, \hat{b}_f\} \triangleq \arg \left\{ \max_{k_f \in \mathfrak{K}_f, b_f \in \mathfrak{B}_f} J(b_f, k_f) \right\}, \quad (4.34)$$

where  $J(b_f, k_f)$  is the joint posterior PMF of the RVs underlying  $k_f$  and  $b_f$ . It can be rewritten, by means of the Bayes' rule, as

$$J(b_f, k_f) = \frac{p(\mathcal{D}_{k_a} | \hat{s}, b_f, k_f) m(b_f | \hat{s}) m(k_f | \hat{s}, k_a)}{p(\mathcal{D}_{k_a} | \hat{s})}.$$

Note that the denominator of the right-hand side of the above expression does not depend on  $b_f$  and  $k_f$ , and that  $m(k_f | \hat{s}, k_a)$  is a non-informative PMF. Thus, one can use the reduced function  $\bar{J}(b_f, k_f) = p(\mathcal{D}_{k_a} | \hat{s}, k_f, b_f) m(b_f | \hat{s})$ . From both Lemma 4.5 and the explicit form of  $m(b_f | \hat{s})$ ,  $\bar{J}$  can be rewritten as

$$\bar{J}(b_f, k_f) = a_1 \sum_{b \in \mathfrak{B}_f} P(b | \hat{s}) \delta_{b_f - b} \exp \left\{ -\frac{1}{2} b_f^2 \xi^{(\hat{s})}(k_f) + b_f \zeta^{(\hat{s})}(k_f) \right\}. \quad (4.35)$$

Finally, by eliminating the factor  $a_1$ , which does not depend on  $b_f$  and  $k_f$ , and by applying the natural logarithmic function, the optimization in (4.34) can be seen to be equivalent to

$$\left\{ \hat{k}_f, \hat{b}_f \right\} = \arg \left\{ \min_{k_f \in \mathfrak{K}_f, b_f \in \mathfrak{B}_f} \check{J}(b_f, k_f) \right\},$$

where  $\check{J}(b_f, k_f) = b_f^2 \xi^{(\hat{s})}(k_f) - 2b_f \zeta^{(\hat{s})}(k_f) - 2 \ln \left( \sum_{b \in \mathfrak{B}_f} P(b | \hat{s}) \delta_{b_f - b} \right)$ .  $\square$

On the basis of the above two theorems, the following algorithm summarizes Stage 1 of the FTTS filter that is suitable for discrete fault magnitudes.

**Algorithm 4.16** Stage 1 of the FTTS filter for discrete fault magnitudes:

1. Estimation of  $s$ :

- for  $\forall i \in \mathcal{I}$ , compute  $T_i(\mathcal{D}_{k_a})$  using equation (4.29);
- $\hat{s} = \arg \{ \max_{i \in \mathcal{I}} T_i(\mathcal{D}_{k_a}) \}$ ;

2. Estimation of  $k_f$  and  $b_f$ :

- $\{\hat{k}_f, \hat{b}_f\} = \arg \{\min_{k_f \in \mathfrak{R}_f, b_f \in \mathfrak{B}_f} \check{J}(b_f, k_f)\}$ , where  $\check{J}(\cdot, \cdot)$  is given by equation (4.33);

### 4.3 Stage 2: state estimation

The three FTTS filters have the same second stage, which carries out state estimation by correcting the fault-free KF using the fault estimate provided by Stage 1. It is worth recalling that from Lemma 3.3, if the fault sequence,  $\{\mathbf{f}_k\}$ , are exactly known, the MMSE estimates of the system states could be computed by

$$\hat{\mathbf{x}}_{k|k}^{opt} = \check{\mathbf{x}}_{k|k} + \mathbf{h}_k, \quad (4.36)$$

where  $\check{\mathbf{x}}_{k|k}$  is the estimate provided by the fault-free KF at instant  $k$  and

$$\mathbf{h}_k = \bar{\mathbf{K}}_k \mathbf{A}_{k-1} \mathbf{h}_{k-1} + \bar{\mathbf{K}}_k \bar{\boldsymbol{\Xi}}_{k-1} \mathbf{f}_{k-1} - \mathbf{K}_k \boldsymbol{\Theta}_{k-1} \mathbf{f}_k, \quad (4.37)$$

with initial condition  $\mathbf{h}_0 = \mathbf{0}$ .

In spite of the optimality of the above state estimator, it cannot be used in practice, since the true fault sequence is usually unknown. Nevertheless, an heuristic but implementable version of this estimator can be obtained by replacing the true fault  $\mathbf{f}_k$  by its estimate

$$\hat{\mathbf{f}}_k = \hat{b}_f \mathbf{e}_{j(\hat{s})} \vartheta^{(\hat{s})} (k - \hat{k}_f), \quad (4.38)$$

which is computed by using the estimates of the fault parameters,  $\hat{s}$ ,  $\hat{k}_f$ , and  $\hat{b}_f$ , provided by Stage 1.

**Definition 4.17** Let the instant of correction be defined as  $k_c \triangleq k_a + M_1 - 1$ . Denote the filtered estimates of the FTTS filters at instant  $k$  by  $\hat{\mathbf{x}}_{k|k}$ . The *state estimation* stage (Stage 2) of the three FTTS filters is given by

- If  $k \leq k_c$ , then  $\hat{\mathbf{x}}_{k|k} = \check{\mathbf{x}}_{k|k}$

- If  $k > k_c$ , then  $\hat{\mathbf{x}}_{k|k} = \check{\mathbf{x}}_{k|k} + \hat{\mathbf{h}}_k$

where  $\hat{\mathbf{h}}_k$  is recursively given by  $\hat{\mathbf{h}}_k = \bar{\mathbf{K}}_k \mathbf{A}_{k-1} \hat{\mathbf{h}}_{k-1} + \bar{\mathbf{K}}_k \bar{\boldsymbol{\Xi}}_{k-1} \hat{\mathbf{f}}_{k-1} - \mathbf{K}_k \boldsymbol{\Theta}_{k-1} \hat{\mathbf{f}}_k$ , with initial condition  $\hat{\mathbf{h}}_{k_f-1} = \mathbf{0}$ .

Note that during the time interval  $k < k_f$ , the state estimator of Definition 4.17 corresponds to the optimal one. However, during the time interval  $k_f \leq k < k_c$ , owing to the effects of the fault, the state estimates might present a diverging behavior. In this phase, nothing can be done in order to improve the state estimates since the fault estimate is not yet available. When the correction becomes effective, i.e., for  $k \geq k_c$ , an improvement of performance is expected. The following algorithm summarizes Stage 2 of the FTTS filters.

**Algorithm 4.18** The  $k$ -th iteration of Stage 2 of the FTTS filters is given by

1. State prediction:

$$\begin{aligned}\check{\mathbf{x}}_{k|k-1} &= \mathbf{A}_{k-1} \check{\mathbf{x}}_{k-1|k-1} + \mathbf{B}_{k-1} \mathbf{u}_{k-1} \\ \mathbf{P}_{k|k-1} &= \mathbf{A}_{k-1} \mathbf{P}_{k-1|k-1} \mathbf{A}'_{k-1} + \boldsymbol{\Gamma}_{k-1} \mathbf{Q}_{k-1} \boldsymbol{\Gamma}'_{k-1}\end{aligned}$$

2. Innovation generation:

$$\begin{aligned}\mathbf{r}_k &= \mathbf{y}_k - \mathbf{C}_k \check{\mathbf{x}}_{k|k-1} \\ \mathbf{V}_k &= \mathbf{C}_k \mathbf{P}_{k|k-1} \mathbf{C}'_k + \mathbf{R}_k\end{aligned}$$

3. State update:

$$\begin{aligned}\mathbf{K}_k &= \mathbf{P}_{k|k-1} \mathbf{C}'_k (\mathbf{V}_k)^{-1} \\ \check{\mathbf{x}}_{k|k} &= \check{\mathbf{x}}_{k|k-1} + \mathbf{K}_k \mathbf{r}_k \\ \mathbf{P}_{k|k} &= (\mathbf{I}_{n_x} - \mathbf{K}_k \mathbf{C}_k) \mathbf{P}_{k|k-1}\end{aligned}$$

4. State correction:

$$\begin{aligned}\text{If } k < k_c, \text{ then } \hat{\mathbf{h}}_k &= \mathbf{0} \\ \text{if } k = k_c, \text{ then for } j = \hat{k}_f : k, \hat{\mathbf{h}}_j &= \bar{\mathbf{K}}_j \mathbf{A}_{j-1} \hat{\mathbf{h}}_{j-1} + \bar{\mathbf{K}}_j \bar{\boldsymbol{\Xi}}_{j-1} \hat{\mathbf{f}}_{j-1} - \mathbf{K}_j \boldsymbol{\Theta}_{j-1} \hat{\mathbf{f}}_j \\ \text{if } k > k_c, \text{ then } \hat{\mathbf{h}}_k &= \bar{\mathbf{K}}_k \mathbf{A}_{k-1} \hat{\mathbf{h}}_{k-1} + \bar{\mathbf{K}}_k \bar{\boldsymbol{\Xi}}_{k-1} \hat{\mathbf{f}}_{k-1} - \mathbf{K}_k \boldsymbol{\Theta}_{k-1} \hat{\mathbf{f}}_k \\ \hat{\mathbf{x}}_{k|k} &= \check{\mathbf{x}}_{k|k} + \hat{\mathbf{h}}_k\end{aligned}$$

## 4.4 Illustrative Examples

In this section, the three FTTS filters are illustrated using a simulated permanent-magnet DC motor coupled to a rotational inertia. Subsection 4.4.1 presents the dynamical model of the fault-prone system, while Subsection 4.4.2 evaluates the performance of the FTTS filters on the basis of Monte Carlo simulations.

### 4.4.1 System modeling

For describing the dynamics of the servomechanism, consider the physical model depicted in Figure 4.1. In this model, the armature of the motor is represented by a series circuit connecting a resistance,  $R_A$ , an inductance,  $L_A$ , and a counter-electromotive force,  $e$ , which is proportional to the shaft angular velocity,  $\omega$ , and opposes the armature voltage,  $v_A$ . The interaction between the main magnetic field (produced by the permanent magnet) and the magnetic field generated by the flow of the armature current,  $i_A$ , through the circuit induces a torque,  $T_m$ . This torque drives a rotational body, whose moment of inertia is  $J$  and is subject to a viscous linear friction with coefficient  $B$ . The system is equipped with a potentiometer (for measuring the angular position,  $\theta$ ) and a tachometer (for measuring the angular velocity,  $\omega$ ). As mentioned before, three illustrative fault modes are considered: an impulsive error in the angular position observations (Fault 1), a constant bias in the angular velocity observations (Fault 2), and a sinusoidal interference in the armature voltage (Fault 3). The physical parameters of the system are shown in Table 4.1.

TABLE 4.1 – Physical parameters of the servomechanism.

Description	Symbol	Value
Armature resistance	$R_A$	$2 \Omega$
Armature inductance	$L_A$	$0.05 H$
Torque constant	$k_T$	$0.1 Nm/A$
EMF constant	$k_\omega$	$0.1 V/(rad/s)$
Friction	$B$	$0.005 Nm/(rad/s)$
Moment of inertia	$J$	$0.02 kgm^2$

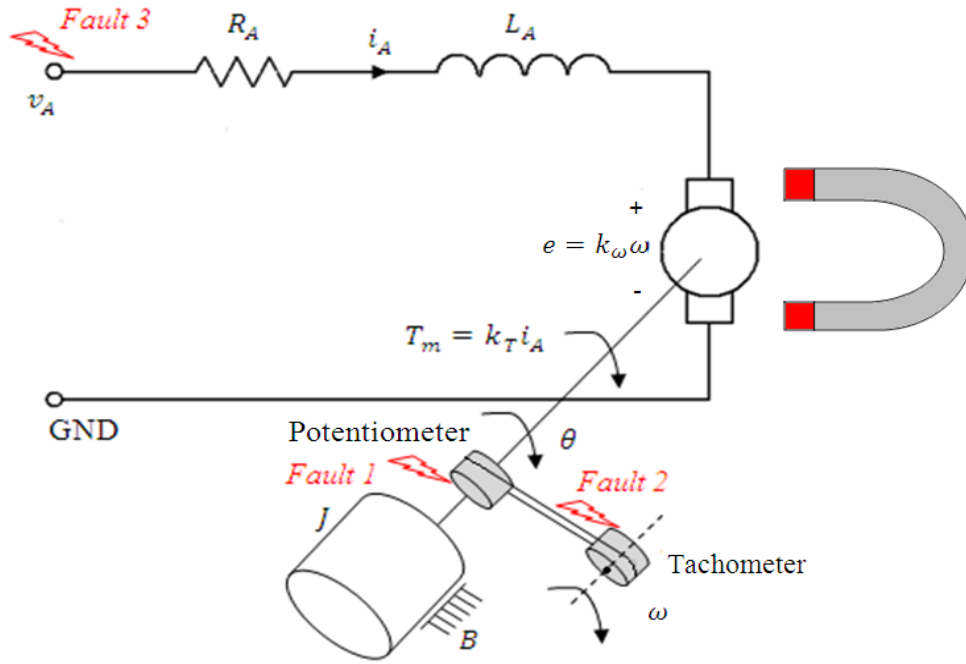


FIGURE 4.1 – Physical model of the servomechanism.

Define a state vector  $\mathbf{x} = [x_1 \ x_2 \ x_3]'$ , with  $x_1 \triangleq \theta$ ,  $x_2 \triangleq \omega$ , and  $x_3 \triangleq i_A$ , and a control input  $\mathbf{u}_k \triangleq v_A$ . By adopting a sample time of  $T = 0.1s$  and taking into account the parameters of Table 4.1, the following time-invariant model can be obtained for describing the dynamics of the servomechanism<sup>2</sup>:

$$\mathbf{x}_{k+1} = \mathbf{A}\mathbf{x}_k + \mathbf{B}\mathbf{u}_k + \mathbf{\Gamma}\mathbf{w}_k + \mathbf{\Xi}\mathbf{f}_k, \quad (4.39)$$

$$\mathbf{y}_k = \mathbf{C}\mathbf{x}_k + \mathbf{v}_k + \mathbf{\Theta}\mathbf{f}_k, \quad (4.40)$$

where

$$\mathbf{A} = \begin{bmatrix} 1 & 0.098 & 0.009 \\ 0 & 0.957 & 0.119 \\ 0 & -0.048 & 0.013 \end{bmatrix}, \quad \mathbf{B} = \begin{bmatrix} 0.008 \\ 0.186 \\ 0.484 \end{bmatrix}, \quad \mathbf{\Gamma} = \mathbf{I}_3, \quad \mathbf{\Xi} = \begin{bmatrix} 0 & 0 & 0.008 \\ 0 & 0 & 0.186 \\ 0 & 0 & 0.484 \end{bmatrix},$$

<sup>2</sup>For the sake of simplicity, the continuous-time model is not presented here. However, it can be found in many textbooks on control theory. See, e.g., (SHINNERS, 1992), p. 143.



$$\mathbf{C} = \begin{bmatrix} 1 & 0 & 0 \\ 0 & 1 & 0 \end{bmatrix}, \quad \Theta = \begin{bmatrix} 1 & 0 & 0 \\ 0 & 1 & 0 \end{bmatrix}.$$

The noise terms,  $\mathbf{w}_k$  and  $\mathbf{v}_k$ , and the initial state,  $\mathbf{x}_0$ , are assumed to be zero-mean Gaussian vectors with covariances  $\mathbf{Q}_k = 10^{-6}\mathbf{I}_3$ ,  $\mathbf{R}_k = 10^{-4}\mathbf{I}_2$ , and  $\mathbf{P}_0 = \mathbf{I}_3$ , respectively. Moreover,  $\{\mathbf{w}_k\}$ ,  $\{\mathbf{v}_k\}$ , and  $\mathbf{x}_0$  are mutually independent.

The fault vector at instant  $k$  is assumed to have the structure  $\mathbf{f}_k = b_f \mathbf{e}_{j(s)} \vartheta^{(s)}(k - k_f)$ , with  $\mathbf{e}_{j(s)} \in \mathbb{R}^3$ , where  $s$ ,  $b_f$ , and  $k_f$  are the unknown fault parameters. As mentioned before, three fault modes are considered in the present illustration. They are described in Table 4.2.

TABLE 4.2 – The fault modes for the illustrative example.

$s$	$\mathbf{f}_k = b_f \mathbf{e}_{j(s)} \vartheta^{(s)}(k - k_f)$	Description
1	$b_f \mathbf{e}_1 \delta_{k-k_f}$	Impulsive error in $y_1$
2	$b_f \mathbf{e}_2 1_{k-k_f}$	Stepwise bias in $y_2$
3	$b_f \mathbf{e}_3 \sin(0.1\pi [k - k_f]) 1_{k-k_f}$	Sinusoidal interference in $v_A$ with frequency of 0.5 Hz

#### 4.4.2 Simulation-based evaluation of the FTTS filters

The servomechanism is simulated ten thousand times in the discrete-time interval  $k \in [1, 200]$  by using equations (4.39)-(4.40) and by adopting the open-loop control input  $\mathbf{u}_k = 2.0 \times 1_{k-10}$ . For simplicity, in all of the runs, the alarm events are considered to occur at instant  $k_a = 100$ <sup>3</sup>. With regard to the prior knowledge about the fault parameters, let the fault modes of Table 4.2 be equiprobable and let the fault instants be drawn from the PMF  $m(k_f | s, k_a) = U([96, 100])$ , for  $s = 1, 2, 3$ . The three fault magnitude cases (Gaussian, *gamma*, and discrete) are considered separately in the subsequent items. Table 4.3 shows the fault magnitude statistics adopted in each case.

The index  $I_k^x \triangleq \|x_{1,k} - \hat{x}_{1,k|k}\|$  is employed for measuring the state estimation error.

<sup>3</sup>In a practical application of the FTTS filters, the alarm event may be generated, for instance, by the  $\chi^2$  detection test that decides for the fault condition if  $\epsilon_k > t_\alpha$ , where  $\epsilon_k \triangleq \sum_{l=k-M_d+1}^k \mathbf{r}_l' \mathbf{V}_l^{-1} \mathbf{r}_l$  is the statistic of the test and  $t_\alpha$  is a given threshold. In the absence of faults, since  $\{\mathbf{r}_k\}$  is a zero-mean white Gaussian sequence with covariances  $\{\mathbf{V}_k\}$ ,  $\epsilon_k$  is a central  $\chi^2$  RV with  $M_d n_y$  degrees of freedom (PAPOULIS; PILLAI, 2002). Therefore,  $t_\alpha$  might be chosen in order to achieve a given probability of false alarm  $\alpha$  by using the expression  $P(\epsilon_k \leq t_\alpha) = 1 - \alpha$ .

TABLE 4.3 – The prior statistics of the fault magnitudes in SI units.

$s$	Gaussian	$gamma$	discrete
1	$\mathcal{N}_{b_f}(0.2000, 0.0025)$	$\mathcal{G}_{b_f}(2, 0.50)$	$\mathcal{K}_{b_f}(1/3, 1/3, 1/3), b_f \in \{0.010, 0.050, 0.080\}$
2	$\mathcal{N}_{b_f}(0.0300, 0.0001)$	$\mathcal{G}_{b_f}(2, 0.02)$	$\mathcal{K}_{b_f}(1/3, 1/3, 1/3), b_f \in \{0.005, 0.010, 0.020\}$
3	$\mathcal{N}_{b_f}(0.0100, 0.0001)$	$\mathcal{G}_{b_f}(2, 0.01)$	$\mathcal{K}_{b_f}(1/3, 1/3, 1/3), b_f \in \{0.008, 0.020, 0.050\}$

For measuring the estimation errors associated with the fault instant estimates and with the fault magnitude estimates, consider the indices  $I^{k_f} \triangleq |k_f - \hat{k}_f|$  and  $I^{b_f} \triangleq |(b_f - \hat{b}_f)/b_f|$ , respectively. Note that the above indices are positive and, furthermore, the more accurate the estimation, the smaller the value of the corresponding index. Finally, the number of correct identification of the fault mode index, which is denoted by  $N_c$ , is employed to evaluate the methods with respect to the estimation of  $s$ .

- *Case 1: Gaussian fault magnitudes*

Monte Carlo simulations are carried out by considering the Gaussian PDFs given in Table 4.3 and by executing the FTTS filter for Gaussian fault magnitudes (Algorithm 4.9 + Algorithm 4.18). Figure 4.2 depicts the sample means,  $\bar{I}_k^x$ , and standard deviations,  $\sigma_k^x$ , of the state estimation index,  $I_k^x$ , obtained for different values of  $M_1$  (data set length) by considering each value of  $s$  separately. In all scenarios, note that the state estimates start diverging at some instant  $k \in [96, 100]$  with the onset of the fault. Moreover, the errors rapidly return to the proximity of the initial level soon after the reconfiguration performed at  $k_c = 99 + M_1$ . Therefore, in general, the larger the value of  $M_1$ , the longer the state estimates remain affected by the fault. Particularly, it is worth noting that in the scenarios where  $s = 1$  (impulsive error at  $y_1$ ), the fault effect is transient and, hence, it would vanish even without reconfiguration. In other words, the conventional KF might be sufficiently robust for dealing with such an impulsive fault.

Table 4.4 shows the statistics of the fault parameter estimation errors. For the scenarios considered here, in general, the larger the data set length,  $M_1$ , the larger the number of correct identification of the fault mode index,  $N_c$ . Moreover, for  $s = 2$  (stepwise fault in  $y_2$ ) and  $s = 3$  (sinusoidal fault in  $v_A$ ), note that the fault magnitude estimation is improved by adopting a larger data set. However, the same improvement is not verified

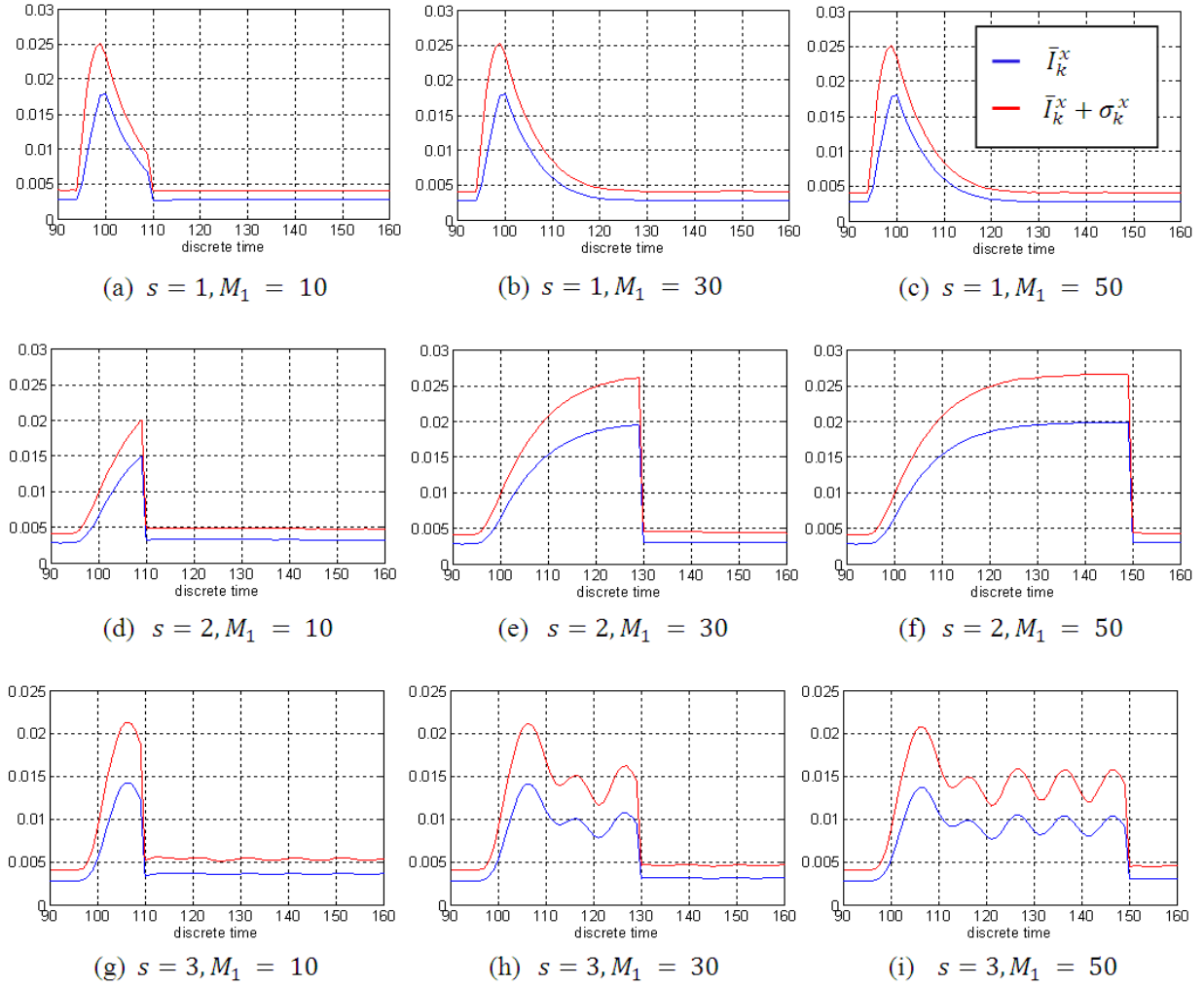


FIGURE 4.2 – The state estimation index – Case 1.

when  $s = 1$ . Such behavior can be explained by inspecting Figure 4.3, which shows three realizations of the innovation sequence of the fault-free KF. For  $s = 1$ , the fault signature on the innovation practically vanishes after about  $k = 120$ . Therefore, one can reason that the ensuing data would not be able to improve the estimation of  $b_f$ , since they have a poor signal-to-noise ratio. For  $s = 2$ , after a transient period, the fault signature stays around a fixed level. In this case, note that further innovations do not bring information about  $k_f$ . In fact, for  $s = 2$ , the estimation of  $k_f$  is slightly impaired by increasing  $M_1$ , as verified in Table 4.4.

With regard to  $b_f$ , for  $s = 2$  and  $s = 3$ , a more significant improvement of accuracy is verified when  $M_1$  is changed from 10 to 30. As a consequence, after reconfiguration, more accurate state estimates are provided by the second stage of the filter, as one can confirm

TABLE 4.4 – The fault parameter estimation errors – Case 1.

$s$	$M_1$	$N_c$	$(\bar{I}^{k_f}, \sigma^{k_f})$	$(\bar{I}^{b_f}, \sigma^{b_f})$
1	10	9833	(0.906, 0.939)	(0.150, 0.171)
	30	9886	(0.927, 0.948)	(0.149, 0.168)
	50	9901	(0.946, 0.957)	(0.151, 0.176)
2	10	9660	(1.105, 0.972)	(0.076, 0.074)
	30	9872	(1.114, 1.006)	(0.049, 0.050)
	50	9927	(1.122, 1.029)	(0.040, 0.043)
3	10	7738	(0.567, 0.687)	(0.312, 2.110)
	30	7900	(0.267, 0.479)	(0.136, 0.482)
	50	7999	(0.198, 0.419)	(0.097, 0.155)

by comparing Figure 4.2(d) with Figure 4.2(e) and Figure 4.2(g) with Figure 4.2(h).

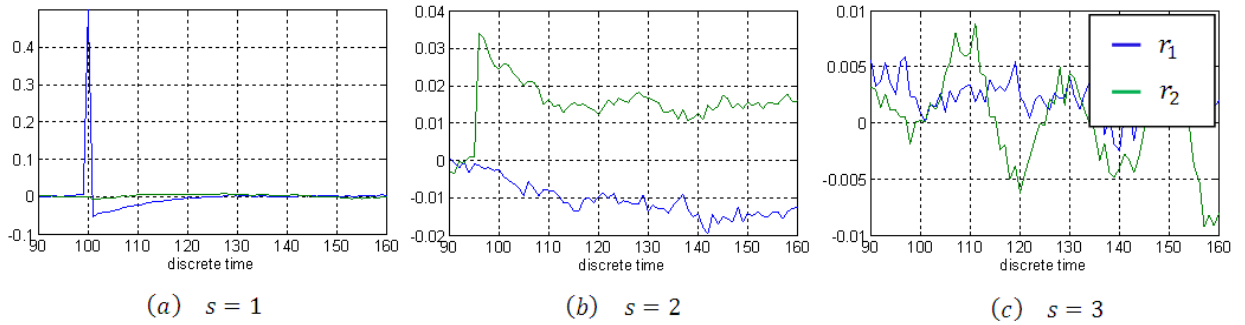


FIGURE 4.3 – Realizations of the innovation sequence of the fault-free KF for different fault modes.

The following two items present the simulation results referring to the FTTS filters for the *gamma* distributed and discrete fault magnitudes. Note that similar conclusions can be made about the performance of these filters. Hence, the details addressed above are not repeated below.

- *Case 2: gamma fault magnitudes*

Now, Monte Carlo simulations are carried out by considering the *gamma* PDFs given in Table 4.3 and by executing the FTTS filter for *gamma* fault magnitudes (Algorithm 4.13 + Algorithm 4.18). The results concerning the state estimation are presented in Figure 4.4, while the fault parameter estimation results are shown in Table 4.5.

- *Case 3: discrete fault magnitudes*

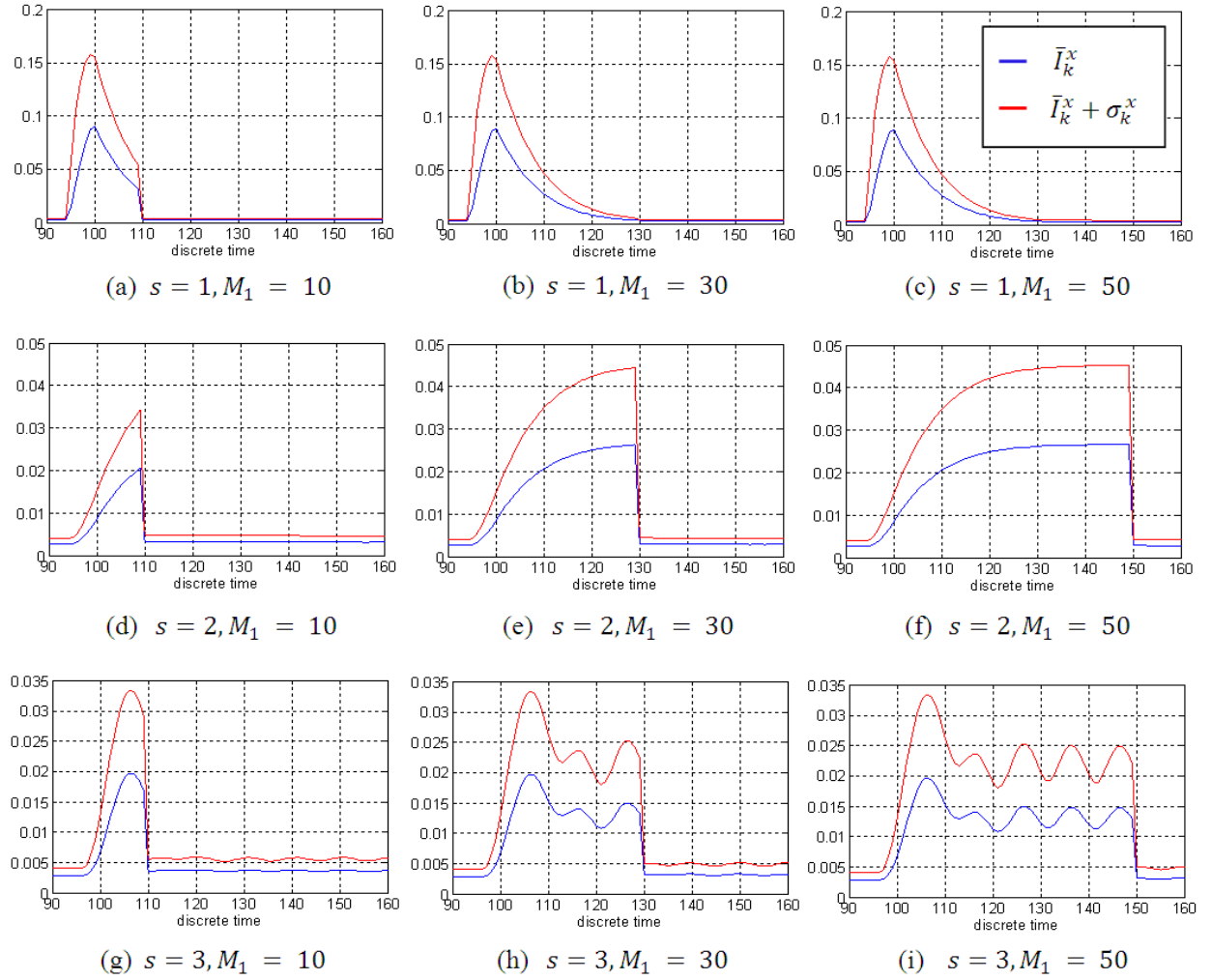


FIGURE 4.4 – The state estimation index – Case 2.

Finally, Monte Carlo simulations are carried out by considering the discrete distributions given in Table 4.3 and by executing the FTTS filter for discrete fault magnitudes (Algorithm 4.16 + Algorithm 4.18). The state estimation results are presented in Figure 4.5, while the fault parameter estimation results are shown in Table 4.6.

## 4.5 Comments on performance analysis

A quantitative performance analysis of the FTTS filters is a formidable problem and it will not be tackled in the present work. Instead, some qualitative insights are provided.

TABLE 4.5 – The fault parameter estimation errors – Case 2.

$s$	$M_1$	$N_c$	$(\bar{I}^{k_f}, \sigma^{k_f})$	$(\bar{I}^{b_f}, \sigma^{b_f})$
1	10	9827	(0.710, 0.817)	(0.096, 0.115)
	30	9882	(0.750, 0.855)	(0.102, 0.127)
	50	9916	(0.753, 0.859)	(0.104, 0.139)
2	10	9484	(1.026, 1.008)	(0.073, 0.101)
	30	9864	(1.053, 1.041)	(0.058, 0.116)
	50	9924	(1.051, 1.043)	(0.048, 0.110)
3	10	9959	(0.526, 0.796)	(0.215, 0.822)
	30	9970	(0.258, 0.523)	(0.138, 0.551)
	50	9974	(0.198, 0.448)	(0.107, 0.479)

TABLE 4.6 – The fault parameter estimation errors – Case 3.

$s$	$M_1$	$N_c$	$(\bar{I}^{k_f}, \sigma^{k_f})$	$(\bar{I}^{b_f}, \sigma^{b_f})$
1	10	9616	(1.264, 1.154)	(0.518, 1.212)
	30	9909	(1.282, 1.156)	(0.565, 1.285)
	50	9957	(1.283, 1.157)	(0.565, 1.285)
2	10	8892	(1.630, 1.304)	(0.080, 0.247)
	30	9446	(1.655, 1.311)	(0.029, 0.154)
	50	9759	(1.656, 1.309)	(0.011, 0.098)
3	10	8563	(0.354, 0.556)	(0.003, 0.056)
	30	9880	(0.189, 0.394)	(0.000, 0.000)
	50	9988	(0.153, 0.360)	(0.000, 0.000)

### 4.5.1 Fault estimation

First consider the estimation of the fault mode index,  $s$ . The corresponding performance could be measured by the probability of correct identification of  $s$ ,  $P_c$ . As commented in Section 3.3, for the purpose of computing  $P_c$ , it is necessary to know the PDFs of the statistics of test and these statistics have to be mutually independent statistically. Note that, in fact, the PDFs of the statistics given in Theorems 4.7, 4.10, and 4.14 cannot be determined analytically. Moreover, the statistical independence requirement cannot be attained, unless the proposed statistics of test could be approximated by Gaussian RVs and the fault modes were chosen such that their signatures on the KF innovations are mutually orthogonal.

Now, consider the estimation of  $k_f$  and  $b_f$ . The performance of estimators for such parameters is commonly evaluated by their biases and variances. However, these proper-

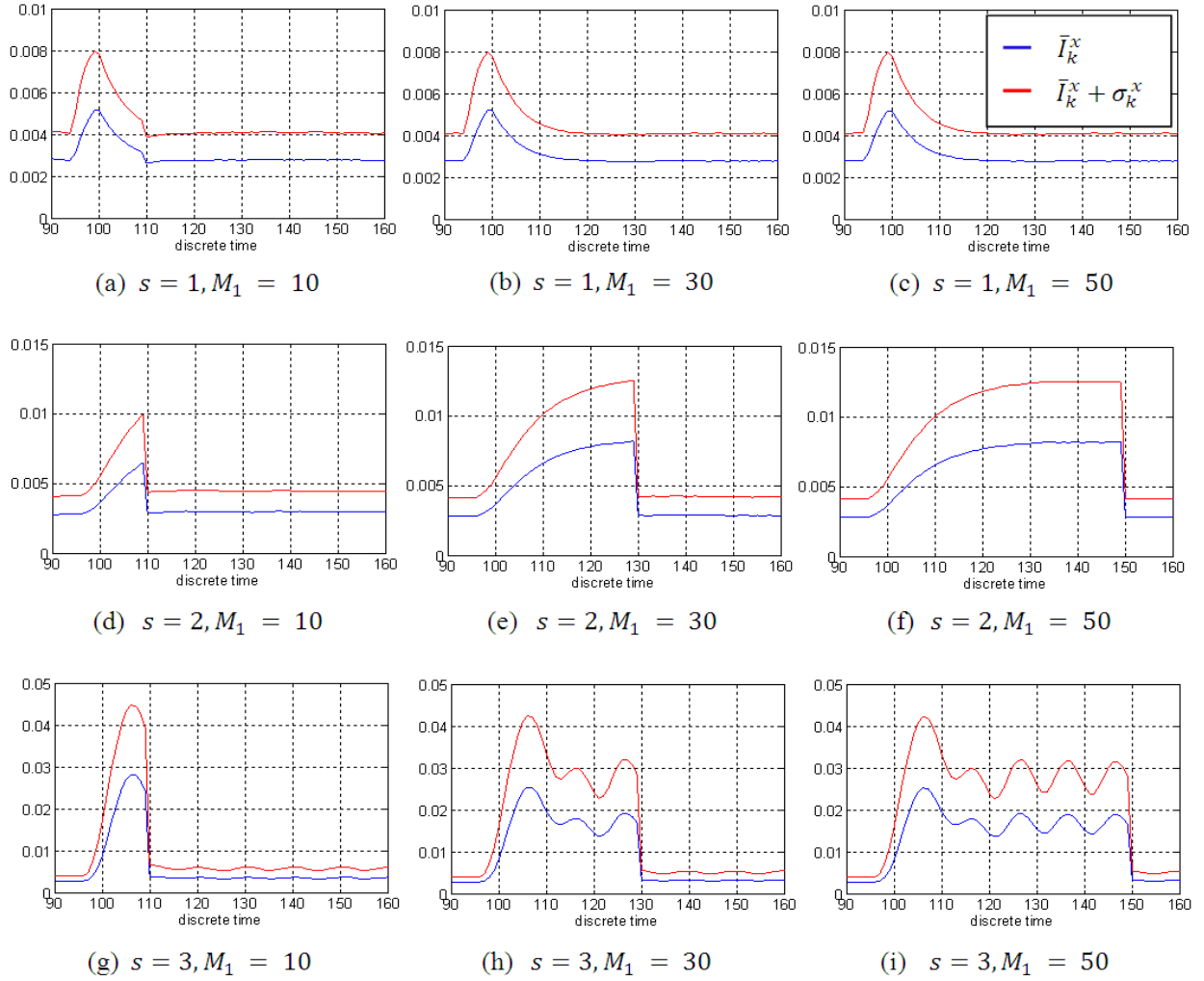


FIGURE 4.5 – The state estimation index – Case 3.

ties cannot be exploited here since the estimators given by Theorems 4.8, 4.12, and 4.15 are not completely explicit owing to the discrete-valued fault parameters ( $k_f$  and  $b_f$  in the discrete magnitude case).

## 4.5.2 State estimation

In the curves presented in Figures 4.2, 4.4, and 4.5, one can generally distinguish three time phases. The first phase corresponds to the time interval  $k < k_f$ . In this phase, the state estimators are equivalent to the fault-free KF and, therefore, they are optimal in the MMSE sense. The second phase corresponds to the time interval  $k_f \leq k \leq k_c$ , in which the fault detection and the fault estimation are carried out. In this phase, the FTTS filters may exhibit a diverging behavior, with severities that depend on the fault

magnitude. Finally, the third phase corresponds to the time interval  $k > k_c$ . Here, the state estimates are obtained as a consequence of correcting the fault-free KF outputs using the proposed methodology. In this phase, the state estimators exhibit suboptimal performance, which depends on the accuracy of the fault estimate provided by Stage 1. In other words, the better the accuracy of the fault estimate, the better the state estimation performance in this phase.

## 4.6 Summary

This chapter was concerned with the proposal of a method to solve Problem 2.4 by using a decision-theoretic approach to the joint state and fault estimation. This approach was called fault-tolerant two-stage (FTTS) filtering. By considering the three plausible models for the prior knowledge about the fault magnitudes (Assumption 2.3), three different FTTS filters were put forward. In general terms, the filters can be described as following. The first stage carries out fault estimation by statistically processing the innovation sequence of a fault-free KF. The second stage performs state estimation by correcting the fault-free KF estimates using the fault estimate provided by the first stage. For illustration purposes, the three FTTS filters were applied to a simulated DC servomechanism.



# 5 A Fault-Tolerant Model Predictive Satellite Attitude Controller

The present chapter proposes a scheme for fault-tolerant attitude control of rigid-body satellites. The scheme integrates the FTTS filter for Gaussian fault magnitudes (see Chapter 4) with a fault-reconfigurable version of a conventional model predictive controller (MPC). It will be called Fault-Tolerant Model Predictive Satellite Attitude Controller (FTMPSAC). The text is organized in the following manner. Section 5.1 presents the fault-prone system model. Relying on this model, the FTMPSAC is introduced and detailed in Section 5.2. Section 5.3 is concerned with the evaluation of the overall system performance by means of computational simulations. Finally, Section 5.4 summarizes the present chapter.

## 5.1 Fault-prone system model

The system under consideration consists of a rigid-body satellite that moves in a low-Earth orbit and includes reaction wheels, rate gyros, solar sensors, and magnetometers. A detailed description of this system as well as the derivation of a fault-free deterministic state-space model of its attitude dynamics is presented in Appendix A. Here, assume that the system is subject to faults so that it can suitably be described by the fault-prone discrete-time linear Gaussian model given by equations (2.1)-(2.2). For convenience, these

equations are repeated:

$$\mathbf{x}_{k+1} = \mathbf{A}_k \mathbf{x}_k + \mathbf{B}_k \mathbf{u}_k + \mathbf{\Gamma}_k \mathbf{w}_k + \mathbf{\Xi}_k \mathbf{f}_k, \quad (5.1)$$

$$\mathbf{y}_k = \mathbf{C}_k \mathbf{x}_k + \mathbf{v}_k + \mathbf{\Theta}_k \mathbf{f}_k, \quad (5.2)$$

with  $\mathbf{x}_k \triangleq [(\mathbf{p}^{rb})', (\boldsymbol{\omega}_b^{br})']'$ , where  $\mathbf{p}^{rb}$  is the MRP representing the attitude of  $S_b$  with respect to  $S_r$  and  $\boldsymbol{\omega}_b^{br}$  is the angular velocity of  $S_b$  with respect to  $S_r$ . The observation vector is  $\mathbf{y}_k \triangleq [(\mathbf{b}_b - \mathbf{b}_r)', (\mathbf{s}_b - \mathbf{s}_r)', \boldsymbol{\omega}'_b]'$ , where  $\mathbf{b}_b$  and  $\mathbf{b}_r$  are representations of the local geomagnetic density observation,  $\mathbf{s}_b$  and  $\mathbf{s}_r$  are representations of the local Sun direction vector observation, and  $\boldsymbol{\omega}_b$  is the observation of the inertial angular velocity of  $S_b$ . The matrices  $\mathbf{A}_k$ ,  $\mathbf{B}_k$ , and  $\mathbf{C}_k$  are given in Section A.4 of Appendix A. Additionally, the state noise gain matrix is assumed to be  $\mathbf{\Gamma}_k = \mathbf{I}_6$ , the statistics of the state and measurement noises are both considered to be known, and the continuous-time fault gain matrices are assumed to have the following structures:

$$\mathbf{\Xi} = \begin{bmatrix} \mathbf{0}_{3 \times 3} & \mathbf{0}_{3 \times 3} & \mathbf{0}_{3 \times 3} \\ \mathbf{B}_2 & \mathbf{0}_{3 \times 3} & \mathbf{0}_{3 \times 3} \end{bmatrix}, \quad (5.3)$$

$$\mathbf{\Theta} = \begin{bmatrix} \mathbf{0}_{3 \times 3} & \mathbf{I}_3 & \mathbf{0}_{3 \times 3} \\ \mathbf{0}_{3 \times 3} & \mathbf{0}_{3 \times 3} & \mathbf{0}_{3 \times 3} \\ \mathbf{0}_{3 \times 3} & \mathbf{0}_{3 \times 3} & \mathbf{I}_3 \end{bmatrix}, \quad (5.4)$$

where  $\mathbf{B}_2$  is defined in equation (A.21). The corresponding discrete-time matrices,  $\mathbf{\Xi}_k$  and  $\mathbf{\Theta}_k$ , are obtained by discretizing  $\mathbf{\Xi}$  and  $\mathbf{\Theta}$ , respectively, by using the same procedure employed to calculate  $\mathbf{B}_k$  (see equations (A.38)-(A.42)). By inspecting the above fault gain matrices, one can conclude that the fault vector  $\mathbf{f}_k$  has dimension  $n_f = 9$ , with the first three components representing additive actuator faults, the three middle ones representing additive magnetometer faults, and the last three components corresponding to additive rate gyro faults.

As defined in Chapter 2, the fault sequence,  $\{\mathbf{f}_k\}$ , is assumed to be a structured sequence parameterized by three unknown parameters: the fault magnitude, the fault instant, and the fault mode index. These parameters are assumed to be realizations of the RVs characterized in Assumption 2.3. Particularly, only the Gaussian fault magnitude case is taken into consideration in the present chapter. Table 5.1 specifies the fault modes used in the present illustration. In all the cases, the fault has a stepwise form. The nine fault modes are assumed to be equiprobable, i.e,  $P(s) = 1/9, s = 1, 2, \dots, 9$ . The solar sensors are assumed to be ideal in the sense that they always operate under fault-free conditions.

TABLE 5.1 – The illustrative fault modes.

$s$	$\mathbf{f}_k = b_f \mathbf{e}_{j(s)} \vartheta^{(s)}(k - k_f)$	$m(k_f   s, k_a)$	$p(b_f   s)$
1	$b_f \mathbf{e}_1 1_{k-k_f}$	$\mathcal{U}_{k_f}([k_a - 20, k_a])$	$\mathcal{N}_{b_f}(5 \times 10^{-4}, 6.25 \times 10^{-8}) [Nm]$
2	$b_f \mathbf{e}_2 1_{k-k_f}$	$\mathcal{U}_{k_f}([k_a - 20, k_a])$	$\mathcal{N}_{b_f}(5 \times 10^{-4}, 6.25 \times 10^{-8}) [Nm]$
3	$b_f \mathbf{e}_3 1_{k-k_f}$	$\mathcal{U}_{k_f}([k_a - 20, k_a])$	$\mathcal{N}_{b_f}(5 \times 10^{-4}, 6.25 \times 10^{-8}) [Nm]$
4	$b_f \mathbf{e}_4 1_{k-k_f}$	$\mathcal{U}_{k_f}([k_a - 20, k_a])$	$\mathcal{N}_{b_f}(2 \times 10^{-6}, 1 \times 10^{-12}) [T]$
5	$b_f \mathbf{e}_5 1_{k-k_f}$	$\mathcal{U}_{k_f}([k_a - 20, k_a])$	$\mathcal{N}_{b_f}(2 \times 10^{-6}, 1 \times 10^{-12}) [T]$
6	$b_f \mathbf{e}_6 1_{k-k_f}$	$\mathcal{U}_{k_f}([k_a - 20, k_a])$	$\mathcal{N}_{b_f}(2 \times 10^{-6}, 1 \times 10^{-12}) [T]$
7	$b_f \mathbf{e}_7 1_{k-k_f}$	$\mathcal{U}_{k_f}([k_a - 20, k_a])$	$\mathcal{N}_{b_f}(1 \times 10^{-3}, 2.5 \times 10^{-7}) [rad/s]$
8	$b_f \mathbf{e}_8 1_{k-k_f}$	$\mathcal{U}_{k_f}([k_a - 20, k_a])$	$\mathcal{N}_{b_f}(1 \times 10^{-3}, 2.5 \times 10^{-7}) [rad/s]$
9	$b_f \mathbf{e}_9 1_{k-k_f}$	$\mathcal{U}_{k_f}([k_a - 20, k_a])$	$\mathcal{N}_{b_f}(1 \times 10^{-3}, 2.5 \times 10^{-7}) [rad/s]$

## 5.2 The fault-tolerant control method

This section presents the fault-tolerant satellite attitude control method that integrates a model predictive controller (MPC) with the FTTS filter for Gaussian fault magnitudes (see Chapter 4). The resulting method will hereafter be called Fault-Tolerant Model Predictive Satellite Attitude Controller (FTMPSAC). The satellite attitude motion is assumed to be slow and close to the reference coordinate system (see Figure A.1) so that the linear model given by equations (5.1)-(5.2) can effectively approximate its dynamics.

### 5.2.1 The scheme for fault-tolerant control

A block diagram of the FTMPSAC is shown in Figure 5.1. It is composed of two parts: the fault-tolerant attitude determination (FTAD) module, and the reconfigurable MPC (RMPC) module. Besides estimating the system states  $\mathbf{x}$  (the attitude and angular velocity of the satellite), the FTAD can also detect and estimate a fault  $\mathbf{f}$ , in case the system undergoes one. It performs these functions by using the model given by equations (5.1)-(5.2) as well as the data from the output measurements,  $\mathbf{y}$ , and the control inputs,  $\mathbf{u}$ . The RMPC consists of a state-space formulated MPC whose prediction model accounts for the fault estimate,  $\hat{\mathbf{f}}$ , provided by the FTAD module. The role of the RMPC is to compute the control input  $\mathbf{u}$  that makes the controlled output  $\mathbf{z}$  to track a desired reference trajectory  $\mathbf{z}_r$  in a certain optimal sense. The following two subsections detail the FTAD and the RMPC modules.

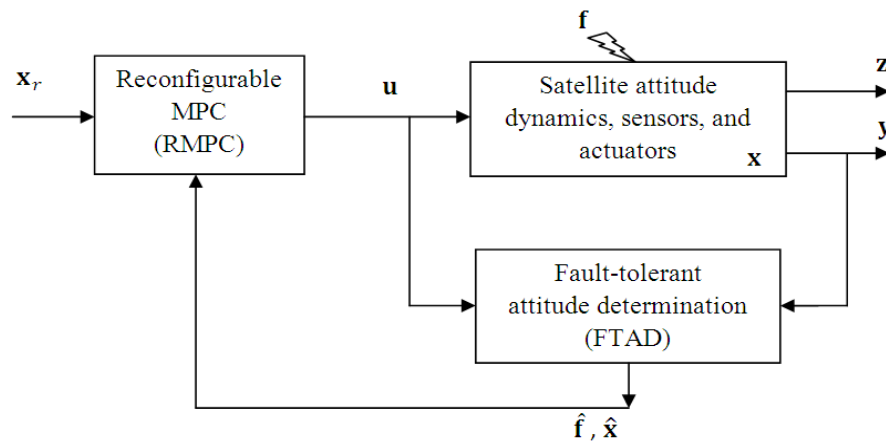


FIGURE 5.1 – The overall fault-tolerant control scheme.

### 5.2.2 Fault-tolerant attitude determination

Conventional satellite attitude determination (AD) methods ([BAR-ITZHACK; REINER, 1984](#)) ([BAR-ITZHACK; OSHMAN, 1985](#)) ([BAR-ITZHACK; IDAN, 1987](#)) ([LEFFERTS \*et al.\*, 1982](#)) are commonly concerned with the attitude estimation relying on Kalman filtering and using vector observations (e.g., the observations of the Sun direction and of the geomagnetic flux density). These methods also consider the availability of angular velocity measures,

which are used for propagating the attitude information between consecutive acquisitions of the vector observations. In the mentioned methods, only the kinematic equations of motion are taken into account when deriving the system state equations. The Euler's moment equations are obviated by treating the angular velocity measures as known inputs, rather than measured outputs. Consequently, these methods yield a reduced computational burden and, moreover, avoid the need for using complex models for the disturbance torques. Regardless of these advantageous characteristics, the conventional AD methods may not perform satisfactorily in the presence of faults in actuators or sensors. In this context, the present subsection proposes a fault-tolerant attitude determination (FTAD) method, which is expected to perform better than the conventional ones when the system is under fault conditions.

Let the system dynamics be described by equations (5.1)-(5.2). It is worth noting that, unlike the conventional methods, here, the state vector  $\mathbf{x}_k$  includes the angular velocity vector. Therefore, the angular velocity observations are not treated as known inputs any longer. This consideration yields a state equation that is augmented with respect to the ones of the conventional methods. However, the resulting augmented model (5.1)-(5.2) has the form required by the FTTS filters. Therefore, by particularly considering that the magnitudes of the fault modes shown in Table 5.1 are realizations of Gaussian RVs, the FTTS filter for Gaussian fault magnitudes (Algorithm 4.9 + Algorithm 4.18) is adopted as the FTAD method.

Rather than reproducing the equations of the FTTS filter, a corresponding block diagram is presented in Figure 5.2. In this diagram, the fault-free KF, which is implemented using equations (5.1)-(5.2), but considering  $\mathbf{f}_k = \mathbf{0}, \forall k$ , is shown to provide the uncorrected state estimates,  $\tilde{\mathbf{x}}_{k|k}$ , by processing the control inputs,  $\mathbf{u}_k$ , and the measured outputs,  $\mathbf{y}_k$ . In Stage 1, the innovation sequence of the fault-free KF,  $\{\mathbf{r}_k\}$ , as well as the corresponding covariance sequence,  $\{\mathbf{V}_k\}$ , is used as data for detecting the fault, identifying the fault mode, and estimating the fault instant and magnitude. After the estimation of the fault parameters, the fault estimate vectors are computed by using the appropriate fault sequence structure hypothesized in Table 5.1. In Stage 2, the estimates of the fault-free

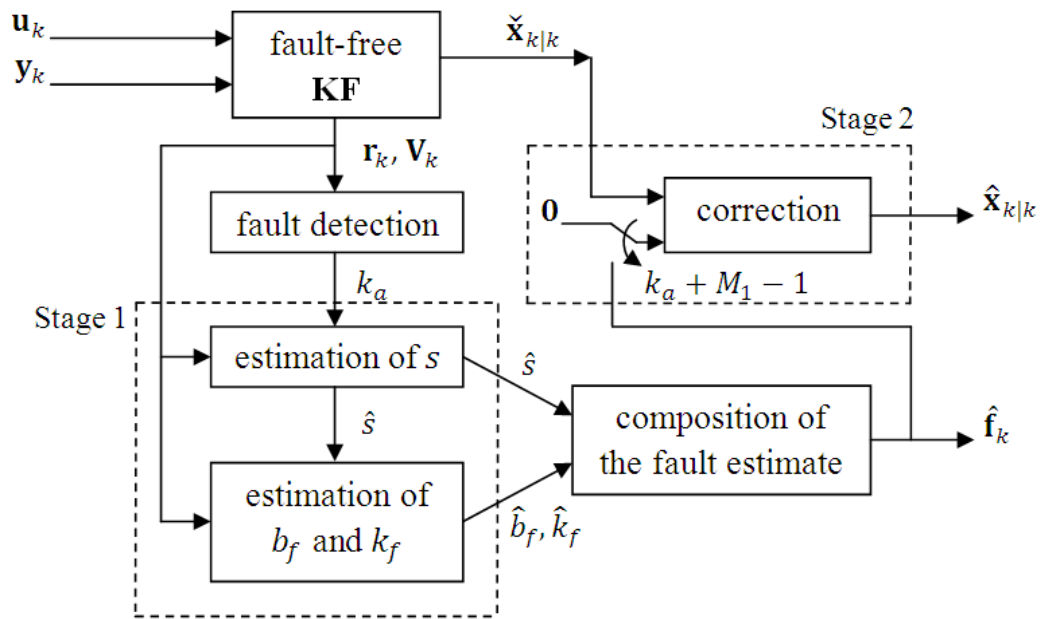


FIGURE 5.2 – The fault-tolerant attitude determination method.

KF,  $\check{\mathbf{x}}_{k|k}$ , are corrected on the basis of the fault estimates computed in Stage 1 so as to provide the corrected state estimates,  $\hat{\mathbf{x}}_{k|k}$ , which, together with the fault estimates, are the outputs of the FTAD module.

### 5.2.3 Reconfigurable MPC

The reconfigurable MPC (RMPC) corresponds to a conventional state-space MPC formulation that has been modified in order to account for actuator fault estimates when predicting the system controlled outputs,  $\mathbf{z}_k \in \mathbb{R}^{n_z}$ . It is worth noting that the sensor faults are compensated for in the FTAD module, which already provides the RMPC with corrected state estimates.

To begin with the derivations, the true fault,  $\mathbf{f}$ , is supposed to be exactly known. On the basis of this assumption, the following lemma provides the optimal MMSE predictor for the controlled output.

**Lemma 5.1** Let the controlled output at instant  $k + i$  be defined as  $\mathbf{z}_{k+i} \triangleq \mathbf{C}^z \mathbf{x}_{k+i}$ ,  $\mathbf{z}_{k+i} \in \mathbb{R}^{n_z}$ , where  $\mathbf{C}^z$  is a known matrix with appropriate dimensions. Therefore, given

the control input sequence,  $\mathbf{u}_{k:k+i-1}$ , the true fault sequence,  $\mathbf{f}_{k:k+i-1}$ , and the MMSE state estimate at instant  $k$ ,  $\hat{\mathbf{x}}_{k|k}^{opt}$ , the optimal MMSE predictor of  $\mathbf{z}_{k+i}$ ,  $\forall i \geq 1$ , is

$$\begin{aligned} \hat{\mathbf{z}}_{k+i|k} = & \mathbf{C}^z \prod_{j=1}^i \mathbf{A}_{k+i-j} \hat{\mathbf{x}}_{k|k}^{opt} + \mathbf{C}^z \sum_{j=1}^i \prod_{l=1}^{j-1} \mathbf{A}_{k+i-l} \mathbf{B}_{k+i-j} \mathbf{u}_{k+i-j} + \dots \\ & \dots + \mathbf{C}^z \sum_{j=1}^i \prod_{l=1}^{j-1} \mathbf{A}_{k+i-l} \mathbf{\Xi}_{k+i-j} \mathbf{f}_{k+i-j}. \end{aligned} \quad (5.5)$$

**Proof.** By repeatedly replacing equation (5.1) into itself,  $\mathbf{x}_{k+i}$  can be expressed in terms of  $\mathbf{u}_{k:k+i-1}$ ,  $\mathbf{f}_{k:k+i-1}$ , and  $\mathbf{x}_k$ , as

$$\begin{aligned} \mathbf{x}_{k+i} = & \prod_{j=1}^i \mathbf{A}_{k+i-j} \mathbf{x}_k + \sum_{j=1}^i \prod_{l=1}^{j-1} \mathbf{A}_{k+i-l} \mathbf{B}_{k+i-j} \mathbf{u}_{k+i-j} + \sum_{j=1}^i \prod_{l=1}^{j-1} \mathbf{A}_{k+i-l} \mathbf{\Gamma}_{k+i-j} \mathbf{w}_{k+i-j} + \dots \\ & \dots + \sum_{j=1}^i \prod_{l=1}^{j-1} \mathbf{A}_{k+i-l} \mathbf{\Xi}_{k+i-j} \mathbf{f}_{k+i-j}, \end{aligned} \quad (5.6)$$

and, hence, the controlled output  $\mathbf{z}_{k+i} = \mathbf{C}^z \mathbf{x}_{k+i}$  can be rewritten as

$$\begin{aligned} \mathbf{z}_{k+i} = & \mathbf{C}^z \prod_{j=1}^i \mathbf{A}_{k+i-j} \mathbf{x}_k + \mathbf{C}^z \sum_{j=1}^i \prod_{l=1}^{j-1} \mathbf{A}_{k+i-l} \mathbf{B}_{k+i-j} \mathbf{u}_{k+i-j} + \dots \\ & \dots + \mathbf{C}^z \sum_{j=1}^i \prod_{l=1}^{j-1} \mathbf{A}_{k+i-l} \mathbf{\Gamma}_{k+i-j} \mathbf{w}_{k+i-j} + \mathbf{C}^z \sum_{j=1}^i \prod_{l=1}^{j-1} \mathbf{A}_{k+i-l} \mathbf{\Xi}_{k+i-j} \mathbf{f}_{k+i-j}. \end{aligned} \quad (5.7)$$

On the other hand, it is well-known that the MMSE estimate of  $\mathbf{z}_{k+i}$  based on the measured outputs up to instant  $k$  corresponds to the conditional expectation  $\hat{\mathbf{z}}_{k+i|k} = E\{\mathbf{z}_{k+i} | \mathcal{Y}_k\}$  (ANDERSON; MOORE, 1979). Thus, by applying this conditional expectation to equation (5.7) and by noting that  $\{\mathbf{w}_k\}$  is zero-mean, equation (5.5) is obtained.  $\square$

It is worth noting that, in practice, one cannot realize predictions by using equation (5.5), since, in general, the true fault sequence,  $\mathbf{f}_{k:k+i-1}$ , and the optimal state estimate,  $\hat{\mathbf{x}}_{k|k}^{opt}$ , are both unavailable. In this work, in order to yield a practical predictor for the controlled output, the fault sequence estimate provided by the FTAD module is employed

to replace the corresponding true fault sequence in (5.5). Moreover, the suboptimal state estimate,  $\hat{\mathbf{x}}_{k|k}$ , is used instead of  $\hat{\mathbf{x}}_{k|k}^{opt}$ . The resulting prediction model is summarized in the following definition.

**Definition 5.2** The controlled output prediction model adopted by the RMPC for predicting  $\mathbf{z}_{k+i}$ ,  $\forall i \geq 1$ , is given by

$$\begin{aligned} \bar{\mathbf{z}}_{k+i|k} = & \mathbf{C}^z \prod_{j=1}^i \mathbf{A}_{k+i-j} \hat{\mathbf{x}}_{k|k} + \mathbf{C}^z \sum_{j=1}^i \prod_{l=1}^{j-1} \mathbf{A}_{k+i-l} \mathbf{B}_{k+i-j} \mathbf{u}_{k+i-j} + \dots \\ & \dots + \mathbf{C}^z \sum_{j=1}^i \prod_{l=1}^{j-1} \mathbf{A}_{k+i-l} \boldsymbol{\Xi}_{k+i-j} \hat{\mathbf{f}}_{k+i-j}, \end{aligned} \quad (5.8)$$

where  $\hat{\mathbf{f}}_{k:k+i-1}$  and  $\hat{\mathbf{x}}_{k|k}$  are both provided by the FTAD module.

The essential difference between the prediction model given by Definition 5.2 and the prediction model used by the conventional state-space formulation of the MPC (MACIEJOWSKI, 2002; CAMACHO; BORDONS, 1999; ROSSITER, 2004) consists of the presence of the last term on the right-hand side of equation (5.8), which accounts for the fault estimate sequence provided by the FTAD module.

In the sequel, the RMPC problem is formulated.

**Definition 5.3** Let  $\mathbf{u}_k^*$  denote the control input vector provided by the *Reconfigurable MPC* at instant  $k$ . Additionally, let  $\{\mathbf{z}_k^r\}$  denote a specified reference trajectory for the controlled output of the system. The vector  $\mathbf{u}_k^*$  is defined to be the first element of the sequence  $\mathbf{u}_{k:k+N_2-1}$ , which minimizes the cost functional

$$\mathcal{J}_k [\mathbf{u}_{k:k+N_2-1}] = \sum_{i=N_1}^{N_2} \|\bar{\mathbf{z}}_{k+i|k} - \mathbf{z}_{k+i}^r\|_{\mathbf{Q}_i^c}^2 + \sum_{i=1}^{N_2} \|\mathbf{u}_{k+i-1}\|_{\mathbf{R}_i^c}^2, \quad (5.9)$$

subject to

$$\Delta \mathbf{u}_{min} \leq \Delta \mathbf{u}_{k+i} \leq \Delta \mathbf{u}_{max}, i = 0, 1, \dots, N_2 - 1, \quad (5.10)$$



$$\mathbf{u}_{min} \leq \mathbf{u}_{k+i} \leq \mathbf{u}_{max}, i = 0, 1, \dots, N_2 - 1, \quad (5.11)$$

$$\mathbf{z}_{min} \leq \mathbf{z}_{k+i} \leq \mathbf{z}_{max}, i = N_1, N_1 + 1, \dots, N_2, \quad (5.12)$$

where  $\bar{\mathbf{z}}_{k+i|k} \in \mathbb{R}^{n_z}$  is the controlled output prediction provided by equation (5.8). The design parameters  $N_1$  and  $N_2$  are, respectively, the inferior and superior limits of the prediction horizon. The matrices  $\mathbf{Q}_i^c \in \mathbb{R}^{n_z \times n_z}$  and  $\mathbf{R}_i^c \in \mathbb{R}^{n_u \times n_u}$  are positive-definite weighting parameters. The vectors  $\Delta \mathbf{u}_{min} \in \mathbb{R}^{n_u}$ ,  $\Delta \mathbf{u}_{max} \in \mathbb{R}^{n_u}$ ,  $\mathbf{u}_{min} \in \mathbb{R}^{n_u}$ ,  $\mathbf{u}_{max} \in \mathbb{R}^{n_u}$ ,  $\mathbf{z}_{min} \in \mathbb{R}^{n_z}$ , and  $\mathbf{z}_{max} \in \mathbb{R}^{n_z}$  are the constraint parameters.

The optimization problem that appears in the previous definition consists of the minimization of a quadratic function subject to linear inequality constraints. For convenience purpose, before solving this optimization problem, it will firstly be recast into the standard format of a quadratic programming (QP) problem. To begin with, consider the following lemma, which provides a compact representation of the controlled output predictions along the prediction horizon,  $[k + N_1, k + N_2]$ .

**Lemma 5.4** The controlled output predictions along the prediction horizon are given, in a compact form, by

$$\mathbf{Z}_k = \Phi_k^x \hat{\mathbf{x}}_{k|k} + \Phi_k^f \mathbf{F}_k + \Phi_k^u \mathbf{U}_k, \quad (5.13)$$

where  $\mathbf{Z}_k \triangleq [\bar{\mathbf{z}}'_{k+N_1|k} \dots \bar{\mathbf{z}}'_{k+N_2|k}]'$ ,  $\mathbf{F}_k \triangleq [\hat{\mathbf{f}}'_k \dots \hat{\mathbf{f}}'_{k+N_2-1}]'$ ,  $\mathbf{U}_k \triangleq [\mathbf{u}'_k \dots \mathbf{u}'_{k+N_2-1}]'$ , and, for  $q = x, u$ , and  $f$ ,

$$\Phi_k^q \triangleq \begin{bmatrix} \mathbf{C}^z \phi_{N_1,k}^q \\ \mathbf{C}^z \phi_{N_1+1,k}^q \\ \dots \\ \mathbf{C}^z \phi_{N_2,k}^q \end{bmatrix}, \quad (5.14)$$

with, for  $i = N_1, \dots, N_2$ ,

$$\phi_{i,k}^x \triangleq \prod_{j=1}^i \mathbf{A}_{k+i-j},$$

$$\phi_{i,k}^f \triangleq \begin{bmatrix} \prod_{l=1}^{i-1} \mathbf{A}_{k+i-l} \mathbf{\Xi}_k & \prod_{l=1}^{i-2} \mathbf{A}_{k+i-l} \mathbf{\Xi}_{k+1} & \dots & \mathbf{A}_{k+i-1} \mathbf{\Xi}_{k+i-2} & \mathbf{\Xi}_{k+i-1} & \mathbf{0}_{n_x \times (N_2-i)n_f} \end{bmatrix},$$

$$\phi_{i,k}^u \triangleq \begin{bmatrix} \prod_{l=1}^{i-1} \mathbf{A}_{k+i-l} \mathbf{B}_k & \prod_{l=1}^{i-2} \mathbf{A}_{k+i-l} \mathbf{B}_{k+1} & \dots & \mathbf{A}_{k+i-1} \mathbf{B}_{k+i-2} & \mathbf{B}_{k+i-1} & \mathbf{0}_{n_x \times (N_2-i)n_u} \end{bmatrix},$$

where  $\phi_{i,k}^x \in \mathbb{R}^{n_x \times n_x}$ ,  $\phi_{i,k}^f \in \mathbb{R}^{n_x \times N_2 n_f}$ , and  $\phi_{i,k}^u \in \mathbb{R}^{n_x \times N_2 n_u}$ .

**Proof.** To obtain (5.13), it suffices to write out the output predictions  $\bar{\mathbf{z}}_{k+N_1|k}$ ,  $\bar{\mathbf{z}}_{k+N_1+1|k}$ ,  $\dots$ ,  $\bar{\mathbf{z}}_{k+N_2|k}$ , by using equation (5.8), and after, to arrange them into an appropriate matrix form.  $\square$

In the following lemma, the minimization problem of Definition 5.3 is rewritten in the standard form of a QP problem.

**Lemma 5.5** The optimal control sequence,  $\mathbf{u}_{k:k+N_2-1}^*$ , which solves the minimization problem of Definition 5.3 can equivalently be obtained by solving the QP problem that minimizes

$$\bar{\mathcal{J}}_k[\mathbf{U}_k] = \frac{1}{2} \mathbf{U}_k' ((\mathbf{\Phi}_k^u)' \mathcal{Q} \mathbf{\Phi}_k^u + \mathcal{R}) \mathbf{U}_k + \gamma_k' \mathcal{Q} \mathbf{\Phi}_k^u \mathbf{U}_k, \quad (5.15)$$

subject to

$$\mathcal{A} \mathbf{U}_k \leq \mathcal{B}, \quad (5.16)$$

where  $\mathbf{U}_k$  and  $\mathbf{\Phi}_k^u$  were defined in Lemma 5.4,  $\mathbf{Z}_k^r \triangleq \begin{bmatrix} (\mathbf{z}_{k+N_1}^r)' & (\mathbf{z}_{k+N_1+1}^r)' & \dots & (\mathbf{z}_{k+N_2}^r)' \end{bmatrix}'$ ,  $\gamma_k \triangleq \mathbf{\Phi}_k^x \hat{\mathbf{x}}_{k|k} + \mathbf{\Phi}_k^f \mathbf{F}_k - \mathbf{Z}_k^r$ ,  $\mathcal{Q}$  and  $\mathcal{R}$  are the block diagonal matrices given by

$$\mathcal{Q} \triangleq \begin{bmatrix} \mathbf{Q}_{N_1}^c & \mathbf{0} & \mathbf{0} & \dots & \mathbf{0} \\ \mathbf{0} & \mathbf{Q}_{N_1+1}^c & \mathbf{0} & \dots & \mathbf{0} \\ \dots & & & & \\ \mathbf{0} & \mathbf{0} & \mathbf{0} & \dots & \mathbf{Q}_{N_2}^c \end{bmatrix}, \quad \mathcal{R} \triangleq \begin{bmatrix} \mathbf{R}_1^c & \mathbf{0} & \mathbf{0} & \dots & \mathbf{0} \\ \mathbf{0} & \mathbf{R}_2^c & \mathbf{0} & \dots & \mathbf{0} \\ \dots & & & & \\ \mathbf{0} & \mathbf{0} & \mathbf{0} & \dots & \mathbf{R}_{N_2}^c \end{bmatrix},$$

and the constraint parameters  $\mathcal{A}$  and  $\mathcal{B}$  are

$$\mathcal{B} \triangleq \begin{bmatrix} \Delta \mathbf{U}_{max} + \mathbf{U}_{k-1}^0 \\ -\Delta \mathbf{U}_{max} - \mathbf{U}_{k-1}^0 \\ \mathbf{U}_{max} \\ -\mathbf{U}_{max} \\ \mathbf{Z}_{max} - \Phi_k^x \hat{\mathbf{x}}_{k|k} - \Phi_k^f \mathbf{F}_k \\ -\mathbf{Z}_{min} + \Phi_k^x \hat{\mathbf{x}}_{k|k} + \Phi_k^f \mathbf{F}_k \end{bmatrix}, \quad \mathcal{A} \triangleq \begin{bmatrix} \mathcal{A}_1 \\ -\mathcal{A}_1 \\ \mathbf{I}_{N_2 n_u} \\ -\mathbf{I}_{N_2 n_u} \\ \Phi_k^u \\ -\Phi_k^u \end{bmatrix},$$

with

$$\mathcal{A}_1 \triangleq \begin{bmatrix} \mathbf{I}_{n_u} & \mathbf{0} & \mathbf{0} & \dots & \mathbf{0} & \mathbf{0} \\ -\mathbf{I}_{n_u} & \mathbf{I}_{n_u} & \mathbf{0} & \dots & \mathbf{0} & \mathbf{0} \\ \mathbf{0} & -\mathbf{I}_{n_u} & \mathbf{I}_{n_u} & \dots & \mathbf{0} & \mathbf{0} \\ \dots & & & & & \\ \mathbf{0} & \mathbf{0} & \mathbf{0} & \dots & -\mathbf{I}_{n_u} & \mathbf{I}_{n_u} \end{bmatrix},$$

$$\Delta \mathbf{U}_{min} \triangleq \begin{bmatrix} \Delta \mathbf{u}_{min} \\ \Delta \mathbf{u}_{min} \\ \vdots \\ \Delta \mathbf{u}_{min} \end{bmatrix}, \quad \Delta \mathbf{U}_{max} \triangleq \begin{bmatrix} \Delta \mathbf{u}_{max} \\ \Delta \mathbf{u}_{max} \\ \vdots \\ \Delta \mathbf{u}_{max} \end{bmatrix}, \quad \mathbf{U}_{min} \triangleq \begin{bmatrix} \mathbf{u}_{min} \\ \mathbf{u}_{min} \\ \vdots \\ \mathbf{u}_{min} \end{bmatrix}, \quad \mathbf{U}_{max} \triangleq \begin{bmatrix} \mathbf{u}_{max} \\ \mathbf{u}_{max} \\ \vdots \\ \mathbf{u}_{max} \end{bmatrix},$$

$$\mathbf{Z}_{min} \triangleq \begin{bmatrix} \mathbf{z}_{min} \\ \mathbf{z}_{min} \\ \vdots \\ \mathbf{z}_{min} \end{bmatrix}, \quad \mathbf{Z}_{max} \triangleq \begin{bmatrix} \mathbf{z}_{max} \\ \mathbf{z}_{max} \\ \vdots \\ \mathbf{z}_{max} \end{bmatrix}, \quad \mathbf{U}_{k-1}^0 \triangleq \begin{bmatrix} \mathbf{u}_{k-1} \\ \mathbf{0} \\ \vdots \\ \mathbf{0} \end{bmatrix},$$

where  $\mathbf{u}_{k-1}$  is the control input vector generated by the RMPC at instant  $k-1$ . The dimensions of the above matrices are summarized in Table 5.2.

**Proof.** First, if one takes into account the matrices  $\mathbf{Z}_k$  and  $\mathbf{U}_k$  defined in Lemma 5.4, and the matrices  $\mathbf{Z}_k^r$ ,  $\mathcal{Q}$ , and  $\mathcal{R}$  defined in the enunciation of Lemma 5.5, then the cost

TABLE 5.2 – The dimensions of the RMPC matrices.

Matrix	Dimension
$\Delta \mathbf{U}_{min}, \Delta \mathbf{U}_{max}, \mathbf{U}_{min}, \mathbf{U}_{max}, \mathbf{U}_{k-1}^0$	$N_2 n_u \times 1$
$\mathbf{Z}_{min}, \mathbf{Z}_{max}$	$(N_2 - N_1 + 1) n_z \times 1$
$\mathcal{A}_1, \mathcal{R}$	$N_2 n_u \times N_2 n_u$
$\mathcal{A}$	$[(4N_2 n_u + 2(N_2 - N_1 + 1) n_z) \times N_2 n_u$
$\mathcal{B}$	$[(4N_2 n_u + 2(N_2 - N_1 + 1) n_z) \times 1$
$\mathcal{Q}$	$(N_2 - N_1 + 1) n_z \times (N_2 - N_1 + 1) n_z$

function (5.9) can be rewritten as

$$\mathcal{J}_k [\mathbf{U}_k] = (\mathbf{Z}_k - \mathbf{Z}_k^r)' \mathcal{Q} (\mathbf{Z}_k - \mathbf{Z}_k^r) + \mathbf{U}_k' \mathcal{R} \mathbf{U}_k. \quad (5.17)$$

Replacing equation (5.13) into equation (5.17), and making some algebraic manipulations, the latter becomes

$$\mathcal{J}_k [\mathbf{U}_k] = \gamma_k' \mathcal{Q} \gamma_k + \mathbf{U}_k' (\Phi_k^u)' \mathcal{Q} \Phi_k^u \mathbf{U}_k + 2\gamma_k' \mathcal{Q} \Phi_k^u \mathbf{U}_k + \mathbf{U}_k' \mathcal{R} \mathbf{U}_k. \quad (5.18)$$

By noting that the first term on the right-hand side of the above equation does not depend on  $\mathbf{U}_k$  and, therefore, can be neglected, the equivalent cost function (5.15) can immediately be obtained. Now, it remains to show the equivalence between equations (5.10)-(5.12) and equation (5.16). Note that the constraints in equation (5.10) can be written out as

$$\begin{bmatrix} \Delta \mathbf{u}_{min} \\ \Delta \mathbf{u}_{min} \\ \vdots \\ \Delta \mathbf{u}_{min} \end{bmatrix} \leq \begin{bmatrix} \mathbf{u}_k - \mathbf{u}_{k-1} \\ \mathbf{u}_{k+1} - \mathbf{u}_k \\ \vdots \\ \mathbf{u}_{k+N_2-1} - \mathbf{u}_{k+N_2-2} \end{bmatrix} \leq \begin{bmatrix} \Delta \mathbf{u}_{max} \\ \Delta \mathbf{u}_{max} \\ \vdots \\ \Delta \mathbf{u}_{max} \end{bmatrix}. \quad (5.19)$$

From equation (5.19), the following two inequalities are obtained:

$$\mathcal{A}_1 \mathbf{U}_k \leq \Delta \mathbf{U}_{max} + \mathbf{U}_{k-1}^0, \quad (5.20)$$

$$-\mathcal{A}_1 \mathbf{U}_k \leq -\Delta \mathbf{U}_{min} - \mathbf{U}_{k-1}^0, \quad (5.21)$$

where  $\mathcal{A}_1$ ,  $\Delta \mathbf{U}_{max}$ ,  $\Delta \mathbf{U}_{min}$ , and  $\mathbf{U}_{k-1}^0$  were defined in the enunciation of Lemma 5.5.

Now, consider explicitly writing the constraints (5.11), which become

$$\begin{bmatrix} \mathbf{u}_{min} \\ \mathbf{u}_{min} \\ \vdots \\ \mathbf{u}_{min} \end{bmatrix} \leq \begin{bmatrix} \mathbf{u}_k \\ \mathbf{u}_{k+1} \\ \vdots \\ \mathbf{u}_{k+N_2-1} \end{bmatrix} \leq \begin{bmatrix} \mathbf{u}_{max} \\ \mathbf{u}_{max} \\ \vdots \\ \mathbf{u}_{max} \end{bmatrix}. \quad (5.22)$$

From equation (5.22), the following two inequalities are obtained:

$$\mathbf{I}_{N_2 n_u} \mathbf{U}_k \leq \mathbf{U}_{max}, \quad (5.23)$$

$$-\mathbf{I}_{N_2 n_u} \mathbf{U}_k \leq \mathbf{U}_{min}, \quad (5.24)$$

where  $\mathbf{I}_{N_2 n_u}$  is the identity matrix of dimension  $N_2 n_u$ , and  $\mathbf{U}_{max}$  and  $\mathbf{U}_{min}$  are as defined in the enunciation of Lemma 5.5. Finally, the constraints given by equation (5.12), can be rewritten as

$$\begin{bmatrix} \mathbf{z}_{min} \\ \mathbf{z}_{min} \\ \vdots \\ \mathbf{z}_{min} \end{bmatrix} \leq \begin{bmatrix} \bar{\mathbf{z}}_{k+N_1|k} \\ \bar{\mathbf{z}}_{k+N_1+1|k} \\ \vdots \\ \bar{\mathbf{z}}_{k+N_2|k} \end{bmatrix} \leq \begin{bmatrix} \mathbf{z}_{max} \\ \mathbf{z}_{max} \\ \vdots \\ \mathbf{z}_{max} \end{bmatrix}, \quad (5.25)$$

which, by using the prediction model (5.13), yields

$$\Phi_k^u \mathbf{U}_k \leq \mathbf{Z}_{max} - \Phi_k^x \hat{\mathbf{x}}_{k|k} - \Phi_k^f \mathbf{F}_k, \quad (5.26)$$

$$-\Phi_k^u \mathbf{U}_k \leq \mathbf{Z}_{min} + \Phi_k^x \hat{\mathbf{x}}_{k|k} + \Phi_k^f \mathbf{F}_k. \quad (5.27)$$

Thus, by putting together the inequalities (5.20), (5.21), (5.23), (5.24), (5.26), and (5.27), equation (5.16) is obtained.  $\square$

The previous lemma has recast the problem of generating the control input,  $\mathbf{u}_k$ , to a

standard optimization problem, for which numerous solution methods are available. MA-CIEJOWSKI (2002) suggests using *interior point* or *active set* methods for solving problems such as the one given in Lemma 5.5. In the particular RMPC problem without constraints on  $\mathbf{U}_k$ , the unique solution can be determined in closed form, as given by the following theorem.

**Theorem 5.6** The unique unconstrained solution to the QP problem of Lemma 5.5 is given by

$$\mathbf{U}_k^* = - \left( (\Phi_k^u)' \mathcal{Q} \Phi_k^u + \mathcal{R} \right)^{-1} (\Phi_k^u)' \mathcal{Q} \gamma_k. \quad (5.28)$$

**Proof.** By differentiating  $\bar{\mathcal{J}}_k$  (which is given by equation (5.15)) with respect to  $\mathbf{U}_k$ , one gets

$$\frac{\partial \bar{\mathcal{J}}_k}{\partial \mathbf{U}_k} = \left( (\Phi_k^u)' \mathcal{Q} \Phi_k^u + \mathcal{R} \right) \mathbf{U}_k + (\Phi_k^u)' \mathcal{Q} \gamma_k, \quad (5.29)$$

which can be differentiated again with respect to  $\mathbf{U}_k$ , yielding the Hessian matrix:

$$\frac{\partial^2 \bar{\mathcal{J}}_k}{\partial \mathbf{U}_k^2} = (\Phi_k^u)' \mathcal{Q} \Phi_k^u + \mathcal{R}. \quad (5.30)$$

Recall that in Definition 5.3, it was established that the weighting matrices  $\mathbf{R}_i^c$  and  $\mathbf{Q}_i^c$ , for  $\forall i$ , are positive-definite. Hence, it follows immediately that the Hessian in equation (5.30) is also positive-definite. In this case,  $\bar{\mathcal{J}}_k$  is a convex quadratic function of  $\mathbf{U}_k$  and, therefore, its unique global unconstrained minimum is attained at  $\mathbf{U}_k^*$ , which can be found by simply making the right-hand side of (5.29) equal to zero and solving the resulting expression for  $\mathbf{U}_k$ . This procedure yields

$$\left( (\Phi_k^u)' \mathcal{Q} \Phi_k^u + \mathcal{R} \right) \mathbf{U}_k^* + (\Phi_k^u)' \mathcal{Q} \gamma_k = \mathbf{0}, \quad (5.31)$$

which immediately results in equation (5.28).  $\square$

## 5.3 Simulation Results

In this section, the FTMP SAC method is evaluated in three different fault scenarios by means of computational simulations.

### 5.3.1 Simulation of the satellite motion

The attitude motion of the satellite is simulated by integrating the nonlinear differential equations (A.12)-(A.13) derived in Appendix A. The initial condition is given by  $[(\mathbf{p}^{rb})' \ (\boldsymbol{\omega}_b^{br})']' \sim \mathcal{N}_{\mathbf{x}_0}(\bar{\mathbf{x}}_0, \mathbf{P}_0)$ , with  $\bar{\mathbf{x}}_0 = \mathbf{0}_{6 \times 1}$  and

$$\mathbf{P}_0 = \begin{bmatrix} 0.01\mathbf{I}_3 & \mathbf{0}_{3 \times 3} \\ \mathbf{0}_{3 \times 3} & 0.0001\mathbf{I}_3 \end{bmatrix}.$$

The fourth-order Runge-Kutta method with an integration step of  $h = 1s$  is used. The reference CCS ( $S_r$ ) is assumed to be aligned with the inertial CCS ( $S_i$ ), i.e.,  $\mathbf{D}^{ri} = \mathbf{I}_3$ . The axes of the body CCS ( $S_b$ ) are assumed to be the principal axes of inertia and the principal moments of inertia of the body are  $I_x = 6.5 \text{ kgm}^2$ ,  $I_y = 8.0 \text{ kgm}^2$ , and  $I_z = 6.5 \text{ kgm}^2$ . The moment of inertia of each reaction wheel is  $I_w = 1.0 \text{ kgm}^2$ . The  $S_b$ -representation of the vector of residual magnetic moments is  $\delta \mathbf{m}_b = [-1 \ 1 \ -1]' \text{ Am}^2$ . The orbital motion is simulated by using a Keplerian model with the orbital parameters given in Table 5.3. The simulation epoch starts at 1:00 A.M. (GMT) on June 10, 2005, and has a duration of 500 seconds.

TABLE 5.3 – Orbital parameters.

Parameter	Value
Semimajor axis	7128 km
Eccentricity	0
Inclination	25 degree
Right ascension	-40 degree
Argument of perigee	12 degree
Perigee time	0

The solar sensors are assumed to directly provide measurements of the  $S_b$ -representations

of the unit vectors pointing towards the Sun. These vectors are computed by using an analytical model for the translational motion of the Earth around the Sun [see (VALLADO, 2004), pg. 276]. For the sake of simplicity, eclipses are not considered to occur, so that the data from the solar sensors are always available. The magnetometers provide local measurements of the  $S_b$ -representations of the geomagnetic flux density. These vectors are computed using the World Magnetic Model WMM2005 (MCLEAN *et al.*, 2004). Noise terms with zero means and Gaussian distributions are added to all of the measurements. Table 5.4 shows the statistics of these measurement noises.

TABLE 5.4 – Covariance matrices of the measurement noises.

Measurement	Covariance
Geomagnetic field vector	$4.0 \times 10^{-14} \mathbf{I}_3 [T^2]$
Sun direction	$1.0 \times 10^{-4} \mathbf{I}_3 [dimensionless]$
Inertial angular velocity	$1.0 \times 10^{-10} \mathbf{I}_3 [(rad/s)^2]$

The FTMP SAC is evaluated in three fault scenarios. In scenario A, the fault belongs to the mode  $s = 1$ , i.e., it consists of a step friction torque acting on the reaction wheel that is aligned with  $X_b$  (see Table 5.1). In scenario B, the fault is of the mode  $s = 5$ , corresponding to a bias on the magnetometer that is aligned with  $Y_b$ . In scenario C, the fault belongs to the mode  $s = 9$ , consisting of a bias on the rate gyro that is aligned with  $Z_b$ . As in Chapter 4, for simplicity, the fault detection module is assumed to always generate the alarm events at a fixed instant,  $k_a = 200$ .

### 5.3.2 Configuration of the FTMP SAC

The parameters of the FTAD module are given in Table 5.5. The length of the data set for fault estimation,  $M_1$ , may have three optional values, whose effects on the system performance will be evaluated. The covariance  $\mathbf{Q}_k$  has been adjusted by trial and error in order to reach a good convergence rate. Note that  $\mathbf{R}_k$  and  $\mathbf{P}_0$  are equal to the covariances used for simulating the measurement noises and the initial state condition, respectively.

The parameters of the RMPC are given in Table 5.6. Note that the value of  $\mathbf{C}^z$  is such that the controlled output corresponds to the MRP vector. The limits of the prediction



TABLE 5.5 – Parameters of the FTAD module in SI units.

Parameter	Value
$M_1$	3; 5; 10
$\mathbf{P}_0$	$\text{diag}(1.0 \times 10^{-2} \mathbf{I}_3, 1.0 \times 10^{-4} \mathbf{I}_3)$
$\hat{\mathbf{x}}_{0 0}$	$\mathbf{0}_{6 \times 1}$
$\mathbf{Q}_k$	$1.0 \times 10^{-12} \mathbf{I}_6, \forall k$
$\mathbf{R}_k$	$\text{diag}(4.0 \times 10^{-14} \mathbf{I}_3, 1.0 \times 10^{-4} \mathbf{I}_3, 1.0 \times 10^{-10} \mathbf{I}_3), \forall k$

horizon,  $N_1$  and  $N_2$ , as well as the weighting matrices,  $\mathbf{Q}_i^c$  and  $\mathbf{R}_i^c$ , have been chosen by trial and error in order to yield a reasonable control performance with a moderate energy consumption by the reaction wheels. The MPC constraint parameters have been selected so that the constraint inequality (5.16) always stays inactive throughout the optimization processes, avoiding the need for dealing with an eventual infeasibility problem.

TABLE 5.6 – Parameters of the RMPC in SI units.

Parameter	Value
$\mathbf{C}^z$	$[\mathbf{I}_3 \quad \mathbf{0}_{3 \times 3}]$
$N_1$	2
$N_2$	15
$\mathbf{Q}_i^c$	$\mathbf{I}_3, \forall i$
$\mathbf{R}_i^c$	$0.01 \mathbf{I}_3, \forall i$
$\mathbf{z}_{min}, \mathbf{z}_{max}$	$-0.51 \mathbf{1}_{N_2}, 0.51 \mathbf{1}_{N_2}$
$\mathbf{u}_{min}, \mathbf{u}_{max}$	$-0.21 \mathbf{1}_{N_2}, 0.21 \mathbf{1}_{N_2}$
$\Delta \mathbf{u}_{min}, \Delta \mathbf{u}_{max}$	$-0.11 \mathbf{1}_{N_2}, 0.11 \mathbf{1}_{N_2}$

### 5.3.3 Monte Carlo simulation results

For evaluating the performance of the proposed control system, consider the following four indices:

$$I_c = \arccos \left( \frac{1}{2} [\text{tr}(\mathbf{D}^{rb}) - 1] \right), \quad (5.32)$$

$$I_e = \arccos \left( \frac{1}{2} [\text{tr}(\hat{\mathbf{D}}^{rb} \mathbf{D}^{rb}) - 1] \right), \quad (5.33)$$

$$I_u = \|\mathbf{u}\|, \quad (5.34)$$

$$I_w = \|\boldsymbol{\omega}_b^{wb}\|, \quad (5.35)$$

where  $\mathbf{D}^{rb}$  is the true attitude matrix,  $\hat{\mathbf{D}}^{rb}$  is the estimate of the attitude matrix (which corresponds to the estimate of the MRP,  $\hat{\mathbf{p}}^{rb}$ ),  $\mathbf{u}$  is the control input generated by the reaction wheels, and  $\boldsymbol{\omega}_b^{wb}$  contains the angular velocities of the wheels relative to the satellite body. It is worth noting that the indices  $I_c$  and  $I_e$  correspond to the angles of the *Euler axis/angle* attitude representations that are equivalent to the matrices  $\mathbf{D}^{rb}$  and  $\hat{\mathbf{D}}^{rb}\mathbf{D}^{rb}$ , respectively [see reference (WERTZ, 1978), p. 412]. Therefore, by inspection, one can see that  $I_c$  is a measure of the attitude *control error*, while  $I_e$  is a measure of the attitude *estimation error*. The indices  $I_u$  and  $I_w$  are adopted to evaluate the usage of the reaction wheels along the system operation. The indices  $I^{k_f}$ ,  $I^{b_f}$ , and  $N_c$  defined in Subsection 4.4.2 are also adopted here to evaluate the performance with regard to the estimation of  $k_f$ ,  $b_f$ , and  $s$ , respectively.

For each of the three scenarios, three Monte Carlo simulations of 10000 runs of the overall fault-tolerant system were carried out  $M_1$ . The sample statistics (mean and standard deviation) of the indices  $I_c$ ,  $I_e$ ,  $I_u$ , and  $I_w$  obtained for  $M_1 = 10$  in scenarios A, B, and C are shown, respectively, in Figure 5.3, Figure 5.4, and Figure 5.5. The statistics of the fault parameter estimation indices,  $I^{k_f}$  and  $I^{b_f}$ , are summarized in Table 5.7. Some comments are presented below.

- *Scenario A:* In Figure 5.3(a), it can be observed that from the onset of the fault at some instant  $k_f \in [180, 200]$  up to the reconfiguration instant around  $k = 210$ , the estimation errors exhibit a diverging behavior. However, this tendency is immediately eliminated after reconfiguration. The same behavior is observed in the control error index (Figure 5.3(b)), which is observed to be lower limited by the estimation error index. Therefore, as expected, to reach a good feedback control performance, it is necessary to have a good estimation performance. Regarding the actuator usage, Figure 5.3(c) shows that  $I_u$  has a transitory increase at the reconfiguration, after which the actuator torques become essentially constant, but slightly

larger than those applied before the fault occurrence. This is explained by the fact that the fault, in this scenario, is indeed a torque and, therefore, additional torque is required for compensating for its effects. One of the consequences is observed in Figure 5.3(d), which shows that the reaction wheels start accelerating after reconfiguration. Table 5.7 shows that, for scenario A, by increasing  $M_1$  from 3 to 10, both the identification of the fault mode and the estimation of  $k_f$  and  $b_f$  are improved.

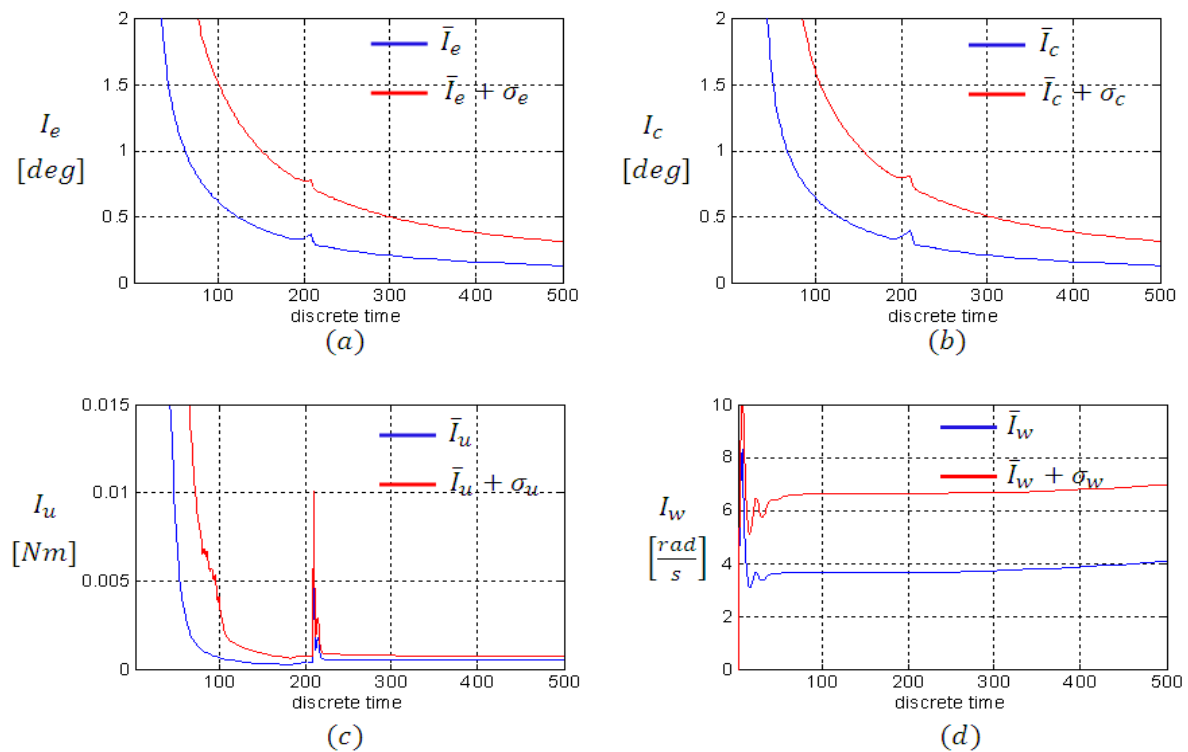
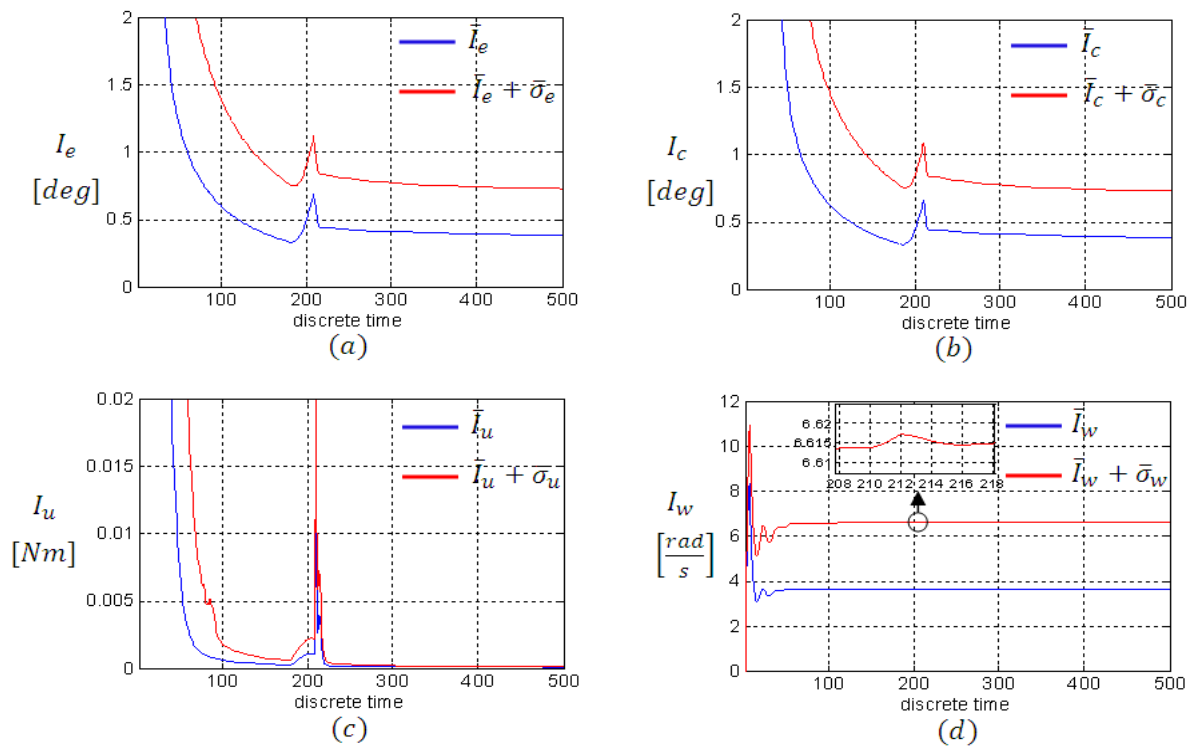


FIGURE 5.3 – Simulation results for scenario A and  $M_1 = 10$ .

- *Scenario B*: As observed in Figure 5.4, regarding the indices  $I_e$  and  $I_c$ , the results for scenario B are very similar to those obtained for scenario A. However, Figure 5.4(c) shows that after the reconfiguration transient, the control torque returns to its previous level. In consequence, as observed in Figure 5.4(d), the velocities of the wheels only undergo a transitory oscillation. Note that, different from the previous scenario, the controller does not provide additional compensating torque, since the fault of scenario B is just a measurement bias whereas in scenario A it was a friction torque. Table 5.7 shows that, for scenario B, by increasing  $M_1$  from 3 to 10, both the identification of the fault mode and the estimation of  $k_f$  and  $b_f$  are improved.


 FIGURE 5.4 – Simulation results for scenario B and  $M_1 = 10$ .

- *Scenario C*: The results for this scenario are similar to the previous case, which also corresponds to a sensor fault. The major difference observed here consists of the insignificant degradation of the state estimation after reconfiguration with respect to the performance observed before the fault occurrence. This is explained by the fact that even in the absence of the measurements from the rate gyros, the attitude and angular velocity could have been estimated uniquely from the attitude sensors (the solar sensors and magnetometers) (AZOR *et al.*, 1998). Table 5.7 shows that, for scenario C, by increasing  $M_1$  from 3 to 10, both the identification of the fault mode and the estimation of  $k_f$  and  $b_f$  are improved.

To finalize, for the purpose of comparison, a simple scheme composed by a conventional MPC and a linearized KF is taken into account. For brevity, it is called MPC-KF. All of its configuration parameters are chosen to be equal to the corresponding ones in the FTMP SAC. Figure 5.6 shows the statistics of  $I_e$  for the MPC-KF scheme under scenarios A, B, and C. It is worth noting that, from the beginning of system operation until the reconfiguration instant, both methods, MPC-KF and FTMP SAC, are equivalent.

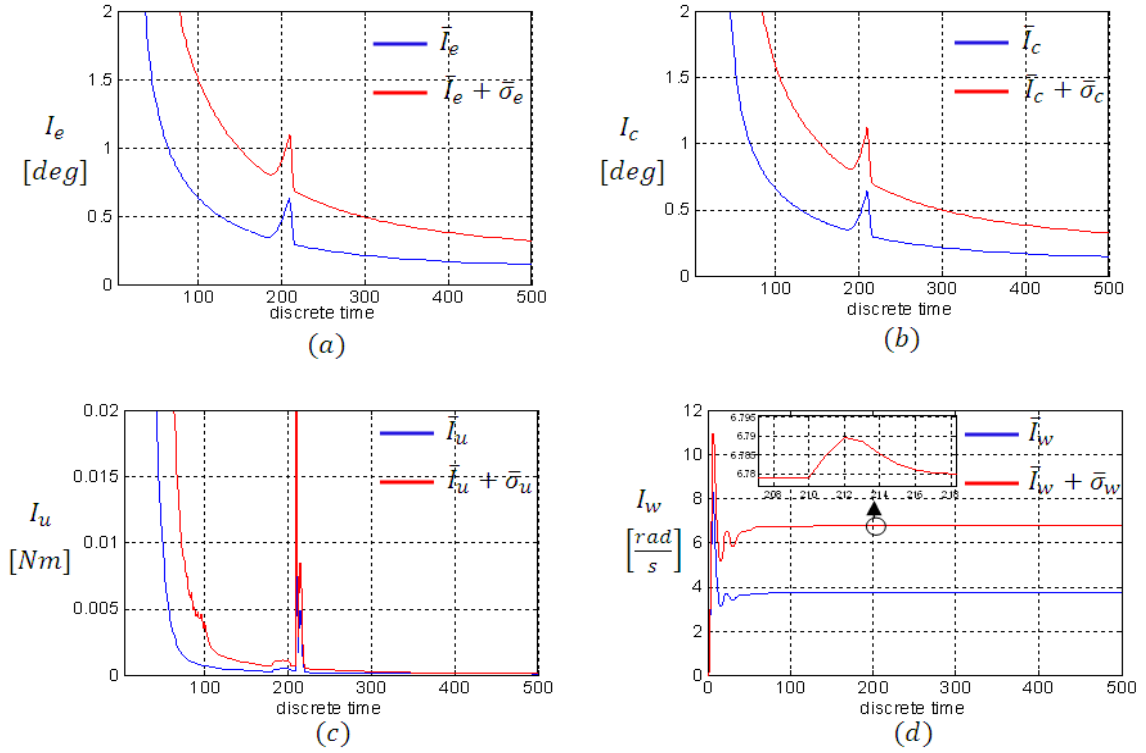


FIGURE 5.5 – Simulation results for scenario C and  $M_1 = 10$ .

Nevertheless, after reconfiguration, the MPC-KF scheme, as expected, presents a degraded performance since it does not adopt any fault remedy.

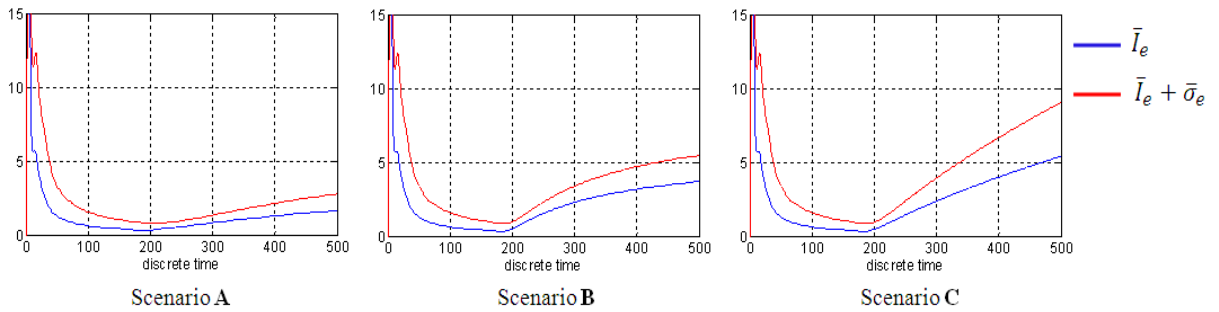


FIGURE 5.6 – State estimation errors obtained with the MPC-KF scheme under scenarios A, B, and C.

## 5.4 Summary

This chapter presented a novel fault-tolerant satellite attitude control method. It is suitable for controlling rigid-body satellites equipped with reaction wheels, rate gyros, solar sensors, and magnetometers. This method consists of an integration of an FTTF

TABLE 5.7 – The fault parameter estimation errors.

Scenario	$M_1$	$N_c$	$(\bar{I}^{k_f}, \sigma^{k_f})$	$(\bar{I}^{b_f}, \sigma^{b_f})$
<i>A</i>	3	9814	(0.6151, 1.5095)	(0.0499, 0.2256)
	5	9849	(0.4324, 1.2330)	(0.0308, 0.1214)
	10	9877	(0.3036, 1.0114)	(0.0219, 0.1467)
<i>B</i>	3	9797	(8.6299, 5.6667)	(0.0971, 0.5738)
	5	9825	(8.5010, 5.6382)	(0.0860, 0.5865)
	10	9834	(8.2433, 5.5858)	(0.0752, 0.5586)
<i>C</i>	3	9916	(0.3041, 0.9364)	(0.0135, 0.0493)
	5	9934	(0.2216, 0.7707)	(0.0100, 0.0317)
	10	9952	(0.1756, 0.7503)	(0.0073, 0.0473)

filter with a fault-reconfigurable version of a conventional state-space formulation of the MPC. Computational simulations were carried out. The results demonstrated the effectiveness of the FTMP SAC method when the system was considered to operate in three fault scenarios: a friction torque in a reaction wheel, a bias in the measurements of a rate gyro, and a bias in the measurements of a magnetometer.

In future works, the FTMP SAC method could be improved by augmenting the set of inequality constraints of the RMPC in order to include limitations on the angular velocities of the reaction wheels. One can conjecture that such an improvement may prevent the wheels of undergoing speed saturation conditions.

## 6 Conclusion

This thesis has been concerned with the joint state and fault estimation of discrete-time linear systems subject to additive faults. Unlike the literature on state estimation of systems subject to unknown inputs (GILLIJNS; MOOR, 2007b; HSIEH, 2010; WILLISKY; JONES, 1976; HMIDA *et al.*, 2010), in the present work, prior knowledge about the fault parameters was assumed to be available and compactly represented by appropriately defined probability distributions. The investigation can be summarized as follows:

- In Chapter 2, a fault-tolerant state estimation (FTSE) problem has been defined (Problem 2.4). It is a joint state and fault estimation in a recursive filtering framework. Problem 2.4 has assumed that the system dynamics can be described by a discrete-time linear Gaussian state-space model subject to additive faults on both the state and measurement equations. The sequence of fault vectors has been defined as a structured sequence parameterized by three fault parameters: the fault magnitude (which represents the severity of the fault), the fault instant (which represents the onset of the fault), and the fault mode index (which represents the form and location of the fault). These parameters have been considered as realizations of particularly defined random variables, which account for the prior knowledge about the fault.
- In Chapter 4, Problem 2.4 has been tackled by a suboptimal (but implementable) fault-tolerant two-stage (FTTS) filtering approach. By separately taking into account the three alternative models for the prior knowledge about the fault magnitude parameter, three FTTS filters have been derived. In general, the structure of the

FTTS filters can be described as follows. In the first stage, the fault parameters are estimated by statistically processing the innovation sequence of a fault-free KF. For this end, it has been adopted the Bayesian approach, with which the prior knowledge about the fault parameters can naturally be considered. On the other hand, the second stage of the filters carries out state estimation by correcting the fault-free KF on the basis of the fault estimate provided by the first stage. This correction is such that the state estimates would be the optimal (MMSE) ones if the fault estimate were replaced by the true fault. It has been pointed out in Section 4.5 that the formal analysis of the FTTS filters is a mathematically intractable problem. Hence, numerical simulations have been carried out in order to evaluate their performance on a specific illustrative system.

- In Chapter 5, the FTTS filter for Gaussian fault magnitudes has been employed in a fault-tolerant attitude control system for rigid body satellites equipped with rate gyros, magnetometers, solar sensors, and reaction wheels. A conventional state-space formulation of the model predictive control (MPC) has been adopted as the basic control strategy. However, the internal prediction model of the proposed fault-tolerant MPC (FTMPC) has been modified so as to account for the fault estimate provided by an FTTS filter. Simulation results have shown the capability of the method to accommodate the effects of both sensor and actuator faults. Although the above FTMPC method has been introduced in the context of satellite attitude control, it is worth mentioning that it can be applied to any system whose dynamics can be described by the fault-prone system model defined in Chapter 2.

Some future works that might be developed on the basis of the framework established in the present investigation are listed below.

1. To attempt solving Problem 2.4 by using the Bayesian filtering approach. Note that, in this case, one firstly needs to look for the joint posterior PDF of the state and fault parameters. Then, to obtain the required estimates, it is necessary to evaluate mean values from such PDF. Although this is a mathematically intricate



problem, Sequential Monte Carlo techniques might be employed in order to achieve approximate solutions. The resulting methods could be compared with the FTTS filters.

2. To implement the FTTS filters in a real-time computer for embedded system applications. In such a work, the computational complexity of the filters should be assessed. More efficient algorithms might be necessary for attaining satisfactory numerical accuracy. The resulting real-time computer could be tested in a Hardware-in-the-Loop (HIL) simulation scheme.
3. To fit the fault parameter PDFs established in Assumption 2.3 to historical experimental fault data sets. Such an investigation might be able to evaluate in practice the statistical models considered throughout the present work for representing the prior knowledge about the fault parameters. Moreover, different model types might be revealed thereby.
4. To extend Problem 2.4 for dealing with multiple faults. Problem 2.4 has only treated single faults. However, in practice, as a consequence of a first fault, some other faults may develop in the system. By using multiple fault estimations and corrections, the FTTS filters could be extended to tackle such multiple fault situations.
5. To extend Problem 2.4 for dealing with multiplicative faults. Note that the difficulty of applying the FTTS filtering approach for treating multiplicative faults stems from the impossibility of exactly predicting the fault mode signatures on the innovation of the fault-free KF. Hence, the fault estimation problem cannot be recast into the statistical processing framework established in Problem 4.3, unless those signatures could be approximated somehow. On the other hand, note that by using the Bayesian filtering approach, at first sight, both additive and multiplicative faults can be addressed indistinctly.
6. To extend Problem 2.4 for dealing with nonlinear systems. Like in the above item, it would not be possible to exactly compute the fault mode signatures on the fault-free KF innovations if the system model were nonlinear. In this case, for extending

the FTTS filters, one could attempt to adopt simulated signatures rather than analytically computed signatures. Alternatively, note that such extended problem may be tackled by using the Bayesian filtering approach together with sequential Monte Carlo techniques.

7. To evaluate the performance of the FTTS filters in a quantitative, but not necessarily analytical manner. From such analysis, one could derive a criterion for selecting the data set length,  $M_1$ . Additionally, it is important to address the robustness of the filters with respect to both model uncertainties and unpredicted fault modes.
8. To derive new versions of the fault-estimation stage of the FTTS filters by considering either a unique hypothesis test or a unique MAP parameter estimator. Such alternative derivations may be compared with the ones proposed in Section 4.2.

# Bibliography

ANDERSON, B. D. O.; MOORE, J. B. **Optimal Filtering**. [S.l.]: Englewood Cliffs: Prentice-Hall, 1979.

ATKINSON, K. E. **An Introduction to Numerical Analysis**. [S.l.]: New York: John Wiley & Sons, 1989.

AZOR, R.; BAR-ITZHACK, I. Y.; HARMAN, R. R. Satellite angular rate estimation from vector measurements. **Journal of Guidance, Control, and Dynamics**, v. 21(3), p. 450–457, 1998.

BAR-ITZHACK, I. Y.; IDAN, M. Recursive attitude determination from vector observations: Euler angle estimation. **Journal of Guidance**, v. 10(2), p. 152–157, 1987.

BAR-ITZHACK, I. Y.; OSHMAN, Y. Attitude determination from vector observations: quaternion estimation. **IEEE Transactions on Aerospace and Electronic Systems**, AES-21(1), p. 128–135, 1985.

BAR-ITZHACK, I. Y.; REINER, J. Recursive attitude determination from vector observations: direction cosine matrix identification. **Journal of Guidance**, v. 7(1), p. 51–56, 1984.

BAR-SHALOM, Y.; LI, X.-R. **Estimation and Tracking: Principles, Techniques, and Software**. [S.l.]: Norwood: Artech House, 1993.

BLANKE, M.; IZADI-ZAMANABADI, R.; BOGH, S.; LUNAU, C. Fault-tolerant control system - a holistic view. **Control Engineering Practice**, v. 5(5), p. 693–702, 1997.

BLANKE, M.; KINNAERT, M.; LUNZE, J.; STAROSWIECKI, M. **Diagnosis and fault-tolerant control**. [S.l.]: Berlin: Springer-Verlag, 2003.

BUENO, R.; CHOW, E. Y.; DUNN, K.-P.; GERSHWIN, S. B.; WILLSKY, A. S. Status report on the generalized likelihood ratio failure detection technique, with application to the f-8 aircraft. In: **In: Decision and Control including the 15th Symposium on Adaptive Processes, 1976 IEEE Conference on**. [S.l.: s.n.], 1976. p. 38–47.

CAGLAYAN, A. K.; LANCRAFT, R. E. A separate-bias identification and state estimation algorithm for nonlinear system. **Automatica**, v. 19(5), p. 561–570, 1983.

CAMACHO, E. F.; BORDONS, C. **Model Predictive Control**. [S.l.]: London: Springer & Verlag, 1999.

CHAN, Y. T.; HU, A. G. C.; PLANT, J. B. A kalman filter based tracking scheme with input estimation. **IEEE Transactions on Aerospace and Electronic Systems**, AES-15(2), p. 237–244, 1979.

CHANG, C. B.; DUNN, K. P. On glr detection and estimation of unexpected inputs in linear discrete system. **IEEE Transactions on Automatic Control**, AC-24(3), p. 499–501, 1979.

DAROUACH, M.; ZASADZINSKI, M.; BOUTAYEB, M. Extension of minimum variance estimation for systems with unknown inputs. **Automatica**, v. 39, p. 867–876, 2003.

DOUCET, A.; FREITAS, N. de; GORDON, N. (Ed.). **Sequential Monte Carlo Methods in Practice**. [S.l.]: Berlin: Springer-Verlag, 2001.

FRANKLIN, G. F.; POWELL, J. D.; EMAMI-NAEINI, A. **Feedback control of dynamic systems**. 6th. ed. [S.l.]: New Jersey: Prentice Hall, 2010.

FREITAS, N. de. Rao-blackwellised particle filtering for fault diagnosis. In: **IEEE Aerospace Conference Proceedings**. [S.l.: s.n.], 2002. p. 1767–1772.

FRIEDLAND, B. Treatment of bias in recursive filtering. **IEEE Transactions on Automatic Control**, AC-14(4), p. 359–367, 1969.

GELB, A. **Applied Optimal Estimation**. [S.l.]: Cambridge: MIT Press, 1974.

GILLIJNS, S.; MOOR, B. D. Unbiased minimum-variance input and state estimation for linear discrete-time systems. **Automatica**, v. 43, p. 111–116, 2007.

GILLIJNS, S.; MOOR, B. D. Unbiased minimum-variance input and state estimation for linear discrete-time systems with direct feedthrough. **Automatica**, v. 43, p. 934–937, 2007.

GOLDSTEIN, H. **Classical Mechanics**. [S.l.]: San Francisco: Addison-Wesley, 2002.

GOODWIN, G. C.; PAYNE, R. L. **Dynamic System Identification: Experiment Design and Data Analysis**. [S.l.]: New York: Academic Press, 1977.

HMIDA, F. B.; KHÉMIRI, K.; RAGOT, J.; GOSSA, M. Unbiased minimum-variance filter for state and fault estimation of linear time-varying systems with unknown disturbances. **Mathematical Problems in Engineering**, 2010.

HSIEH, C. Extension of unbiased minimum-variance input and state estimation for systems with unknown inputs. **Automatica**, v. 45, p. 2145–2153, 2009.

HSIEH, C.-S. On the global optimality of unbiased minimum-variance state estimation for systems with unknown inputs. **Automatica**, v. 46, p. 708–715, 2010.

HSIEH, C.-S.; CHEN, F.-C. Optimal solution of the two-stage kalman estimator. **IEEE Transactions on Automatic Control**, v. 44(1), p. 194–199, 1999.

IGNAGNI, M. An alternate derivation and extension of friedlands two-stage kalman estimator. **IEEE Transactions on Automatic Control**, AC-26(3), p. 746–750, 1981.

IGNAGNI, M. Separate-bias kalman estimator with bias state noise. **IEEE Transactions on Automatic Control**, v. 35(3), p. 338–341, 1990.

IGNAGNI, M. Optimal and suboptimal separate-bias kalman estimators for a stochastic bias. **IEEE Transactions on Automatic Control**, v. 45(3), p. 547–551, 2000.

ISERMANN, R. **Fault-diagnosis systems - an introduction from fault detection to fault tolerance**. [S.l.]: Berlin: Springer-Verlag, 2006.

JAZWINSKI, A. H. **Stochastic process and filtering theory**. [S.l.]: New York: Academic Press, 1970.

KAILATH, T. A view of three decades of linear filtering theory. **IEEE Transactions on Information Theory**, IT-20(2), p. 146–181, 1974.

KAILATH, T.; SAYED, A. H.; HASSIBI, B. **Linear Estimation**. [S.l.]: New Jersey: Prentice Hall, 2000.

KALMAN, R. E. A new approach to linear filtering and prediction problems. **Transactions of the ASME–Journal of Basic Engineering**, v. 82, n. Series D, p. 35–45, 1960.

KAY, S. M. **Fundamentals of Statistical Signal Processing: Detection Theory.**

[S.l.]: New Jersey: Prentice Hall, 1998.

KAY, S. M. **Fundamentals of Statistical Signal Processing: Estimation Theory.**

[S.l.]: New Jersey: Prentice Hall, 1998.

KIM, K. H.; LEE, J. G.; PARK, C. G. Adaptive two-stage extended kalman filter for a fault-tolerant ins-gps loosely coupled system. **IEEE Transactions on Aerospace and Electronic Systems**, v. 45(1), p. 125–137, 2009.

KITANIDIS, P. K. Unbiased minimum-variance linear state estimation. **Automatica**, v. 23(6), p. 775–778, 1987.

KOLMOGOROV, A. N. Interpolation and extrapolation of stationary random processes.

**Bull. Acad. Sci. USSR**, v. 5, 1941.

KUO, B. C.; GOLNARAGHI, M. F. **Automatic Control Theory.** [S.l.]: John Wiley & Sons, 2003.

LEFFERTS, E. J.; MARKLEY, F. L.; SHUSTER, M. D. Kalman filtering for spacecraft attitude estimation. **Journal of Guidance, Control, and Dynamics**, v. 5(5), p. 417–429, 1982.

MACIEJOWSKI, J. M. **Predictive Control with Constraints.** [S.l.]: Harlow: Prentice Hall, 2002.

MAHMOUD, M.; JIANG, J.; ZHANG, Y. **Active Fault Tolerant Control Systems - Stochastic Analysis and Synthesis.** In *Lecture Notes in Control and Information Sciences*. [S.l.]: Berlin: Springer-Verlag, 2003.

- MCAULAY, R. J.; DENLINGER, E. A decision-directed adaptive tracker. **IEEE Transactions on Aerospace and Electronic Systems**, AES-9(2), p. 229–236, 1973.
- MCLEAN, S.; MACMILLAN, S.; MAUS, S.; LESUR, A.; THOMSON, D.; DATER, D. **The US/UK World Magnetic Model for 2005-2010**. [S.l.], 2004.
- MENDEL, J. M. Extension of friedland's bias filtering technique to a class of nonlinear systems. **IEEE Transactions on Automatic Control**, AC-21, p. 296–298, 1976.
- NARASIMHAN, S.; MAH, R. S. H. Generalised likelihood ratios for gross errors identification in dynamic systems. **AIChE J**, v. 34, n. 1, p. 1321–1332, 1988.
- OGATA, K. **Modern control engineering**. [S.l.]: New Jersey: Prentice Hall, 1970.
- ORCHARD, M. E. **A Particle filtering-based framework for on-line fault diagnosis and failure prognosis**. Tese (Doutorado) — Georgia Institute of Technology, 2007.
- PAPOULIS, A.; PILLAI, S. U. **Probability, Random Variables, and Stochastic Processes**. [S.l.]: New York: McGraw-Hill, 2002.
- PATTON, R. J. Fault-tolerant control systems: 1997 situation. In: **In Proceedings of the IFAC Symposium SAFEPROCESS 1997, Hull, UK**. [S.l.: s.n.], 1997. p. 1033–1054.
- PRAKASH, J.; NARASIMHAN, S.; PATWARDHAN, S. C. Integrating model based diagnosis with model predictive control. **Ind. Eng. Chem. Res.**, v. 44, n. 2, p. 4344–4260, 2005.



PRAKASH, J.; PATWARDHAN, S. C.; NARASIMHAN, S. A supervisory approach to fault-tolerant control of linear multivariable systems. **Ind. Eng. Chem. Res.**, v. 41, p. 2270–2281, 2002.

RAPOPORT, I.; OSHMAN, Y. Efficient fault tolerant estimation using the IMM methodology. In: **AIAA Guidance, Navigation, and Control Conference and Exhibit**. Providence, Rhode Island: [s.n.], 2004. p. 1–18.

RAPOPORT, I.; OSHMAN, Y. Fault tolerant particle filtering using IMM-based Rao-Blackwellization. In: **AIAA Guidance, Navigation, and Control Conference and Exhibit**. Providence, Rhode Island: [s.n.], 2004. p. 1–13.

ROSSITER, J. A. **Model-Based Predictive Control**. [S.l.]: New York: CRC Press, 2004.

SANTOS, D. A. dos; YONEYAMA, T. Fault-tolerant attitude determination system of an earth-pointing satellite. In: **20th International Congress of Mechanical Engineering**. Gramado-RS, Brazil: [s.n.], 2009.

SANTOS, D. A. dos; YONEYAMA, T. Diagnóstico bayesiano de falhas utilizando sequência de inovação. In: **XVIII Congresso Brasileiro de Automática**. Bonito-MS, Brazil: [s.n.], 2010. p. 2883–2890.

SANTOS, D. A. dos; YONEYAMA, T. A bayesian solution to the multiple composite hypothesis testing for fault diagnosis in dynamic systems. **Automatica**, v. 47(1), n. 1, p. 158–163, 2011.

SANYAL, P.; SHEN, C. N. Bayes decision rule for rapid detection and adaptive estimation scheme with space applications. **IEEE Transactions on Automatic Control**, v. 19(3), p. 228–231, 1974.

SCHARF, L. L. **Statistical Signal Processing: Detection, Estimation, and Time Series Analysis**. [S.l.]: Addison-Wesley Publishing Company, 1991.

SHINNERS, S. M. **Modern Control System Theory and Design**. [S.l.]: New York: John Wiley & Sons, 1992.

SHUSTER, M. D. A survey of attitude representations. **The Journal of the Astronautical Sciences**, v. 41(4), p. 439–517, 1993.

SIGALOV, D.; OSHMAN, Y. A new formulation of fault-tolerant estimation problems and some solutions. In: **IEEE 26-th Convention of Electrical and Electronics Engineers in Israel**. [S.l.: s.n.], 2010. p. 626–630.

SORENSEN, H. W. Least-squares estimation: from gauss to kalman. **IEEE Spectrum**, p. 63–68, 1970.

SORENSEN, H. W. **Kalman Filtering: Theory and Application**. [S.l.]: Montvale: IEEE Press, 1985.

TUNG, W. **Group Theory in Physics**. [S.l.]: Philadelphia: World Scientific, 1985.

VALLADO, D. A. **Fundamentals of Astrodynamics and Applications**. [S.l.]: Microcosm Press, 2004.

VERMA, V. **Tractable particle filters for robot fault diagnosis**. Tese (Doutorado) — Carnegie Mellon University, 2004.

WAHNON, E.; BENVENISTE, A.; GHAOUI, L. E.; NIKOUKHAH, R. An optimum robust approach to statistical failure detection and identification. In: **Proceedings of the 30th Conference on Decision and Control**. Brighton, England: [s.n.], 1991. p. 650–655.

WERTZ, J. R. (Ed.). **Spacecraft attitude determination and control**. [S.l.]: Kluwer Academic Publisher, 1978.

WIENER, N. **Extrapolation, Interpolation, and Smoothing of Stationary Time Series**. [S.l.]: New York: Technology Press and Wiley, 1949.

WILLSKY, A. S. Detection of abrupt changes in dynamic systems. In: **Lecture Notes in Control and Information Sciences**, v. 77, p. 27–49, 1986.

WILLSKY, A. S.; JONES, H. L. A generalized likelihood ratio approach to the detection and estimation of jumps in linear systems. **IEEE Transactions on Automatic Control**, AC-21, n. 1, p. 108–112, 1976.

ZHANG, Y.; JIANG, J. Bibliographical review on reconfigurable fault-tolerant control systems. In: **Proceeding of the 5th IFAC Symposium on Fault Detection, Supervision and Safety for Technical Processes**. Washington, D.C., USA: [s.n.], 2003. p. 265–276.

ZHANG, Y.; LI, X. R. Detection and diagnosis of sensor and actuator failures using imm estimator. **IEEE Transactions on Aerospace and Electronic Systems**, v. 34(4), n. 4, p. 1293–1313, 1998.

---

ZHOU, D. H.; SUN, Y. X.; XI, Y. G.; ZHANG, Z. J. Extension of friedlands separate-bias estimation to randomly time-varying bias of nonlinear systems. **IEEE Transactions on Automatic Control**, v. 38(8), p. 1270–1273, 1993.

# Appendix A - Satellite Attitude

## Dynamics

The present appendix provides a detailed derivation of a deterministic state-space model for the attitude dynamics of a rigid-body satellite. The text is organized in the following manner. Section A.1 presents some preliminary definitions and notations. Section A.2 derives the nonlinear dynamic models for the satellite attitude motion. Moreover, it presents the nonlinear measurement models relating the data from rate gyros, magnetometers, and solar sensors with the satellite attitude and angular velocity. Section A.3 provides a deterministic continuous-time linearized state-space model. Finally, Section A.4 presents a discretized state-space model.

### A.1 Preliminary definitions

Three Cartesian coordinate systems (CCS) will be considered throughout. They are illustrated in Figure A.1. The body CCS, denoted by  $S_b = \{X_b, Y_b, Z_b\}$ , is centered at the satellite center of mass (CM) and is fixed in its body. The reference CCS, denoted by  $S_r = \{X_r, Y_r, Z_r\}$ , is also centered at CM, but it is not attached to the satellite. Its axes are aligned with a required direction that depends on the mission specifications.

The inertial CCS, denoted by  $S_i = \{X_i, Y_i, Z_i\}$ , is Earth-centered and its axes have the following orientation:  $X_i$  points towards the vernal equinox,  $Z_i$  is aligned with the Earth's rotation axis, and  $Y_i$  completes the orthogonal right-hand oriented coordinate system.

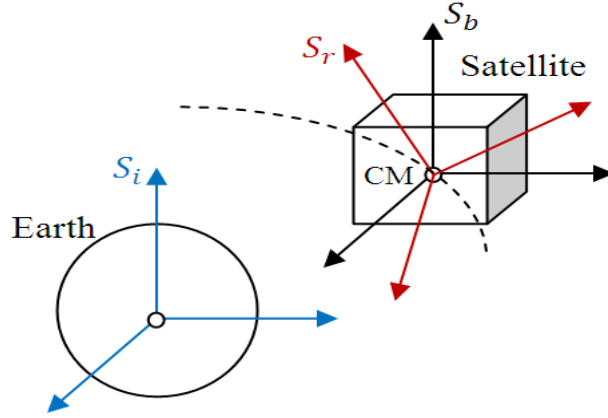


FIGURE A.1 – Cartesian coordinate systems.

Let  $\vec{\mathbf{r}}$  denote a vector representing a physical quantity. It can be represented in any CCS. For example, the representation of  $\vec{\mathbf{r}}$  in  $S_b$ , which will hereafter be called the  $S_b$ -representation of  $\vec{\mathbf{r}}$ , is denoted by  $\mathbf{r}_b \in \mathbb{R}^3$ . Likewise, the  $S_r$ -representation and the  $S_i$ -representation of  $\vec{\mathbf{r}}$  are denoted by  $\mathbf{r}_r$  and  $\mathbf{r}_i$ , respectively. The attitude matrix  $\mathbf{D}^{rb} \in SO(3)$ <sup>1</sup> transforms  $S_r$ -representations into the corresponding  $S_b$ -representations, i.e.,  $\mathbf{r}_b = \mathbf{D}^{rb}\mathbf{r}_r$ . Although such a matrix represents a general coordinate transformation, it is inconvenient to deal with it since it involves nine scalar parameters, while only three ones are sufficient. In this case,  $\mathbf{D}^{rb}$  may be parameterized by a vector  $\mathbf{p} \in \mathbb{R}^{n_p}$ , where  $3 \leq n_p \leq 9$ . In this work,  $\mathbf{p}$  is chosen to be the vector of modified Rodrigues parameters (MRP), whose dimension is  $n_p = 3$ . Let the angular velocity of  $S_b$  with respect to  $S_r$  be  $\vec{\omega}^{br}$ . Therefore, its  $S_b$ -representation is denoted by  $\omega_b^{br}$ . Time-differentiation will often be denoted by the dot notation, e.g.,  $\dot{\mathbf{r}}_b$ . However, in certain cases, a vector representation in some CCS needs being time-differentiated with respect to an observer that is attached

<sup>1</sup>SO(3) denotes the Special Orthogonal Group (TUNG, 1985). A given matrix  $\mathbf{D}$  belongs to SO(3) if  $\mathbf{D} \in \mathbb{R}^{3 \times 3}$ ,  $\mathbf{D}'\mathbf{D} = \mathbf{I}_3$ , and  $\det(\mathbf{D}) = 1$ .

to another CCS. In such situations, the notation exemplified by  $\overset{r}{\mathbf{r}}_b$  is adopted. It means that the  $S_b$ -representation  $\mathbf{r}_b$  is time-differentiated by an observer that is attached to  $S_r$ .

It is useful to make explicit the relationship between time derivatives of vectors with respect to different CCSs. It can be shown that (GOLDSTEIN, 2002) given a representation  $\mathbf{r}$  of a vector  $\vec{\mathbf{r}}$ ,

$$\overset{i}{\dot{\mathbf{r}}} = \overset{b}{\dot{\mathbf{r}}} + \boldsymbol{\omega}^{bi} \times \mathbf{r}, \quad (\text{A.1})$$

where  $\boldsymbol{\omega}^{bi}$  is the angular velocity of  $S_b$  with respect to  $S_i$ . Note that the subscripts for denoting the CCS in which the vectors are represented are omitted here. In fact, this equation is valid for vectors represented in any CCS.

Note that the  $S_b$ -representation of the vector product  $\vec{\mathbf{a}} \times \vec{\mathbf{b}}$  can be rewritten as the matrix multiplication  $[\mathbf{a}_b \times] \mathbf{b}_b$ , where

$$[\mathbf{a}_b \times] = \begin{bmatrix} 0 & -a_3 & a_2 \\ a_3 & 0 & -a_1 \\ -a_2 & a_1 & 0 \end{bmatrix}, \quad (\text{A.2})$$

with  $\mathbf{a}_b = [a_1 \ a_2 \ a_3]'$ .

To complete the preliminary definitions, it is useful to present the *strapdown equation*, which relates the time-derivative of the attitude matrix  $\mathbf{D}^{rb}$  with the angular velocity  $\boldsymbol{\omega}^{br}$ . Such equation is just a form of representing the kinematic attitude model. Mathematically, it is given by (WERTZ, 1978)

$$\dot{\mathbf{D}}^{rb} = -[\boldsymbol{\omega}^{br} \times] \mathbf{D}^{rb}. \quad (\text{A.3})$$

## A.2 System Modeling

The present section aims at developing the dynamic and measurement models of the satellite illustrated in Figure A.2. These models are used for simulation and design purposes in Chapter 5. The vehicle illustrated here consists of a cubic rigid-body satellite. It can be controlled by three identical reaction wheels mounted in an aligned fashion with respect to the axes of  $S_b$ . They are labeled by  $RW_x$ ,  $RW_y$ , and  $RW_z$ . In order to be capable of estimating the attitude and angular velocity, the satellite is also supposed to be equipped with a triad of rate gyros ( $TG_x$ ,  $TG_y$ , and  $TG_z$ ), a triad of magnetometers ( $TM_x$ ,  $TM_y$ , and  $TM_z$ ), and six two-axis solar sensors ( $SS_1, \dots, SS_6$ ), one on each satellite face. All the sensors are assumed to provide measurements corresponding to  $S_b$ -representations.

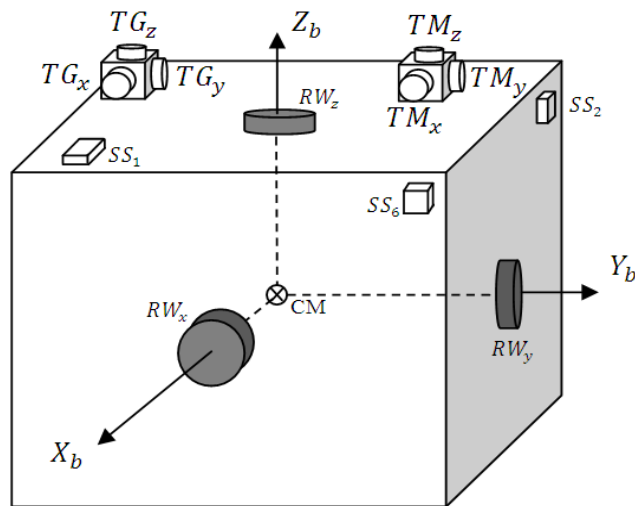


FIGURE A.2 – A cubic rigid-body satellite and its sensors and actuators.



### A.2.1 Satellite attitude dynamics

The  $S_b$ -representation of the Euler's moment equation for the satellite depicted in Figure A.2 is given by

$$\mathbf{M}_b = \dot{\mathbf{H}}_b + [\boldsymbol{\omega}_b^{bi} \times] \mathbf{H}_b, \quad (\text{A.4})$$

where  $\mathbf{M}_b$  represents the external torque acting on the satellite about its CM,  $\mathbf{H}_b$  is the total angular momentum (of the satellite and the reaction wheels) also about CM, and  $\boldsymbol{\omega}_b^{bi}$  corresponds to the inertial angular velocity of the satellite body. The total angular momentum is given by

$$\mathbf{H}_b = {}^s\mathbf{H}_b + {}^w\mathbf{H}_b, \quad (\text{A.5})$$

where  ${}^s\mathbf{H}_b$  is the angular momentum of the satellite body, which is given by  ${}^s\mathbf{H}_b = \mathbf{J}_s \boldsymbol{\omega}_b^{bi}$ , where  $\mathbf{J}_s$  is the satellite inertia matrix with respect to the  $S_b$  axes. On the other hand,  ${}^w\mathbf{H}_b$  represents the angular momentum of the wheels. It is given by  ${}^w\mathbf{H}_b = I_w \mathbf{I}_3 \boldsymbol{\omega}_b^{wi}$ , where  $I_w$  is the moment of inertia of each wheel about its rotation axis, and  $\boldsymbol{\omega}_b^{wi}$  is such that its components correspond to the inertial angular velocities of the wheels. It follows that  $\boldsymbol{\omega}_b^{wi} = \boldsymbol{\omega}_b^{wb} + \boldsymbol{\omega}_b^{bi}$ . Therefore, by taking into consideration the above definitions and replacing equation (A.5) into (A.4), it results

$$\mathbf{M}_b - I_w \mathbf{I}_3 \dot{\boldsymbol{\omega}}_b^{wb} = (\mathbf{J}_s + I_w \mathbf{I}_3) \dot{\boldsymbol{\omega}}_b^{bi} + [\boldsymbol{\omega}_b^{bi} \times] \{(\mathbf{J}_s + I_w \mathbf{I}_3) \boldsymbol{\omega}_b^{bi} + I_w \mathbf{I}_3 \boldsymbol{\omega}_b^{wb}\}. \quad (\text{A.6})$$

Since the goal is to describe the attitude motion of  $S_b$  with respect to  $S_r$ , the angular velocity  $\boldsymbol{\omega}_b^{br}$  has to appear in place of  $\boldsymbol{\omega}_b^{bi}$  in equation (A.6). This is accomplished by just making  $\boldsymbol{\omega}_b^{bi} = \boldsymbol{\omega}_b^{br} + \boldsymbol{\omega}_b^{ri}$ , where  $\boldsymbol{\omega}_b^{ri} = \mathbf{D}^{rb} \boldsymbol{\omega}_r^{ri}$ . Note that  $\mathbf{D}^{rb}$  represents the attitude of the satellite. The quantity  $\boldsymbol{\omega}_r^{ri}$  represents the inertial angular velocity of the reference

CCS, which is assumed to be known. Using the above considerations, equation (A.6) can be rewritten as

$$\begin{aligned} \mathbf{M}_b - I_w \mathbf{I}_3 \dot{\boldsymbol{\omega}}_b^{wb} &= (\mathbf{J}_s + I_w \mathbf{I}_3) \left( \dot{\boldsymbol{\omega}}_b^{br} + \mathbf{D}^{rb} \boldsymbol{\omega}_r^{ri} + \mathbf{D}^{rb} \boldsymbol{\omega}_r^{b\ ri} \right) + \dots \\ &\dots + [(\boldsymbol{\omega}_b^{br} + \mathbf{D}^{rb} \boldsymbol{\omega}_r^{ri}) \times] \{ (\mathbf{J}_s + I_w \mathbf{I}_3) (\boldsymbol{\omega}_b^{br} + \mathbf{D}^{rb} \boldsymbol{\omega}_r^{ri}) + I_w \mathbf{I}_3 \boldsymbol{\omega}_b^{wb} \}. \end{aligned} \quad (\text{A.7})$$

Now, by using equations (A.1) and (A.3), noting that  $\mathbf{D}^{br} = (\mathbf{D}^{rb})'$ , and defining the control torque  ${}^c\boldsymbol{\tau} \triangleq I_w \mathbf{I}_3 \dot{\boldsymbol{\omega}}_b^{wb}$ , the above equation can be rewritten as

$$\begin{aligned} \mathbf{M}_b - {}^c\boldsymbol{\tau} &= (\mathbf{J}_s + I_w \mathbf{I}_3) \left( \dot{\boldsymbol{\omega}}_b^{br} - [\boldsymbol{\omega}_b^{br} \times] \mathbf{D}^{rb} \boldsymbol{\omega}_r^{ri} + \mathbf{D}^{rb} \left( \dot{\boldsymbol{\omega}}_r^{ri} + [\boldsymbol{\omega}_r^{ri} \times] (\mathbf{D}^{rb})' \boldsymbol{\omega}_b^{br} \right) \right) + \dots \\ &\dots + [(\boldsymbol{\omega}_b^{br} + \mathbf{D}^{rb} \boldsymbol{\omega}_r^{ri}) \times] \{ (\mathbf{J}_s + I_w \mathbf{I}_3) (\boldsymbol{\omega}_b^{br} + \mathbf{D}^{rb} \boldsymbol{\omega}_r^{ri}) + I_w \mathbf{I}_3 \boldsymbol{\omega}_b^{wb} \}. \end{aligned} \quad (\text{A.8})$$

The actuation provided by the reaction wheels is explained by the principle of conservation of the total angular momentum (GOLDSTEIN, 2002). There is no other actuator being taken into account in the satellite depicted in Figure A.2. Therefore, in the present application, the external torque term,  $\mathbf{M}_b$ , consists only of perturbation torques. In the sequel, two types of perturbation torques are considered: the gravity-gradient torque,  ${}^{gg}\mathbf{M}_b$ , and the residual magnetic torque,  ${}^{mg}\mathbf{M}_b$ . Such perturbations are relevant when dealing with low-Earth orbits (WERTZ, 1978). Mathematically,

$$\mathbf{M}_b = {}^{gg}\mathbf{M}_b + {}^{mg}\mathbf{M}_b. \quad (\text{A.9})$$

The gravity-gradient torque is produced by the differences in the magnitude of the Earth's gravitational field along the satellite body. It is usually approximated by the following expression (WERTZ, 1978):

$${}^{gg}\mathbf{M}_b \cong \frac{3\mu}{\|\mathbf{r}_r\|^3} [(\mathbf{D}^{rb}\hat{\mathbf{r}}_r) \times] (\mathbf{J}_s + I_w\mathbf{I}_3) \mathbf{D}^{rb}\hat{\mathbf{r}}_r, \quad (\text{A.10})$$

where  $\mathbf{r}_r$  is the  $S_r$ -representation of the satellite position vector with respect to the center of the Earth,  $\hat{\mathbf{r}}_r$  is the unitary vector in the direction of  $\mathbf{r}_r$ , and  $\mu$  is the Earth gravitational constant.

The residual magnetic perturbation torque emerges from the interaction between the geomagnetic field and the satellite residual magnetic field due to its onboard electronics. It is given by (WERTZ, 1978)

$${}^{mg}\mathbf{M}_b = [\delta\mathbf{m}_b \times] \mathbf{D}^{rb}\mathbf{b}_r, \quad (\text{A.11})$$

where  $\delta\mathbf{m}_b$  is the residual *magnetic dipole moment* represented in  $S_b$ , and  $\mathbf{b}_r$  is the  $S_r$ -representation of the geomagnetic flux density at the satellite current position. Therefore, by substituting (A.10) and (A.11) into (A.9), and replacing the resulting expression in (A.8), one finally obtains the nonlinear attitude dynamic equation:

$$\begin{aligned} \dot{\boldsymbol{\omega}}_b^{br} = & (\mathbf{J}_s + I_w\mathbf{I}_3)^{-1} \frac{3\mu}{\|\mathbf{r}_r\|^3} [(\mathbf{D}^{rb}\hat{\mathbf{r}}_r) \times] (\mathbf{J}_s + I_w\mathbf{I}_3) \mathbf{D}^{rb}\hat{\mathbf{r}}_r + (\mathbf{J}_s + I_w\mathbf{I}_3)^{-1} [\delta\mathbf{m}_b \times] \mathbf{D}^{rb}\mathbf{b}_r + \dots \\ & \dots - (\mathbf{J}_s + I_w\mathbf{I}_3)^{-1} [(\boldsymbol{\omega}_b^{br} + \mathbf{D}^{rb}\boldsymbol{\omega}_r^{ri}) \times] ((\mathbf{J}_s + I_w\mathbf{I}_3) (\boldsymbol{\omega}_b^{br} + \mathbf{D}^{rb}\boldsymbol{\omega}_r^{ri}) + I_w\mathbf{I}_3\boldsymbol{\omega}_b^{wb}) + \dots \end{aligned}$$

$$\dots + [\boldsymbol{\omega}_b^{br} \times] \mathbf{D}^{rb} \boldsymbol{\omega}_r^{ri} - \mathbf{D}^{rb} \dot{\boldsymbol{\omega}}_r^{ri} - \mathbf{D}^{rb} [\boldsymbol{\omega}_r^{ri} \times] (\mathbf{D}^{rb})' \boldsymbol{\omega}_b^{br} - (\mathbf{J}_s + I_w \mathbf{I}_3)^{-1} {}^c \boldsymbol{\tau}, \quad (\text{A.12})$$

which corresponds to a system of three coupled nonlinear first-order differential equations.

In order to complete the description of the attitude motion, it remains to write the kinematic equation, relating the time derivatives of the MRP  $\mathbf{p}^{rb} \in \mathbb{R}^3$  (which parameterizes  $\mathbf{D}^{rb}$ ) with  $\boldsymbol{\omega}_b^{br}$ . It is given by (SHUSTER, 1993)

$$\dot{\mathbf{p}}^{rb} = \frac{1}{4} \left\{ \left( 1 - \|\mathbf{p}^{rb}\|^2 \right) \mathbf{I}_3 + 2 [\mathbf{p}^{rb} \times] + 2 \mathbf{p}^{rb} (\mathbf{p}^{rb})' \right\} \boldsymbol{\omega}_b^{br}, \quad (\text{A.13})$$

and the relationship between the attitude matrix  $\mathbf{D}^{rb}$  and the MRP  $\mathbf{p}^{rb}$  is

$$\mathbf{D}^{rb} \triangleq \mathbf{D}(\mathbf{p}^{rb}) = \mathbf{I}_3 + \frac{4}{\left( 1 + \|\mathbf{p}^{rb}\|^2 \right)^2} \left\{ 2 [\mathbf{p}^{rb} \times]^2 - \left( 1 - \|\mathbf{p}^{rb}\|^2 \right) [\mathbf{p}^{rb} \times] \right\}. \quad (\text{A.14})$$

Equations (A.12)-(A.13) completely describe the dynamics of the attitude motion of the satellite depicted in Figure A.2 when it is subject to disturbance torques due to gravity-gradient and residual magnetism.

### A.2.2 Measurement models

Consider that the magnetometers, the solar sensors, and the rate gyros provide measurements of the  $S_b$ -representations, respectively, of the geomagnetic flux density,  $\mathbf{b}_b$ , the unit vector pointing towards the Sun,  $\mathbf{s}_b$ , and the inertial angular velocity of  $S_b$ ,  $\boldsymbol{\omega}_b$ . Moreover, assume that the corresponding  $S_r$ -representations,  $\mathbf{b}_r$ ,  $\mathbf{s}_r$ , and  $\boldsymbol{\omega}_r$  can be computed by using available reference models. Therefore, one can immediately write the following

expressions:

$$\mathbf{b}_b = \mathbf{D}(\mathbf{p}^{rb}) \mathbf{b}_r, \quad (\text{A.15})$$

$$\mathbf{s}_b = \mathbf{D}(\mathbf{p}^{rb}) \mathbf{s}_r, \quad (\text{A.16})$$

and

$$\boldsymbol{\omega}_b = \boldsymbol{\omega}_b^{br} + \boldsymbol{\omega}_b^{ri} = \boldsymbol{\omega}_b^{br} + \mathbf{D}(\mathbf{p}^{rb}) \boldsymbol{\omega}_r^{ri}, \quad (\text{A.17})$$

where the true attitude matrix,  $\mathbf{D}(\mathbf{p}^{rb})$ , is given by equation (A.14). Note that, in equations (A.15)-(A.16), the true  $S_r$ -representations,  $\mathbf{b}_r$  and  $\mathbf{s}_r$ , are simply transformed into the corresponding  $S_b$ -representations,  $\mathbf{b}_b$  and  $\mathbf{s}_b$ , respectively. Equation (A.17) is just a slightly modified expression of the  $S_b$ -representation of the inertial angular velocity of  $S_b$ .

### A.3 Linearized state-space model

For the purpose of designing the linear fault-tolerant control scheme of Chapter 5, it is necessary to derive discrete-time linearized approximations of the nonlinear continuous-time models presented in the previous section. Note that the coordinate system  $S_r$  has not been specified thus far. Therefore, the above equations are valid for any reference CCS centered at the CM of the satellite.

Now, in order to derive the linearized equations, define  $S_r$  to be parallel to  $S_i$ . Hence,  $\mathbf{D}^{ri} = \mathbf{I}_3$ ,  $\boldsymbol{\omega}_r^{ri} = \mathbf{0}$ ,  $\dot{\boldsymbol{\omega}}_r^{ri} = \mathbf{0}$ , and  $\hat{\mathbf{r}}_r = \hat{\mathbf{r}}_i$ . Define the continuous-time state vector as  $\mathbf{x}(t) \triangleq [(\mathbf{p}^{rb})', (\boldsymbol{\omega}_b^{br})']'$ , the continuous-time control input vector as  $\mathbf{u}(t) \triangleq {}^c \boldsymbol{\tau}$ , and the reference state as  $\bar{\mathbf{x}} \triangleq \mathbf{0}_{6 \times 1}$ . Additionally, let the inertia matrix  $\mathbf{J}_s$  be diagonal and define

the notations  $\mathbf{J}_s \triangleq \text{diag}(I_x, I_y, I_z)$ ,  $\delta\mathbf{m}_b \triangleq [\delta m_{bx} \ \delta m_{by} \ \delta m_{bz}]'$ ,  $\mathbf{b}_r \triangleq [b_{rx} \ b_{ry} \ b_{rz}]'$ , and  $\hat{\mathbf{r}}_r \triangleq [\hat{r}_{rx} \ \hat{r}_{ry} \ \hat{r}_{rz}]'$ . Therefore, by truncating the Taylor series expansions of the nonlinearities appearing in equations (A.12)-(A.13) about the reference point  $\bar{\mathbf{x}}$ , a linear continuous-time deterministic state equation,

$$\dot{\mathbf{x}}(t) = \mathbf{A}(t)\mathbf{x}(t) + \mathbf{B}\mathbf{u}(t), \quad (\text{A.18})$$

is obtained, where

$$\mathbf{A}(t) = \begin{bmatrix} \mathbf{0}_{3 \times 3} & \frac{1}{4}\mathbf{I}_3 \\ \mathbf{A}_{21} & [I_w \mathbf{I}_3 \boldsymbol{\omega}_b^{wb} \times] \end{bmatrix}, \quad (\text{A.19})$$

$$\mathbf{B} = \begin{bmatrix} \mathbf{0}_{3 \times 3} \\ -\mathbf{B}_2 \end{bmatrix}, \quad (\text{A.20})$$

$$\mathbf{B}_2 = \text{diag} \{ (I_x + I_w)^{-1}, (I_y + I_w)^{-1}, (I_z + I_w)^{-1} \} \quad (\text{A.21})$$

and

$$\mathbf{A}_{21} = \begin{bmatrix} a_{11} & a_{12} & a_{13} \\ a_{21} & a_{22} & a_{23} \\ a_{31} & a_{32} & a_{33} \end{bmatrix}, \quad (\text{A.22})$$

with

$$a_{11} \triangleq \frac{3\mu(I_z - I_y)}{\|\mathbf{r}_i\|^3 (I_x + I_w)} (4\hat{r}_{rz}^2 - 4\hat{r}_{ry}^2) - \frac{4\delta m_{bz}}{I_x + wI} b_{rz} - 4 \frac{\delta m_{by}}{I_x + wI} b_{ry}, \quad (\text{A.23})$$

$$a_{12} \triangleq \frac{12\mu(I_z - I_y)}{\|\mathbf{r}_i\|^3 (I_x + I_w)} \hat{r}_{rx} \hat{r}_{ry} + \frac{4\delta m_{by}}{I_x + I_w} b_{rx}, \quad (\text{A.24})$$

$$a_{13} \triangleq \frac{-12\mu(I_z - I_y)}{\|\mathbf{r}_i\|^3 (I_x + I_w)} \hat{r}_{rz} \hat{r}_{rx} + \frac{4\delta m_{bz}}{I_x + I_w} b_{rx}, \quad (\text{A.25})$$

$$a_{21} \triangleq \frac{-12\mu(I_x - I_z)}{\|\mathbf{r}_i\|^3 (I_y + I_w)} \hat{r}_{rz} \hat{r}_{ry} + \frac{4\delta m_{bx}}{I_y + I_w} b_{ry}, \quad (\text{A.26})$$

$$a_{22} \triangleq \frac{3\mu(I_x - I_z)}{\|\mathbf{r}_i\|^3 (I_y + I_w)} (-4\hat{r}_{rz}^2 + 4\hat{r}_{rx}^2) - \frac{4\delta m_{bz}}{I_y + I_w} b_{rz} - \frac{4\delta m_{bx}}{I_y + I_w} b_{rx}, \quad (\text{A.27})$$

$$a_{23} \triangleq \frac{12\mu(I_x - I_z)}{\|\mathbf{r}_i\|^3 (I_y + I_w)} \hat{r}_{rz} \hat{r}_{ry} + \frac{4\delta m_{bz}}{I_y + I_w} b_{ry}, \quad (\text{A.28})$$

$$a_{31} \triangleq \frac{12\mu(I_y - I_x)}{\|\mathbf{r}_i\|^3 (I_z + I_w)} \hat{r}_{rz} \hat{r}_{rx} + \frac{4\delta m_{bx}}{I_z + I_w} b_{rz}, \quad (\text{A.29})$$

$$a_{32} \triangleq \frac{-12\mu(I_y - I_x)}{\|\mathbf{r}_i\|^3 (I_z + I_w)} \hat{r}_{rz} \hat{r}_{ry} + \frac{4\delta m_{by}}{I_z + I_w} b_{rz}, \quad (\text{A.30})$$

$$a_{33} \triangleq \frac{3\mu(I_y - I_x)}{\|\mathbf{r}_i\|^3 (I_z + I_w)} (4\hat{r}_{ry}^2 - 4\hat{r}_{rx}^2) - \frac{4\delta m_{by}}{I_z + I_w} b_{ry} - \frac{4\delta m_{bx}}{I_z + I_w} b_{rx}. \quad (\text{A.31})$$

Now, consider the nonlinear measurement equations (A.15)-(A.17). In order to linearize them about  $\bar{\mathbf{x}}$ , first let the quadratic functions of  $\mathbf{p}^{rb}$  appearing in equation (A.14) equal to zero. This procedure yields

$$\mathbf{D}^{rb} \cong \mathbf{I}_3 - 4 [\mathbf{p}^{rb} \times]. \quad (\text{A.32})$$

Therefore, by noting that  $\boldsymbol{\omega}_r^{ri} = \mathbf{0}$ , equations (A.15)-(A.16) become

$$\mathbf{b}_b \cong \mathbf{b}_r + 4 [\mathbf{b}_r \times] \mathbf{p}^{rb}, \quad (\text{A.33})$$

$$\mathbf{s}_b \cong \mathbf{s}_r + 4 [\mathbf{s}_r \times] \mathbf{p}^{rb}, \quad (\text{A.34})$$

$$\boldsymbol{\omega}_b = \boldsymbol{\omega}_b^{br}. \quad (\text{A.35})$$

To cast the above measurement models into the standard form of linear state-space representations, let the observation vector be  $\mathbf{y} \triangleq [(\mathbf{b}_b - \mathbf{b}_r)', (\mathbf{s}_b - \mathbf{s}_r)', \boldsymbol{\omega}'_b]'$ . Hence, the measurement equation becomes

$$\mathbf{y}(t) = \mathbf{C}(t)\mathbf{x}(t), \quad (\text{A.36})$$

with

$$\mathbf{C}(t) = \begin{bmatrix} 4 [\mathbf{b}_r \times] & \mathbf{0}_{3 \times 3} \\ 4 [\mathbf{s}_r \times] & \mathbf{0}_{3 \times 3} \\ \mathbf{0}_{3 \times 3} & \mathbf{I}_3 \end{bmatrix}. \quad (\text{A.37})$$

## A.4 Discretized state-space model

For the purpose of discretizing equation (A.18), assume that, between consecutive sampling instants,  $\mathbf{A}(t)$  and  $\mathbf{u}(t)$  are approximately constant. Particularly, denote two arbitrary consecutive sampling instants by  $t_k$  and  $t_{k+1}$ . Hence, for  $t \in [t_k, t_{k+1})$ , one can write  $\mathbf{A}(t) = \mathbf{A}(t_k)$  and  $\mathbf{u}(t) = \mathbf{u}(t_k)$ . In this context, given  $\mathbf{x}(t_k)$ , the solution of the



differential equation (A.18) at instant  $t_{k+1}$  is [see (KUO; GOLNARAGHI, 2003), p.143]

$$\mathbf{x}(t_{k+1}) = \exp \{ \mathbf{A}(t_k) \times (t_{k+1} - t_k) \} \mathbf{x}_k + \int_{t_k}^{t_{k+1}} \exp \{ \mathbf{A}(t_k) \times (t_{k+1} - \tau) \} \mathbf{B} \mathbf{u}(t_k) d\tau, \quad (\text{A.38})$$

which can be rewritten as

$$\mathbf{x}_{k+1} = \mathbf{A}_k \mathbf{x}_k + \mathbf{B}_k \mathbf{u}_k \quad (\text{A.39})$$

where  $\mathbf{x}_k \triangleq \mathbf{x}(t_k)$ ,  $\mathbf{u}_k \triangleq \mathbf{u}(t_k)$ ,

$$\mathbf{A}_k \triangleq \exp \{ \mathbf{A}(t_k) \times (t_{k+1} - t_k) \}, \quad (\text{A.40})$$

and

$$\mathbf{B}_k \triangleq \int_{t_k}^{t_{k+1}} \exp \{ \mathbf{A}(t_k) \times (t_{k+1} - \tau) \} d\tau \mathbf{B}. \quad (\text{A.41})$$

Finally, by solving the integral over  $\tau$ , equation (A.41) can be rewritten as

$$\mathbf{B}_k = \mathbf{A}(t_k)^{-1} (\mathbf{A}_k - \mathbf{I}_6) \mathbf{B}. \quad (\text{A.42})$$

Since the continuous-time measurement model (A.36) is an algebraic equation, a corresponding discrete-time model can immediately be obtained as

$$\mathbf{y}_k = \mathbf{C}_k \mathbf{x}_k, \quad (\text{A.43})$$

where  $\mathbf{y}_k \triangleq \mathbf{y}(t_k)$  and  $\mathbf{C}_k \triangleq \mathbf{C}(t_k)$ .

In summary, equations (A.39) and (A.43) constitute a deterministic discrete-time linearized state-space model for the system under consideration. In this work, a sample

period of  $T \triangleq t_{k+1} - t_k = 1$  s is adopted.

## FOLHA DE REGISTRO DO DOCUMENTO

1. CLASSIFICAÇÃO/TIPO <p style="text-align: center;"><b>TD</b></p>	2. DATA <p style="text-align: center;">22 de agosto de 2011</p>	3. DOCUMENTO Nº <p style="text-align: center;">DCTA/ITA/TD-018/2011</p>	4. Nº DE PÁGINAS <p style="text-align: center;">130</p>
5. TÍTULO E SUBTÍTULO: Fault-tolerant state estimation of linear Gaussian Systems Subject to Additive Faults			
6. AUTOR(ES): <b>Davi Antônio dos Santos</b>			
7. INSTITUIÇÃO(ÕES)/ÓRGÃO(S) INTERNO(S)/DIVISÃO(ÕES): Instituto Tecnológico de Aeronáutica – ITA			
8. PALAVRAS-CHAVE SUGERIDAS PELO AUTOR: Fault-Tolerant State Estimation; Filtering Theory; Statistical Signal Processing; Bayesian Detection; Model Predictive Control; Satellite Attitude Control			
9. PALAVRAS-CHAVE RESULTANTES DE INDEXAÇÃO: Estimação de estado; Tolerância a falhas; Teoria de filtragem; Processamento de sinais; Análise estatística; Modelos matemáticos; Controle preditivo; Controle			
10. APRESENTAÇÃO: <span style="float: right;"><input checked="" type="checkbox"/> Nacional    <input type="checkbox"/> Internacional</span> ITA, São José dos Campos. Curso de Doutorado. Programa de Pós-Graduação em Engenharia Eletrônica e computação. Área de Sistemas e Controle. Orientador: Takashi Yoneyama. Defesa em 10/08/2011. Publicada em 2011.			
11. RESUMO: <p>Owing to the need for the satisfaction of attributes such as safety, maintainability, and reliability in modern critical engineering devices, the design of automatic feedback control systems has increasingly demanding fault-tolerant methods. In particular, if the system states cannot directly be measured by the available suite of sensors, a fault-tolerant state estimation method turns out to be of paramount importance for achieving fault tolerance. In this context, the present thesis formulates a fault-tolerant state estimation (FTSE) problem consisting of a joint state and fault estimation of linear systems subject to additive faults. The system is described by a discrete-time linear Gaussian state-space model, where the fault appears as unknown inputs affecting both the state and measurement equations. The sequence of fault inputs is assumed to be parameterizable by three fault parameters: the fault magnitude, the fault instant, and the fault mode index. Moreover, these parameters are treated as unknown realizations of random variables (RV) that are defined so as to account for prior knowledge about possible faults. For tackling the above FTSE problem, the present work introduces a fault-tolerant two-stage (FTTS) filtering approach, from which three different FTTS filters are derived by considering three plausible alternative characterizations of the fault magnitude RV. On the basis of computational simulations, one of the FTTS filters is illustrated on a fault-tolerant model predictive control (MPC) scheme for satellite attitude control.</p>			
12. GRAU DE SIGILO: <input checked="" type="checkbox"/> <b>OSTENSIVO</b> <input type="checkbox"/> <b>RESERVADO</b> <input type="checkbox"/> <b>CONFIDENCIAL</b> <input type="checkbox"/> <b>SECRETO</b>			